

TREM2 Associations with Concomitant Pathology in Alzheimer's Disease

By

Rebecca Lynn Winfree

Dissertation
Submitted to the Faculty of the
Graduate School of Vanderbilt University
in partial fulfillment of the requirements
for the degree of

DOCTOR OF PHILOSOPHY

in

Pharmacology

August 31st, 2022

Nashville, TN

Approved:

Joey Barnett, Ph.D.

Angela Jefferson, Ph.D.

Christine Konradi, Ph.D.

Sean Davies, Ph.D.

Timothy J. Hohman, Ph.D.

Dedication

I dedicate this work to my loving husband, Erik. Amongst many tough challenges that come along with the territory of pursuing a graduate education, he has always been there, helping me to re-focus on what is joyful and what is fun.

Acknowledgements

I would like to acknowledge the Vanderbilt Department of Pharmacology for supporting me throughout my graduate career, particularly my committee members and advisor, Dr. Timothy Hohman. I would also like to acknowledge the training grant which provided me with financial support as a trainee in the Vanderbilt Memory and Alzheimer's Center (T32-AG058524). I am very grateful to have been immersed in such an exceptional, multidisciplinary training environment.

TABLE OF CONTENTS

	Page
LIST OF TABLES	v
LIST OF FIGURES	vii
LIST OF ABBREVIATIONS	ix
Chapter	
I. INTRODUCTION	1
Alzheimer’s Disease	1
Prevalence and Clinical Characterization	1
Concomitant Neuropathology	3
Pharmacological Treatments	6
TREM2 and sTREM2 Overview	9
Biological Functions	10
Roles in Neurodegenerative Disease	12
Rationale and Aims	15
II. EVALUATION OF <i>TREM2</i> GENE EXPRESSION ASSOCIATIONS WITH ALZHEIMER’S DISEASE PATHOLOGY AT AUTOPSY	21
Introduction	21
Methods	25
Results	33
Discussion	49
III. BIOLOGICAL CORRELATES OF ELEVATED STREM2 IN CSF	57
Introduction	57
Methods	60
Results	66
Discussion	81
IV. MS4A-ASSOCIATED SNP INTERACTIONS WITH <i>TREM2</i> & STREM2 EXPRESSION ON ALZHEIMER’S DISEASE PATHOLOGY	88

Introduction	88
Methods	92
Results	96
Discussion	114
V. SUMMARY AND FUTURE DIRECTIONS	121
APPENDIX	134
Supplemental tables	134
Supplemental figures	143
REFERENCES	149

LIST OF TABLES

Table	Page
Table 2.1. Cohort characteristics ROS/MAP.....	33
Table 2.2. Main effects of <i>TREM2</i> on amyloid outcome measures	39
Table 2.3. Main effects of <i>TREM2</i> on amyloid outcome measures adjusting for microglial fraction	39
Table 2.4. Main effects of <i>TREM2</i> on tau outcome measures	41
Table 2.5. Main effects of <i>TREM2</i> on tau outcome measures adjusting for microglial fraction	41
Table 2.6. Main effects of <i>TREM2</i> on cerebrovascular outcome measures	42
Table 2.7. Main effects of <i>TREM2</i> on cerebrovascular outcome measures adjusting for microglial fraction	42
Table 2.8. <i>TREM2</i> x neuropathology interactions on activated microglial density in the caudate	43
Table 2.9. Stratified main effects of <i>TREM2</i> on global cognition	47
Table 3.1. VMAP cohort demographics	67
Table 3.2. Main effects of baseline CSF biomarkers on s <i>TREM2</i> measurement	71
Table 3.3. Competitive hierarchical linear regression results	73
Table 3.4. Main effects of baseline CSF s <i>TREM2</i> measurement on neuroimaging measures of cerebrovascular injury	79
Table 3.5. CSF s <i>TREM2</i> interactions on cerebrovascular neuroimaging measures ...	80
Table 4.1. s <i>TREM2</i> X presence of rs1582763 minor allele (A<G) interaction on CSF AD biomarkers	101
Table 4.2. s <i>TREM2</i> X presence of rs6591561 minor allele interaction on CSF AD biomarkers	103
Table 4.3. ADNI cohort demographics	105

Table 4.4. sTREM2 X presence of rs1582763 minor allele interaction on CSF AD biomarkers in ADNI.....	106
Table 4.5. sTREM2 X presence of rs6591561 minor allele interaction on CSF AD biomarkers in ADNI	108
Table 4.6. Main effects of <i>TREM2</i> mRNA on A β neuropathology	109
Table 4.7. MS4A SNP X <i>TREM2</i> mRNA interaction on A β neuropathology	110

LIST OF FIGURES

Figure	Page
Figure 2.1. ROS/MAP brain regions	34
Figure 2.2. <i>TREM2</i> expression across diagnosis	35
Figure 2.3. <i>TREM2</i> expression across <i>APOE</i> - ϵ 4 status	36
Figure 2.4. <i>TREM2</i> correlations with cell-type fraction	37
Figure 2.5. <i>TREM2</i> associations with amyloid	38
Figure 2.6. <i>TREM2</i> associations with tau	40
Figure 2.7. <i>TREM2</i> correlations with microglial density components	44
Figure 2.8. <i>TREM2</i> associations with cognition	46
Figure 2.9. <i>TREM2</i> X amyloid interactions on cognition	48
Figure 3.1. Main effects of AD CSF biomarkers on s <i>TREM2</i> levels	70
Figure 3.2. CSF/plasma albumin X <i>APOE</i> - ϵ 4 status on s <i>TREM2</i>	71
Figure 3.3. Main effects of AD CSF biomarkers on s <i>TREM2</i> ADNI replication	72
Figure 3.4. Tau interactions with diagnosis and <i>APOE</i> - ϵ 4 status on s <i>TREM2</i>	75
Figure 3.5. A β and BBB interactions with diagnosis and <i>APOE</i> - ϵ 4 status on s <i>TREM2</i>	76
Figure 4.1. CSF s <i>TREM2</i> characterization across rs1582763 genotype	98
Figure 4.2. CSF s <i>TREM2</i> characterization across rs6591561 genotype	99
Figure 4.3. rs1582763 X s <i>TREM2</i> interactions on A β peptides	102
Figure 4.4. rs1582763 X s <i>TREM2</i> interaction on CSF/plasma albumin	102
Figure 4.5. rs6591561 X s <i>TREM2</i> interactions on A β peptides	104
Figure 4.6. rs6591561 X s <i>TREM2</i> interaction on CSF/plasma albumin	104
Figure 4.7. rs1582763 X s <i>TREM2</i> interaction on A β peptides ADNI replication	107

Figure 4.8. rs6591561 X sTREM2 interactions on A β peptides in ADNI	108
Figure 4.9. <i>TREM2</i> X rs6591561 interaction on A β 1-38 in ROS/MAP	111
Figure 4.10. rs1582763 X sTREM2 interactions on cognition	113

LIST OF ABBREVIATIONS

Abbreviation

1. Alzheimer's disease (AD)
2. Triggering receptor expressed on myeloid cells-2 (TREM2)
3. Soluble triggering receptor expressed on myeloid cells-2 (sTREM2)
4. Apolipoprotein E epsilon 4 (APOE- ϵ 4)
5. Cerebrospinal fluid (CSF)
6. Amyloid beta (A β)
7. Neurofilament light chain protein (NfL)
8. Proportion of activated microglia (PAM)
9. Mild cognitive impairment (MCI)
10. Normal Cognition (NC)
11. Dorsolateral prefrontal cortex (dlPFC)
12. Posterior cingulate cortex (PCC)
13. Head of the caudate nucleus (CN)
14. Late-onset Alzheimer's disease (LOAD)
15. Vanderbilt Memory and Aging Project (VMAP)
16. Religious Orders Study (ROS)
17. Rush Memory and Aging Project (MAP)
18. Alzheimer's disease neuroimaging initiative (ADNI)
19. Magnetic resonance imaging (MRI)
20. Cerebrovascular disease (CVD)
21. Cerebral amyloid angiopathy (CAA)
22. Neurovascular unit (NVU)
23. Blood-brain barrier (BBB)
24. Membrane-spanning 4-domains, subfamily A (MS4A)
25. Genome-wide association study (GWAS)
26. Single reaction monitoring-based proteomics (SRM)

CHAPTER 1

INTRODUCTION

Alzheimer's Disease

Prevalence and Clinical Characterization

Alzheimer's disease (AD) is a progressive neurodegenerative disease and the most common form of dementia leading to cognitive decline and memory loss. AD was the seventh major cause of death in the U.S. in 2020 and 2021¹; furthermore, the only top ten illness without an effective treatment to slow or cure, as current therapies are not proven successful in preventing eventual decline in cognitive functioning².

Age is the number one risk factor for AD. More than one in nine seniors are affected with AD in the U.S. and this number is expected to grow rapidly as the population of individuals aged 65 and older is projected to expand by 30 million by 2050. While an estimated 6.2 million seniors are currently living with AD, this number is forecasted to double in less than 30 years¹. The lack of disease-modifying treatment and growing prevalence of AD have created a desperate need for novel disease targets and renewed drug discovery approaches.

AD is nosologically defined by two distinct biochemical lesions, both with prion-like activity; extracellular plaques of amyloid- β ($A\beta$) and intraneuronal tangles of hyperphosphorylated tau proteins in brain. Parenchymal $A\beta$ plaques are composed of mainly toxic $A\beta_{1-42}$ species (which aggregate faster and more frequently) and, to a lesser extent, shorter forms such as $A\beta_{1-40}$ and truncated $A\beta$ peptides with relatively

less or slower aggregation potential³. However, neuroimaging technologies such as magnetic resonance imaging (MRI), computerized tomography (CT) and positron emission tomography (PET) used to detect abnormal presence of these two pathologies are costly, and still in the adaptation period for widespread clinical use⁴. Alternatively, or in conjunction with neuroimaging, CSF biomarkers, genetic testing, neuropsychological exams, and more recently, blood biomarkers^{5, 6}, have supplemented the process and allow for the diagnoses of mild cognitive impairment due to AD (MCI due to AD), as well as probable AD. Gold standard AD diagnosis is confirmed through post-mortem autopsy identification of abnormal levels of A β and neurofibrillary tangles in brain.

Despite the colloquial characterization of Alzheimer's disease as a dementia, a substantial portion of the disease continuum exists in the absence of noticeable cognitive deficit before the onset of overt dementia. In fact, it is preceded by both asymptomatic preclinical and mild cognitive impairment (MCI) or "prodromal" periods which are known to span a remarkable time of up to 20+ and 10+ years, respectively⁷. MCI is diagnosed according to the National Institutes of Aging and the Alzheimer's Association (NIA-AA) as the absence of dementia and preserved independent functioning in daily life, paired with a concern about the onset of changes in cognitive functioning, and impairment of at least one cognitive domain, i.e., memory, outside the expected range of scoring given the individual's age and education. And MCI diagnosis paired with abnormal CSF biomarker levels of A β ₁₋₄₂ and tau indicate a diagnosis of MCI due to AD⁸. An estimated 32% of individuals diagnosed with MCI progress to Alzheimer's dementia within five years⁹. Therefore, older individuals with MCI represent a key population of interest for AD biomarker research. This characteristic temporal

progression of AD dementia provides a substantial window in which we may detect pathological changes before irreversible cognitive deficits occur. Identifying and characterizing novel biomarkers in these earlier stages of disease may lead to breakthroughs in the prevention of AD.

Concomitant Neuropathology

Despite AD being the most common cause of dementia, AD-associated A β plaques and neurofibrillary tangles are most frequently accompanied by brain changes linked to other causes of dementia. Examples of these include concomitant neurodegenerative disease pathologies including Lewy bodies or TDP-43, but also concomitant cerebrovascular disease (CVD) pathologies including cerebral infarcts, arteriolosclerosis, atherosclerosis, and cerebral amyloid angiopathy. One post-mortem study showed that over 80% of older individuals had mixed neuropathologies while only 3% had isolated AD neuropathology¹⁰. In fact, 50-84% of brains from persons who lived past 80 years of age show morphological substrates of both CVD and AD^{11, 12}. There is a substantial overlap between the presentation of AD and vascular dementia (VaD) and individuals may also be diagnosed with mixed vascular-Alzheimer's dementia (MVAD)¹³.

The interaction between AD and vascular pathology remains incompletely understood; most studies suggest synergistic effects of the two on cognitive decline^{12, 14-17}, however, the relative degree of permeance and relationship of cerebrovascular pathology to AD remains debated¹⁸⁻²⁵. As we age, particularly as our risk increases for several shared vascular and AD risk factors such as hypertension, sedentary lifestyle²⁶,

or diabetes, our vascular system attempts to compensate in terms of its ability to regulate cerebral blood flow²⁷. Healthy aging causes the vascular endothelium to increasingly bear damage from cerebrovascular and parenchymal pathology and subsequent production of reactive oxidative species and inflammatory mediators; processes which may become exaggerated, and eventually pathological, in AD^{27, 28}. Changes in brain endothelial cells may include deposition of collagen, hypertensive scarring or thickening of the vessel, and subsequent ischemia/hypoxia to the local cerebrum. Specifically, in AD, the pathological burden of both A β and neurofibrillary tangles is indeed known to lead to increases in both the biomechanical and metabolic dysfunction of cerebrovascular cells²⁷. For instance, A β -induced activation of perivascular macrophages leads to NADPH oxidase production of free radicals and subsequent endothelial Ca²⁺ dysregulation. A β is also thought to reduce blood flow and lower the threshold of susceptibility of blood vessels to ischemia. This is in line with the fact that individuals with AD diagnosis have an increased risk of stroke²⁹. Pathological A β accumulation is also known to lead to increases in intracellular filamentous tau pathology. The release of tau into brain interstitial fluid is believed to contribute to perivascular toxicity and thus changes in blood vessel structure and function³⁰. It is also known that tau contributes to mitochondrial dysfunction as well as the neuroinflammatory environment which regulates essential tight junctions and extracellular matrix components of the cerebrovascular system. In these manners, tau pathology is thought to contribute to cerebrovascular impairment in AD.

Supporting this idea of synergism, vascular pathology, in return, has been linked to an increased burden of AD pathology. In fact, vascular risk factors have been shown to

be some of the most important and modifiable in AD³¹. Some of these include hypertension, heart disease, and physical inactivity. Indeed, high blood pressure is known to promote atherosclerosis, lowering cerebral blood supply and oxygenation³², subsequently promoting infarction³³. And cerebrovascular dysfunction in general is thought to contribute to brain atrophy, and protein build-up of A β as well as tau³⁴ via mechanistic links between vasogenic regulation, inflammation, and oxidative stress³⁵⁻³⁷. For example, CAA compromises perivascular drainage of A β and may lead to arterial rupture, further decreasing the threshold for widespread dysregulation of immune and ROS signaling³⁸. Arterial occlusion in aged mice demonstrates profuse white matter damage accompanied by increases in hyperphosphorylation and biofluidic detection of tau³⁴. Additional work in hypertensive rats shows that cerebral hypoperfusion and ischemia promote tau hyperphosphorylation³⁹ suggesting cerebrovascular deficits may promote AD neuropathology independent of disease. Moreover, cerebrovascular dysfunction exists upstream of symptomology in individuals at risk for AD, including increased BBB permeability⁴⁰ and reduced cerebral blood flow⁴¹. This suggests an early contribution of cerebrovascular dysfunction to resultant AD cognitive decline.

The cerebrovascular environment is tightly regulated in concert by a network of diverse cell types, including neurons, glia, pericytes, endothelial, and smooth muscle cells, and this has been termed the neurovascular unit (NVU) which ultimately maintains cerebral blood flow and gates molecular transport across the blood-brain barrier (BBB). While the role of cerebrovascular pathology in AD has been increasingly recognized, underlying immune dysfunction, specifically glial activation, is similarly gaining focus. And glial activation has more recently become recognized as a cardinal feature of the

disease in addition to cerebrovascular pathology. With the advent of TSPO PET neuroimaging, clinical studies have revealed increases in microglial activation in both MCI- and AD-stage patients⁴². Glial activation and neuroinflammation are inextricably linked with AD pathophysiology. And indeed, in 1907, Alois Alzheimer first described morphological deviations in glial cells upon examination of AD patients' brains⁴³. Tissue-resident innate immune cells, namely microglia, are critical regulators of the inflammation status, as well as the health and longevity of neurons in the brain. They are programmed to respond to and help eliminate pathogenic stimuli, however, in the context AD these homeostatic functions may go awry and contribute to the neurodegenerative process⁴⁴. Undoubtedly, microglial dynamics throughout the complex disease process represent a vital window into the etiology of AD.

The variety and prevalence of these different combinations of concomitant brain neuropathology in AD are thought to represent one of the most difficult challenges to AD drug discovery. More specifically, this phenotypic heterogeneity presents a challenge to both target selection and recruitment phases of drug discovery with many individuals harboring vascular or other risk factors that may lead to drug contraindications.

Pharmacological Treatments

There are four FDA-approved pharmacological agents currently available for the treatment of cognitive symptoms associated with AD⁴. In addition, one more recently approved drug, aducanumab, was designed to slow the progression of AD by means of targeting and removing A β plaques in the brain – the first and only disease-modifying

treatment. However, it's accelerated approval process, which leaves the drug under continued phase 4 surveillance by manufacturer, Biogen, after passing a surrogate endpoint (plaque reduction), precludes the determination of robust efficacy in translating improvements in A β burden into cognitive benefits. Such post-approval studies are still needed to demonstrate clinical efficacy. And this has left quite a few questions and even controversies surrounding the approval process^{45, 46}.

While it may take several or more years to fully determine the impact of aducanumab on the treatment of individuals with AD, and while the cost is also projected to be very high for both patients and insurers⁴⁶, this leaves a continued need for other disease-modifying therapeutics, particularly those that may not rely on the direct targeting of A β as have a long line of previously failed anti-A β antibodies. In fact, over 60 clinical trials targeting amyloid have failed, including that of the recent DIAN trial⁴⁷ which includes participants with dominant mutations in the amyloidogenic pathway. Certainly, there are many theories as to why targeting and clearing amyloid along a causal pathway has not yet translated into desired success. This includes recruiting patient populations who have progressed too far along the disease process to reap a desired benefit, which is also a result of a failure to identify and recruit individuals at risk for AD before major pathological developments occur. But also, severe side effects such as amyloid-related imaging abnormalities (ARIA), lack of agreement on dosages, as well as which form of A β in the brain to target (i.e., monomers, oligomers, protofibrils, fibrils, or mature plaque) have all led to major hinderances in this area of drug development. Despite the complicated history of A β -targeting drugs, there is a continued focus on these drugs. For example, early data from Eli Lilly shows

donanemab may have some degree of cognitive benefit⁴⁸. Unlike other monoclonal anti-A β antibodies, donanemab recognizes a pyroglutamate A β form (A β p3-42) which is aggregated in established plaques. Therefore, the potential of the drug to clear existing plaque as opposed to solely preventing the growth of new plaques may have contributed to the retention of amyloid clearance after one year in participants from the TRIALBLAZER-ALZ trial. This hope is balanced with caution as previous plaque-targeting antibodies led to brain microhemorrhaging⁴⁹. Currently, a phase 3 head-to-head comparison of aducanumab and donanemab in terms of their relative efficacy to clear plaque is underway (<https://clinicaltrials.gov/ct2/show/NCT05108922>).

In light of growing evidence of the roles of the neuroimmune system in AD, immune-regulating drugs have been increasingly prevalent in the AD drug development pipeline. Many of these are thought to act upstream of AD neuropathology, including biologics as well as small molecules⁵⁰. This includes an ERK inhibitor, NE3107, in phase 3 trials that selectively inhibits neuroinflammation with insulin-sensitizing properties. Relevant to the focus of this dissertation, Alector and AbbVie have partnered to develop AL002, a humanized monoclonal IgG1 antibody which agonizes the microglial receptor TREM2 (discussed at length below) leading to microglial proliferation and compaction and clearance of A β plaque in 5XFAD as well as APP/PS1 mice after 72 hours. The antibody is well tolerated, and a phase 2 (INVOKE-2) trial is currently running through 2023 enrolling 265 individuals with early AD⁵¹. The current trend in diversifying AD drug targets beyond amyloid and tau may lead to critical advancements in our understanding of the pathogenic features of underlying immune dysregulation in AD while also offering earlier intervention strategies.

Moving away from efforts at disease modification, donepezil, galantamine, rivastigmine, and memantine are currently widely used and prescribed for the alleviation of AD cognitive symptoms, improving memory and thinking in people suffering from AD. The first three drugs are acetylcholinesterase inhibitors which act to increase the amount of acetylcholine available in the synapse. Memantine, however is a low-affinity, uncompetitive, NMDA receptor inhibitor which improves nerve cell communication by reducing excess stimulation which arises from excitotoxic glutamate release⁴. Finally, there is a single drug which is used and approved for sleep abnormality and insomnia in individuals living with AD, suvorexant, which works by antagonizing both the OX1R and OX2R orexin receptors⁵².

In summary, although we have a handful of drugs which are widely used to treat AD symptoms, we are left with a desperate need for a pharmacological prevention of AD as well as a deeper understanding of the etiological causes of AD dementia and cognitive decline. Particularly, there has been increased focus on immune- and cerebrovascular-interplay in AD pathophysiology and the identification and characterization of early-detection biomarkers and immune targets.

TREM2 and sTREM2 Overview

Biological Functions

Triggering Receptor Expressed on Myeloid Cells-2 (TREM2) is a type 1 transmembrane member of the TREM family and immunoglobulin superfamily of receptors, with a molecular weight dependent on the presence and extent of post-

translational modification (~30-50kDa)⁵³. In brain, TREM2 is preferentially expressed on microglia, and to a much lesser degree, infiltrating monocytes, and macrophages^{54, 55}. Of note, is the increased expression of TREM2 on circulating monocytes observed in AD patients as compared to controls⁵⁶ and of individuals converting from MCI to AD as compared to MCI nonconverters⁵⁷. Therefore, it's conserved myeloid-type expression hints at roles in both phagocytic immune regulation as well as peripheral-central nervous system communication. TREM2 and its accompanying signaling machinery are, in the broadest sense, sensors of the tissue microenvironment. As such, TREM2's large extracellular domain harbors a basic patch which aids in the binding of a diversity of anionic ligands through pattern recognition such as bacterial surfaces, DNA, phospholipids, and lipoprotein products^{58, 59}. This includes APOE isoforms and A β molecules. Subsequently, TREM2 happens to exist at the intersections of immune homeostasis, specifically the sensing of tissue degeneration, and plaque accumulation, as well as APOE signaling.

Beyond the extracellular domain, TREM2 contains a single transmembrane helix and a relatively short cytoplasmic tail. Therefore, TREM2 is thought to rely on adaptor proteins for signal transduction. For example, DNAX activating protein of 12 kDa (DAP12 also known as TYROBP) acts as a co-receptor, interacting with the transmembrane region of TREM2, and upon ligand interaction with TREM2, DAP-12 is phosphorylated on tyrosine residues within an immunoreceptor tyrosine-based activation motif (ITAM) recruiting additional signal transduction components such as the activation of spleen tyrosine kinase (Syk) and PI3K (for DAP10)⁵⁸. Transcriptional

regulation downstream of TREM2 activation is associated with microglial survival, mobility, proliferation, phagocytosis, and inflammation regulation^{60, 61}.

Therefore, in a healthy aging individual, TREM2 is designed to be efficient at a number of important microglial regulatory functions including maintaining the balance of pro- and anti-inflammatory mediators, sustaining a healthy density of microglial cells which is known to decrease as we age⁶², and promoting the activation of brain tissue repair pathways⁶³ and the health of neurons and additional cell types, especially in the face of white matter insult or neurodegeneration^{64, 65}. For all of the reasons above, it is no wonder that TREM2 dysfunction is found at the crossroads of numerous genetic and molecular risk factors for AD.

A soluble form of TREM2 (sTREM2) was first discovered in human CSF and serum in 2008 by authors Piccio et al⁶⁶. The molecular weight of sTREM2 was determined to have a wide range typical of its parent form due to post-translational glycosylation (24-40 kDa). Production of sTREM2 was found to occur mainly by ectodomain shedding and by alternative splicing to a lesser extent (20-25%)⁶⁷. Membrane-bound TREM2 may be cleaved by several a disintegrin and metalloproteases (ADAM10/ADAM17) between histidine 157 and serine 158 releasing sTREM2 into the extracellular space^{68, 69}. There is a sequential proteolytic processing of TREM2 where this generation of sTREM2 initiates and reveals the C-terminal fragment which is then cut by γ -secretase aiding in the removal of remaining fragment from the membrane⁷⁰. However, the biological impacts of sTREM2 shedding, including constitutive or disease functions remain incompletely understood.

In fact, it wasn't until 2015 that a functional role for sTREM2 had been outlined in vitro, driving bone marrow derived macrophage (BMDM) expansion and survival in cells from both WT and Trem2^{-/-} mice⁷¹. These same authors found that IL-13 induced a robust increase in sTREM2 levels released from BMDMs which was attenuated in cells from Dap12^{-/-} mice, suggesting DAP12 and IL-13 contributed to sTREM2 production and subsequent sTREM2-dependent functions⁷¹. Despite this finding, receptor shedding may be initiated by various biological mechanisms and other potential regulators of sTREM2 production may remain undiscovered, particularly in disease contexts. Because TREM2 signaling function at the myeloid membrane is critical for numerous homeostatic functions, its removal and subsequent generation of sTREM2 may provide negative feedback for such cellular activity^{72, 73}. However, the overall impact of sTREM2 generation on TREM2 receptor activity is still largely unknown. Using a recombinant sTREM2-Fc protein injected into mouse hippocampi, sTREM2 overexpression was found to significantly increase inflammatory cytokine expression and microglial activation in WT and Trem2^{-/-} mice demonstrating for the first time in vivo biological activity⁷⁴.

Roles in Neurodegenerative Disease

TREM2 receptor has become established as a major central and peripheral nervous system immune signaling hub, sensitive to an array of chronic and acute pathological stimuli. Mutations modulating its expression and/or function have been linked to the risk of several neurodegenerative disorders. While *APOE-ε4* is the largest

single genetic risk factor for late-onset AD (LOAD) with two alleles associated with about a 12-fold risk⁷⁵, the R47H *TREM2* mutation confers about a 3-5-fold risk^{76, 77}, similar to that of a single *APOE-ε4* copy. *TREM2* and DAP12 (*TYROBP*) homozygous mutations are known to cause Nasu-Hakola disease characterized by bone cysts, sclerosing leukoencephalopathy, and presenile dementia⁷⁸⁻⁸⁰. *TREM2* mutations have also been associated with frontotemporal dementia^{76, 81} and Parkinson's disease⁸². Additional heterozygous mutations, particularly in the ligand binding domain of *TREM2* have been associated with increased AD risk. Similar to R47H, this includes another loss of function mutation, R62H, both of which are known to impair *TREM2*-mediated microglial activation and decrease microglial coverage of Aβ plaques. Others are also reported as hypofunctional, affecting expression or folding such as glutamine-33-stop (Q33X) and T66M^{61, 83}. These findings help to understand the importance of functional *TREM2* on the cell surface membrane and implications of *TREM2* dysfunction in the context of Aβ deposition.

Similar to full-length *TREM2*, s*TREM2* signaling was recently shown to regulate microglial clearance of Aβ plaque. Specifically, the pro-inflammatory effect on microglia via s*TREM2* binding to an unknown receptor was shown to ameliorate Aβ pathology in a mouse model of AD by promoting phagocytosis⁸⁴. Therefore, s*TREM2* and *TREM2* both have strong links to AD pathophysiology via their biological roles in innate immune response to pathological deposition of Aβ, however, *TREM2*/s*TREM2* expression in relation to tau pathology and more generally, neurodegeneration in AD remains incompletely observed and obscured due to complex immune dynamics throughout the disease process.

For example, one hypothesis is that early increases in sTREM2 and TREM2 expression seem to be protective in the initial stages of AD, while chronic (or sequential) activation of microglial populations may lead to the dysregulation of this pathway, inflammatory detriment to surrounding neurons contributing to neurodegeneration, and eventually, the metabolic failure of microglia themselves in later stages of AD. This may partially explain contrasting reports of TREM2 function in relation to tau in the preclinical animal model literature⁸⁵⁻⁸⁸ as microglial activation has been proposed to occur both before and after the detection of increased tau markers⁸⁹. And while we know that increases in CSF sTREM2 are robustly correlated with increases in CSF tau biomarkers, potentially marking a tipping point between protective- vs. disease-associated microglial signaling at the onset of neurodegeneration, comprehensive studies of TREM2 gene expression associations with AD neuropathology in humans remain limited in number and size of the cohorts examined^{90, 91}.

An important development in the potential causal roles of the TREM2 pathway in AD came when Deming et. al. searched for genomic variants associated with sTREM2 levels in CSF⁹². Utilizing data from 813 individuals in the Alzheimer's Disease Neuroimaging Initiative and additional replications cohorts (N=580), Deming and co-authors found two common SNPs in the MS4A gene cluster previously linked to the regulation of late-onset AD. One of the variants, rs1582763, is an intergenic variant associated with slower onset and lowered risk of AD, as well as higher CSF sTREM2 concentration. This variant was also shown to promote expression of MS4A4A and MS4A6A (from human eQTL and cell culture studies)⁹². The other variant, rs659156, is a missense variant in the MS4A4A gene which increases AD risk, accelerates onset,

and reduces sTREM2 expression in CSF. Previous GWAS established that variants in this locus modulate AD risk by about 10%^{93, 94}. These SNPs regulate expression of the MS4A protein members themselves and are thought to also regulate TREM2 processing via (at least in part) co-localization and thus a functional interaction. Indeed, authors found that MS4A4A co-localized with TREM2 in the cytoplasm and membrane of human macrophages and promoted sTREM2 expression^{92, 95}. It is possible these MS4A proteins may become viable AD therapeutics themselves, however, this will require digging deeper into the relationship between TREM2 and MS4A proteins in order to reveal immunogenetic contributions to LOAD progression, specifically the interactions of these previously unconnected risk loci on unknown biological pathways underlying the pathological progression of AD.

Rationale and Aims

TREM2 encodes a myeloid transmembrane receptor with immune sensing function⁹⁶ and is therefore an ideal candidate gene to further explore the role of the innate immune system in AD. TREM2 deficiency has been linked to inflammation, impaired microgliosis and amyloidosis in AD models^{60, 97, 98}. Similarly, it is associated with other models of neurodegenerative and inflammatory disease^{63, 82, 99-101}. This non-specific innate immune response likely has direct effects on AD pathology and indirect effects on the clinical manifestation of disease through concomitant pathways of brain injury. Yet, TREM2 associations with concomitant pathways of injury beyond amyloidosis have not been well characterized.

Differential expression of both TREM2 and its soluble fragment have been linked to AD risk in both animal models and humans. However, studies assessing TREM2 expression in AD have been largely focused on associations between TREM2 levels and parenchymal A β burden^{96, 102-105}. Whereas possible associations between TREM2 levels and other concomitant neuropathology, particularly between cerebrovascular health outcomes, remains largely unexplored. This is despite several lines of preclinical evidence linking TREM2 to mechanisms of NVU integrity. TREM2 signaling is known to induce release of NVU modulating mediators such as pro- and anti-inflammatory cytokines, reactive oxygen species, and complement factors^{62, 106, 107}. Beyond its fundamental biological outputs, evidence links TREM2 to several specific mechanisms of NVU integrity. For example, TREM2 localizes near blood vessels in the human brain¹⁰⁸ and has been implicated in a number of cellular processes that drive CVD including cell-cell communication at the NVU¹⁰⁹, blood-brain barrier permeability¹¹⁰, leukocyte trafficking¹¹¹, hypoxia response⁶³, and foam cell formation^{96, 107}. Despite evidence of these biological processes, there has not yet been a comprehensive assessment of TREM2 associations with autopsy measures of cerebrovascular disease and concomitant AD neuropathology (**Aim 1**).

We hypothesize that myeloid TREM2 is important for homeostatic neuroimmune signaling and by these means links immune response to hemodynamic and structural cerebrovascular alterations underlying AD. The results of this aim will help clarify the therapeutic potential of targeting TREM2 pathways for protection against inflammatory-mediated cerebrovascular deficits in aging and AD and may also identify novel expression associations between TREM2 and cerebrovascular pathology.

Furthermore, there is an increased effort to properly identify and interpret efficacious and early biomarkers of immune dysregulation in AD. However, major methodological limitations of in vivo assessments of CNS immune dysregulation in humans have precluded a definitive collection of clinically useful inflammatory biomarkers. And a more granular understanding of underlying immune changes as indicated by specific biomarkers along the spectrum of disease is needed. While it is understood that fluctuations in CSF levels of sTREM2 represent microglial dynamics underlying disease, the exact nature and consequence of sTREM2 elevation in AD is unknown. And sTREM2's relationship to AD pathophysiology beyond microglial activation and parenchymal A β burden remains a largely unexplored area of research. Therefore, given the recent implications of sTREM2 function in the regulation of AD neuropathology as well as its dynamic expression during AD progression, there is an intense need to comprehensively characterize CSF sTREM2's potential as an early AD biomarker. This includes a need to better understand potential biological relationships of sTREM2 and concomitant inflammatory and neuropathological mediators of disease progression including those of cerebrovascular injury (**Aim 2**). Conclusions from this aim contribute to CSF sTREM2's characterization as a complementary biomarker in aging and AD as well as guiding ongoing efforts towards microglial and TREM2-based therapeutics for AD.

After establishing the contribution of various AD inflammatory markers to variance in sTREM2 levels in CSF, it is explored whether or not known genetic regulators of CSF sTREM2 levels modify these biomarkers associations (**Aim 3**). Analysis of a pair of single nucleotide polymorphisms (SNPs) within the membrane-spanning 4-domains

subfamily A (MS4A) gene cluster with opposing functional annotations including association with AD risk and onset, as well as CSF sTREM2 levels (namely, rs1582763 and rs6591561), and their potential interaction with sTREM2 on other biomarker concentrations attempts to answer the question of whether or not genetic regulation of sTREM2 levels by MS4A mutations is included in a causal pathway leading to subsequent modulation of neuropathology. These final analyses contribute a more nuanced understanding of the relationship between this additional AD risk locus and CSF sTREM2 as well as the impact of its genetic regulation on sTREM2 expression associations in aging and disease.

The field has largely focused on amyloid clearance as the primary mechanism underlying innate immune associations in AD, and TREM2 has certainly been implicated in amyloid plaque clearance. However, emerging evidence suggests the innate immune response is also critical for the propagation of tau downstream of amyloidosis and cerebrovascular injury independent of amyloidosis. The over-arching goal of the analyses herein is to elucidate the role of the innate immune system in the pathophysiology of AD, focusing on concomitant pathways of injury beyond parenchymal amyloid plaque deposition associated with TREM2 and sTREM2 expression. The central hypothesis is that TREM2 dysfunction contributes to an inflammatory environment permissive of the propagation of diverse neuropathology. The scope of analyses within this dissertation uses cutting-edge bioinformatic methods, deep transcriptomic and proteomic data from human biospecimen, and detailed phenotypic data from longitudinal cohort studies to comprehensively characterize TREM2 expression associations detailed in the following aims:

Aim 1. Autopsy Approach: To determine whether *TREM2* mRNA transcript is associated with substrates of **(A)** cerebrovascular disease and **(B)** concomitant classical AD neuropathology, A β and tau, over the course of normal aging and AD. Leveraging Religious Orders Study and Rush Memory and Aging Project (ROS/MAP) RNA sequencing data from human brain and linear regression techniques, we comprehensively assessed the association between *TREM2* expression and autopsy measures of cerebrovascular disease including arteriolosclerosis, atherosclerosis, microinfarcts, macroinfarcts, and cerebral amyloid angiopathy. Additional outcome measures include immunohistochemical quantification of hyperphosphorylated tau, A β ₁₋₄₂, and silver staining measurements of neurofibrillary tangles, and A β neuritic plaque.

Aim 2. Biomarker Approach: To determine whether CSF sTREM2 expression is associated with in vivo neuroimaging markers of vascular hemodynamics and small vessel disease, and or inflammatory biomarkers of AD neuropathology in CSF. Thereby to comprehensively understand underlying biological correlates of elevated sTREM2 in AD and relevant inflammatory pathways during an early window of AD development. CSF proteomic data from Vanderbilt Memory and Aging (VMAP) participants was used to test for sTREM2 associations with regional cerebral blood flow, vascular reactivity, and white matter hyperintensities as well as deconvolve associations with other diverse inflammatory biomarkers in CSF (A β ₁₋₄₂, A β _{x-42}, A β _{x-40}, total tau, phosphorylated tau, and neurofilament light) and BBB integrity (CSF/plasma albumin ratio). Linear

regression models were utilized in R examining sTREM2 as an outcome variable to quantify its relative components.

Aim 3. MS4A SNP Interactions with sTREM2/TREM2 on Concomitant

Neuropathology: To assess whether MS4A AD-associated SNPs (rs1582763 and rs6591561) interact with CSF sTREM2 or *TREM2* mRNA expression to modify established main effects on concomitant neuropathology in previous aims, thereby offering valuable insight into possible biological pathways through which MS4A (MS4A4A/MS4A6A) and TREM2 proteins regulate AD risk and progression of diverse neuropathology.

CHAPTER 2

EVALUATION OF *TREM2* GENE EXPRESSION ASSOCIATIONS WITH ALZHEIMER'S DISEASE PATHOLOGY AT AUTOPSY

Introduction

The discovery of increased AD risk in carriers of rare *TREM2* mutations from large GWAS studies^{76, 77} surely jump-started the interest in characterizing the potential roles of *TREM2* protein, and more generally innate immune function, in the progression of disease. Since then, dysregulation of *TREM2* expression has also been documented in neurodegenerative disease, including AD. And *TREM2* signaling has indeed been tied to mechanisms of phenotypic switching of microglia, regulation of neuropathology, and cognition^{60, 97, 98}. However, there has yet to be a comprehensive evaluation of regional brain *TREM2* gene expression association with all three of these critical components of AD. Therefore, the following chapter seeks to expand upon our understanding of how post-mortem *TREM2* mRNA levels in brain relate to disease status in attempt to identify novel regional, neuropathological, and retrospective cognitive functioning associations.

In addition to heterozygous mutation associations with increased LOAD risk, canonical *TREM2* dysregulation is also found in the AD brain. *TREM2* mRNA and protein expression are upregulated in severe AD frontal cortex versus aged control. Furthermore, mRNA expression of *TREM2* has been found to track with both protein levels in the cortex as well as with clinical progression of the disease¹¹². However, *TREM2* expression changes in AD may be regionally-dependent as contrasting reports

of TREM2 expression changes in the hippocampus – another region vulnerable early-on to the accumulation of AD-related pathology -- yielded differential findings depending on the study and form of TREM2 measured, including a glycosylated protein of 33-50kD¹¹²⁻¹¹⁴. A lack of differential expression changes in the frontal cortex was found in individuals with normal cognition and mild AD, which is consistent with the leading hypothesis that upregulation of TREM2 expression is a late event which reflects a compensatory function of this pathway with respect to the accumulation of disease pathology¹¹².

Additionally, from transgenic mouse models of AD several important findings were gleaned concerning expression changes of TREM2 with respect to disease pathology. For example, it was learned that TREM2 protein is enriched in brain regions associated with high levels of amyloid- β accumulation in mice similarly to humans¹¹⁵. Specifically, TREM2 was highly expressed in microglial in temporal cortex surrounding amyloid plaque. This observation supports the most characterized role of TREM2 in microglia regulating pathological plaque development^{51, 61, 74, 84}. It was since determined that plaque-associated microglia upregulate levels of TREM2 and accompanying signaling adapter DAP12, indicating an essential role of this pathway in response to amyloid- β plaque deposition in the brain parenchyma¹¹⁵.

Accompanying this compensatory response of TREM2 protein machinery to plaque development is a transcriptional and phenotypic transition from a maintenance to activated microglial cell. The activated proportion of microglia has been found to be elevated in AD compared to age-matched non-AD subjects^{116, 117}. This increase in glial activation in disease included a reduction of microglial cell arborization consistent with

activation and in the absence of a reduction in total microglial cell density ¹¹⁸.

Furthermore, the proportion of activated microglia in cortical tissue at autopsy has been tied most closely in regression models to increased A β neuropathology as well as positive levels of tau neuropathology, albeit, to a lesser extent ¹¹⁶ using this same ROS/MAP cohort. In the same study, authors found the proportion of activated microglia (PAM) in subcortical regions did not relate to classical AD neuropathology or cognitive decline such as in cortical regions. We wonder, given these previous findings, whether *TREM2* transcription may be important to the proportion of activated microglia in post-mortem tissue and whether or not this may be specific to interactions of microglia with classical AD neuropathology in the cortex. Additionally, whether PAM corresponds to *TREM2* levels in subcortical areas and if this may reflect age- or disease-related cerebrovascular changes as these areas contain smaller blood vessels residing in deeper brain areas which are particularly vulnerable to injury such as inflammation, arteriosclerosis, and ischemic lesions ¹¹⁹.

The broad expression of *TREM2* in human tissues as well as its many immunological functions, including but not limited to those of microglial cells, suggests *TREM2* expression may be associated with post-mortem amyloid- β levels as well as other concomitant pathology related to underlying immune dysregulation. For example, loss of *TREM2* disrupted the response of endothelial cell gene networks to vascular endothelial growth factor, suggesting an impairment in cell-cell networks related to vascular homeostasis known to dysfunction in small vessel disease ^{109, 120}. Strong evidence links chronic inflammation to the development of cardiovascular disease (including atherosclerosis) and dementia. Specifically, *TREM2* variant rs6918289 in

heart has been associated with increased risk of atherosclerosis ¹²¹. Effects of immune activation on blood vessels, such as proinflammatory cytokine, complement or reactive oxygen species release by myeloid cells (microglia, dendritic cells and monocytes), may manifest as localized infarcts, diffuse white matter hyperintensities (WHI) or microbleeds, increasing blood brain barrier (BBB) permeability in old age and disease ¹²². This oxidative and inflammatory stress may affect blood vessels themselves and surrounding NVU components that aid in maintaining their structural and metabolic integrity. Several studies link TREM2 to these critical NVU mechanisms ^{63, 96, 107, 109, 110, 120}.

Despite current progress in the literature associating genetic and/or expression- and function-related associations of TREM2 dysregulation in AD, the exact roles of its dynamic expression changes throughout the course of the disease remain elusive. The present chapter investigates the relationship between *TREM2* bulk transcript with clinical AD, cognitive functioning, and AD-related neuropathology, including measures of cerebrovascular pathology and immunohistochemical quantification of microglial density and activation phenotypes. Results from gene expression analyses in a large dorsolateral prefrontal cortex discovery cohort (dlPFC) will be shared along with corresponding results from independently sampled regions; the posterior cingulate cortex (PCC) and the head of the caudate nucleus (CN). Therefore, the following results help clarify the neuropathological correlates of *TREM2* levels across the brain. We hypothesized that higher cortical expression of *TREM2* mRNA at autopsy will correspond to increases in AD-related pathology including microglial reactivity, cerebrovascular injury, as well as worse cognitive performance.

Methods

Participants

The Religious Orders Study (ROS) and the Rush Memory and Aging Project (MAP), or ROS/MAP, were leveraged using autopsy and cognitive data to conduct this study. Data collection began in 1994 and 1997, respectively, contributing to rich longitudinal clinical-pathologic information concerning risk factors in aging and AD. ROS enrolls religious clergy members from across the United States while MAP enrolls lay persons from northeastern regions of Illinois. Participants are aged 65 years and older, free of dementia at baseline, and are predominantly of European ancestry (see cohort demographics in **Table 2.1**). Importantly, participants have all consented to organ donation. The Rush University Medical Center gave Institutional Review Board approval and guidelines for data sharing within Institutional Review Board protocols. Additionally, analyses were approved by the Vanderbilt University Medical Center IRB. Participant data collection is attributed to collaborators at Rush University with special thanks to Drs. David Bennett, Julie Schneider, Lisa Barnes, Bryan James, and Greg Klein.

Genotyping

Whole blood lymphocytes or frozen brain tissue was used to extract DNA and previously defined quality control (QC) measures were employed¹²³. *APOE* genotyping was performed by investigators blinded to cohort data at Polymorphic DNA

Technologies. The *APOE* gene was sequenced defining differential isoforms of *APOE*- ϵ 2, *APOE*- ϵ 3, and *APOE*- ϵ 4 by codons 112 and 158 on exon 4.

Neuropsychological Composites

Neuropsychological testing details are previously published¹²⁴⁻¹²⁶. There are 19 neuropsychological tests across five cognitive domains (episodic, semantic, and working memory, visuospatial ability/perceptual orientation, and perceptual speed) used in the calculation of a composite representing the global cognition variable in ROS/MAP. This variable is meant to represent a participant's overall cognitive functioning. Raw scores from each test were converted to z-scores using the mean and standard deviation. The final composite score is calculated by converting each test within each domain to a z-score and averaging all z-scores.

Cognitive Diagnosis

A clinical diagnosis of cognitive status was made at each participant visit based on the combination of computerized cognitive tests scores, clinical judgement by a neuropsychologist, and diagnostic classification by a clinician (neurologist, geriatrician, or geriatric nurse practitioner) as previously described¹²⁴⁻¹²⁶. Clinical diagnosis of AD or other dementia followed criteria suggested by the joint working group of the National Institute of Neurological and Communicative Disorders and Stroke and the Alzheimer's Disease and Related Disorders Association (NINCDS/ADRDA). Diagnosis of mild cognitive impairment (MCI) is rendered for persons who are judged to have cognitive

impairment by the neuropsychologist but are classified as not meeting criteria for dementia by the clinician.

Neuropathological Measures

Core AD Pathology

All neuropathological marker quantifications have been previously described¹²⁴⁻¹²⁶. Briefly, quantification of neuritic plaques and neurofibrillary tangles was based on silver staining of five brain regions (midfrontal cortex, midtemporal cortex, inferior parietal cortex, entorhinal cortex, and hippocampus) averaged to obtain a summary score of the overall burden. In addition, immunohistochemistry was performed to calculate semi-quantitative scores for both amyloid- β and phospho-tau abundance in the cortex using antibodies specific to A β ₁₋₄₂ and abnormally phosphorylated tau, AT8 epitope, respectively, based off the average of eight regions.

Cerebrovascular Pathology

Rating of large vessel cerebral atherosclerosis was performed by visual inspection of the vertebral, basilar, posterior cerebral, middle cerebral, and anterior cerebral arteries of the circle of Willis, as well as their proximal branches and graded based on severity including the number of arteries involved and extent of artery involvement (0=no pathology, 4=severe pathology). Additionally, given visual identification of occlusion, an artery was bisected to assess the degree of occlusion which would then

be incorporated into the final score. Arteriolosclerosis severity was classified by a semi-quantitative grading scale (0=no pathology, 3=severe pathology) after characterization of histologic changes in the vascular lumen. These changes included but were not limited to the following histological changes in small vessels: intimal deterioration, smooth muscle degeneration, and fibrohyalinotic thickening of arterioles with consequent narrowing of the vascular lumen. Macro infarcts were visualized by the naked eye on fixed slabs and dissected for confirmation. Micro infarcts were examined on 6 μ m paraffin-embedded sections, stained with hematoxylin/eosin. Gross and micro infarcts were categorized as present (1) or absent (0) based upon visual inspection in nine brain regions (midfrontal, middle temporal, entorhinal, hippocampal, inferior parietal and anterior cingulate cortices, anterior basal ganglia, midbrain, and thalamus). A semi-quantitative score for cerebral amyloid angiopathy (CAA) was measured by amyloid- β immunostaining in neocortical regions (midfrontal, midtemporal, angular, and calcarine cortices), and was scored on a scale from 0 – 4 (0=no pathology, 4=severe pathology). For each brain region a meningeal and parenchymal vessel score was obtained, and the maximum of these was then used in each case. Final scores were averaged across regions.

Autopsy Measures of *TREM2* mRNA Expression

A standard post-mortem biological specimen protocol was utilized across centers where autopsies were performed and has been previously described¹²⁴. RNA extraction from individual brain regions was performed using a Qiagen miRNeasy mini kit and a RNase free DNase Set for quantification on a Nanodrop. An Agilent Bioanalyzer

assessed quality including integrity and purity. A RIN score greater than five was used as inclusion criteria for next generation RNA sequencing in bulk.

Sequencing was carried-out in multiple phases; phase one included initial dorsolateral prefrontal cortex (dlPFC) while phase two added additional dlPFC samples as well as samples from the posterior cingulate cortex (PCC) and head of the caudate nucleus (CN). Phase three ran additional participant samples from the dlPFC. Detailed information on RNA processing and sequencing can be found on synapse: <https://www.synapse.org/#!/Synapse:syn3388564>. In summary, phase one utilized poly-A selection and strand-specific dUTP library preparation and Illumina HiSeq with 101bp paired-end reads achieving a coverage of 150 million reads of the first 12 reference samples. The deep sequencing of these 12 reference samples included two males and two females of non-impaired, mild cognitive impaired, and Alzheimer's disease cases. The remaining samples underwent sequencing with a coverage of 50 million reads. Phase two, library preparation utilized KAPA Stranded RNA-Seq Kit with RiboErase (kapabiosystems) with which ribosomal depletion and fragmentation was performed. Sequencing of this phase was performed on an Illumina NovaSeq6000 sequence using 2x100bp cycles targeting 30 million reads per sample. Phase three, RNA was extracted with a Chemagic RNA tissue kit (Perkin Elmer, CMG-1212) using an Chemagic 360 instrument and ribosomal RNA was depleted using RiboGold (Illumina, 20020599). Sequencing of phase three was performed on a NovaSeq 6000 (Illumina) with 40-50M 2x150bp paired-end reads.

Data processing and QC of RNA sequencing runs was performed by our Computational Neurogenomics Team (CNT) using our own automated pipeline. This

included the combining of the three dIPFC phases (N=631, N=278, and N=104, 1-3 respectively) as well as the other brain regions (PCC; N=571 and CN; N=745). All samples with a RIN score below 4 and/or a post-mortem interval greater than 24 hours were removed. Read counts per million (CPM) values were quantile normalized to adjust for global variability between samples using the R package, *Cqn*, controlling for GC-content and gene length, and then used to align to the hg38 reference genome using STAR with the R package, *ComBat*, to adjust for batch effects. In addition, principal component outliers outside five standard deviations as well as genes missing covariates of interest or those necessary for normalization were removed.

Cellular Fraction Data

A deconvolution technique was employed to obtain cellular fraction data on a subset of ROS/MAP participants ¹²⁷. This method consisted of a subset of bulk RNA samples from the dIPFC (Brodmann area 10) also having single-nucleus data (N= 48 individuals and 80,660 single-nucleus transcriptomes) which was used to find the best predictors of each cellular component (i.e., excitatory neuron, microglia, oligodendrocyte, etc.) using all of the genes in the RNAseq data to build models with the most optimized set of genes. The isolation and extraction of nuclei from frozen tissue has been described previously ¹²⁸. Briefly, analysis of single-nucleus data (snRNA-seq) followed high-throughput droplet technology and massively parallel sequencing following the DroNc-seq protocol (Habib, Avraham-Davidi, Basu et al. 2017), with modification for the 10x Genomics Chromium platform. Gene counts were obtained by alignment of reads to the hg38 reference genome (GRCh38.p5) using CellRanger

software. Unspliced nuclear transcripts were accounted for by counting reads mapped to pre-mRNA. Each individual library was quantified for pre-mRNA and then aggregated to equalize read depth between libraries to generate a gene count matrix.

Quality control for cell inclusion has been previously described in detail ¹²⁷. The final dataset consisted of 17,926 genes in 75,060 nuclei. This snRNA-seq data was utilized in a regression-based approach for the generation of a reference expression profile and decomposition of bulk RNA sequencing data yielding cellular fraction estimates for each sample across multiple cell types (microglia, astrocytes, inhibitory neurons, excitatory neurons, oligodendrocytes, oligodendrocyte progenitors, and endothelial or pericyte cells). These measurements are attributed to collaborators from Columbia University with acknowledgement to Drs. Vilas Menon and Phil De Jager for their work.

Microglial Density Data

Microglial density measurements were obtained from brain samples using immunohistochemistry performed by an Automated Leica Bond immunostainer (Leica Microsystems Inc., Bannockburn IL) and anti-human HLA-DP, DQ, and DR antibodies (clone CR3/43; DakoCytomation, Carpinteria CA; 1:100). A blinded investigator sampled 4% of an ROI with fixed magnification (400x) marking microglia counts and uniquely identifying their phenotypic activation stage. Stage 1 being least or not activated and having thin, ramified processes. Stage 2 being activated with a rounded cell body >14um in size with thickened processes. Stage 3 being activated with criteria

as in stage 2 but in addition having a macrophage appearance. Total counts for different stages were counted separately from adjacent blocks of tissue (0.5-1cm apart) then summed, divided by the area of the sample, and multiplied by 10^6 yielding a composite average density.

Statistical Analyses

Statistical analyses were performed in R v3.6.1 using R Studio IDE (<https://www.rstudio.com/>). To evaluate the data, a multiple linear regression model (for cross-sectional cognition and AD-related pathology outcomes) as well as a linear mixed-effects model (for longitudinal cognition outcomes) were used. For binomial and multinomial cerebrovascular outcome variables, generalized linear and proportional odds models were substituted, respectively. Linear regression models covaried for age at death, sex, post-mortem interval, education, and the interval from the last visit to death. Models assessed *TREM2* gene expression on the following AD clinical and neuropathological outcome measures: cross-sectional and longitudinal global cognition, amyloid- β (IHC), p-tau (IHC), silver staining of neuritic plaques and neurofibrillary tangles, micro and macro cerebral infarcts, CAA, arteriolosclerosis, and atherosclerosis. IHC and silver staining measurements of AD pathology were square root transformed to better approximate a normal distribution.

Secondary analyses investigated *TREM2* x *APOE*- $\epsilon 4$, *TREM2* x sex, and *TREM2* x cognitive diagnosis interactions on the above-mentioned outcomes. Sensitivity analyses were conducted to account for possible variation in model predictions due to cell-type

specific expression of *TREM2* in microglia using both cellular fraction data in the same samples as covariates.

All models were corrected for multiple comparisons using the Benjamini & Hochberg (1995) false discovery rate based on the total number of tests completed, accounting for all gene-tissue combinations across mRNA analyses. Statistical outliers of *TREM2* mRNA outside four standard deviations from the mean were removed.

Results

Participant Demographics

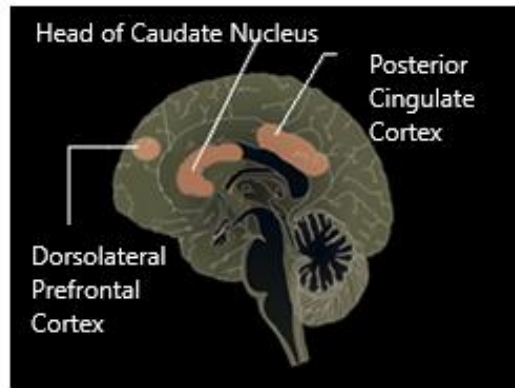
Participant characteristics are summarized in **Table 2.1**. The percentage of male compared to female participants was significantly less in all tissue cohorts. Participants were long-lived (mean age at death, yrs.=89), predominantly White ($\geq 98\%$), and were highly educated (mean >16 yrs.).

Table 2.1. Cohort Characteristics ROS/MAP

Characteristic	dIPFC	PCC	CN
N	908	505	699
AD Diagnosis, no. (%)	327 (36)	152 (30)	231 (33)
APOE4 Carrier, no. (%)	236 (26)	126 (25)	189 (27)
Male, no. (%)	308 (34)	192 (38)	245 (35)
White, no. (%)	890 (98)	495 (98)	692 (99)
Age of death	89.4 +/- 6.6	89.3 +/- 6.4	89.2 +/- 6.5
Education	16.5 +/- 3.6	16.5 +/- 3.6	16.4 +/- 3.6
Global cognition	-0.8 +/- 1.1	-0.7 +/- 1.0	-0.8 +/- 1.1
PMI	7.6 +/- 4.3	7.1 +/- 4.0	7.6 +/- 4.4

Figure 2.1. ROS/MAP brain regions.

These regions are included in tissue sampling for next generation RNA sequencing.



TREM2 mRNA in the dlPFC and PCC was subtly higher in individuals with a cognitive diagnosis of AD compared to NC (**Figure 2.2A**; $p=0.047$, and $p=0.021$, respectively) as well as across *APOE-ε4* carrier status (**Figure 2.3A-B**; $p=0.042$, and $p=0.043$ respectively). Levels of *TREM2* mRNA in the CN neither differed across cognitive diagnosis nor across *APOE-ε4* carrier status (**Figures 2.2** and **2.3C**). When restricting to autopsy confirmed AD diagnosis, dlPFC and PCC *TREM2* levels were higher in individuals with high or intermediate likelihood of AD as compared to individuals without or with low likelihood of AD as classified by NIA-Reagan criteria (**Figure 2.2B**; $p=8.5e-05$, and $p=6.3e-4$, respectively). In contrast, caudal *TREM2* levels did not differ across pathologic tissue diagnosis (**Figure 2.2B**; $p=0.72$). As expected, *TREM2* mRNA was found to be significantly correlated with the microglial cell-type fraction compared to other fractions (**Figure 2.4**; representative data from dlPFC, $r=0.7$).

Figure 2.2. *TREM2* expression across diagnosis. Cortical *TREM2* expression is higher in AD compared to control while caudal *TREM2* expression does not differ across diagnosis. **A:** Clinical cognitive diagnosis at last exam; normal cognition (NC), mild cognitive impairment (MCI) and Alzheimer’s disease dementia (AD). **B:** Tissue diagnosis according to neuropathologic staging (CERAD and Braak) NIA-Reagan criteria. (1) AD present (high or intermediate likelihood) and (0) AD not present (low likelihood or no AD). P-values displayed represent statistical comparison of means by a student’s t-test.

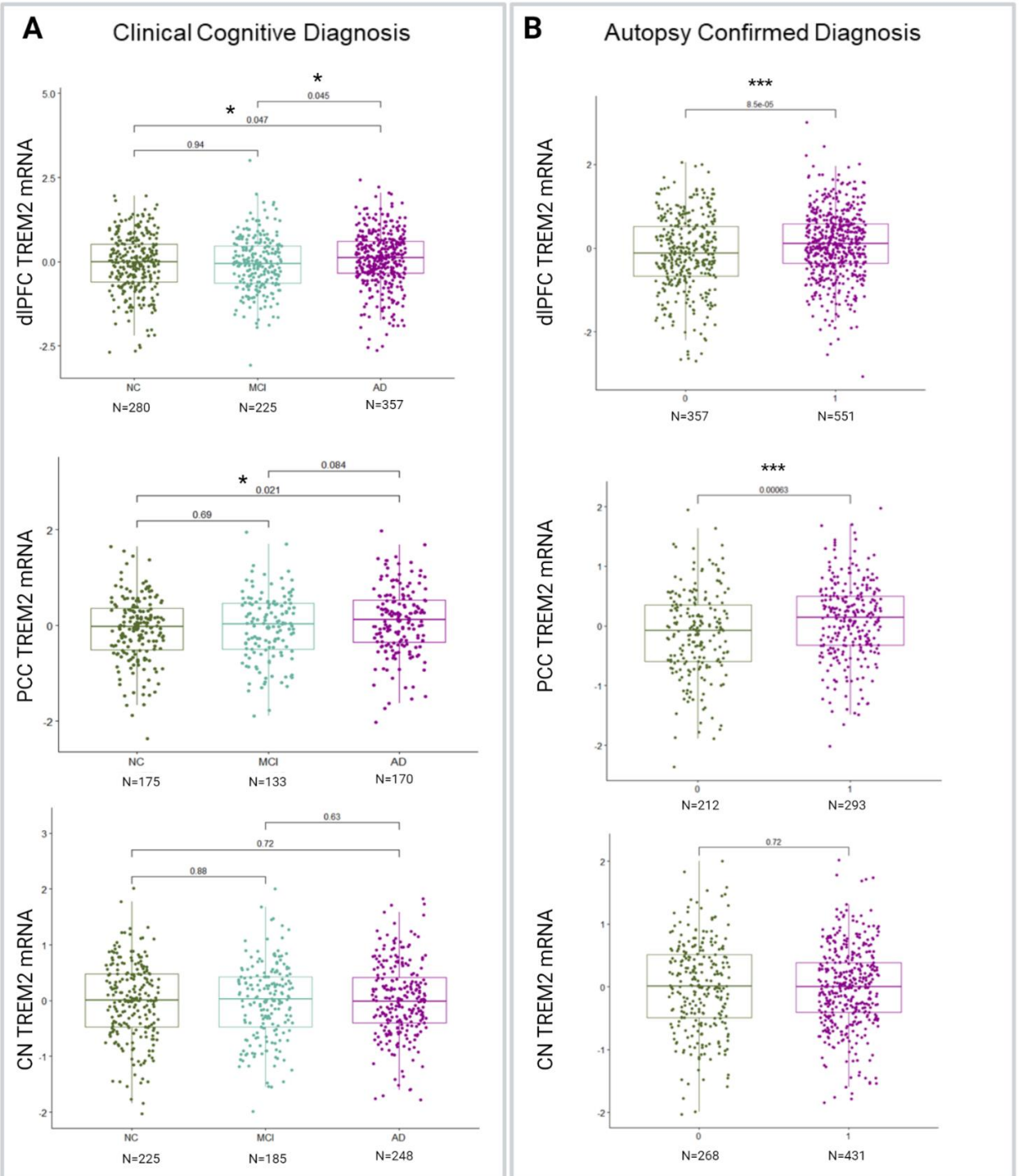


Figure 2.3. *TREM2* expression across *APOE*- ϵ 4 status. Cortical *TREM2* expression is subtly higher in *APOE*- ϵ 4 allele carriers (1) compared to non-carriers (0) while caudal *TREM2* expression does not differ. **A:** Dorsolateral prefrontal cortex (dlPFC) *TREM2* mRNA levels across *APOE* genotype. **B:** Posterior cingulate cortex (PCC) *TREM2* mRNA levels across *APOE* genotype. **C:** Head of caudate nucleus (CN) *TREM2* mRNA levels across *APOE* genotype. P-values displayed represent statistical comparison of means by a student's t-test.

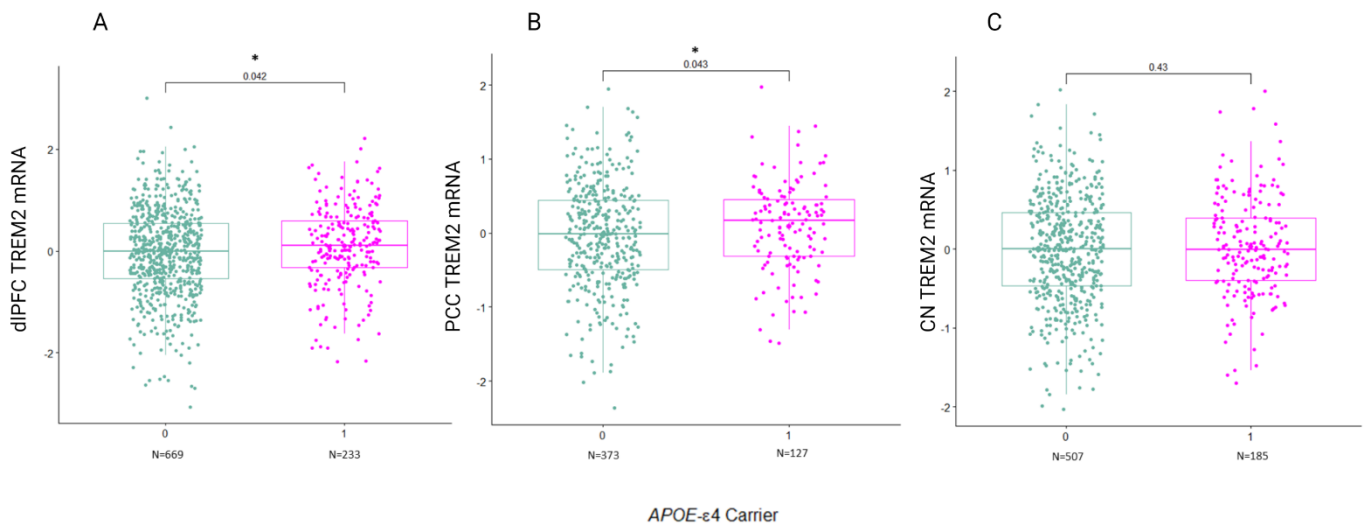
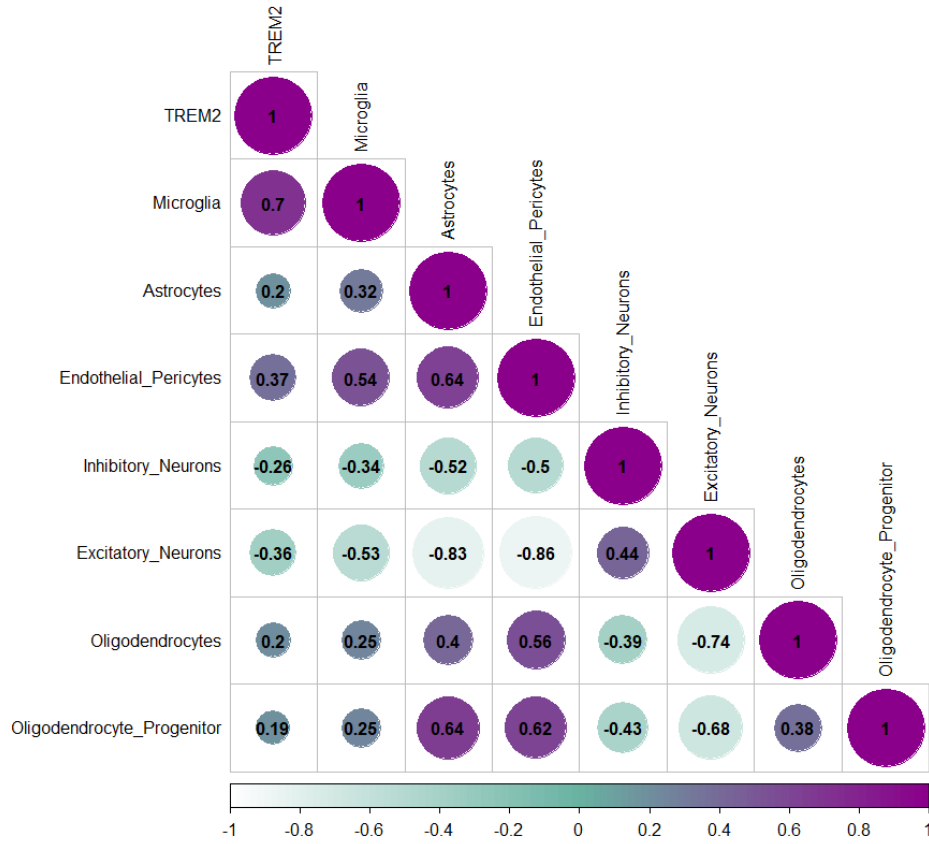


Figure 2.4. *TREM2* correlations with cell-type fraction. *TREM2* mRNA is significantly correlated with microglial cell-type fraction. Representative data shows *TREM2* from the dorsolateral prefrontal cortex (dlPFC) is significantly correlated with microglial cell-type fraction above other cell types examined. A Pearson's correlation coefficient (*r*) is displayed for each comparison.



TREM2 mRNA Associations with Amyloid

As expected, *TREM2* mRNA levels were significantly associated with higher amyloid burden in cortical regions and across outcome measures (Table 2.2-2.3).

TREM2 levels in the CN were not significantly associated with either amyloid outcome measure (Table 2.2 and Figure 2.5).

Figure 2.5. *TREM2* associations with amyloid. Cortical but not caudal *TREM2* mRNA positively associates with amyloid neuropathology. **A-C:** Regional *TREM2* mRNA levels by $A\beta_{1-42}$ burden as measured by immunohistochemistry. **D-F:** Regional *TREM2* mRNA levels by neuritic plaque burden as measured by silver stain. Unadjusted scatter plots and statistical results from linear regression models adjusting for age at death, sex, education, and post-mortem interval.

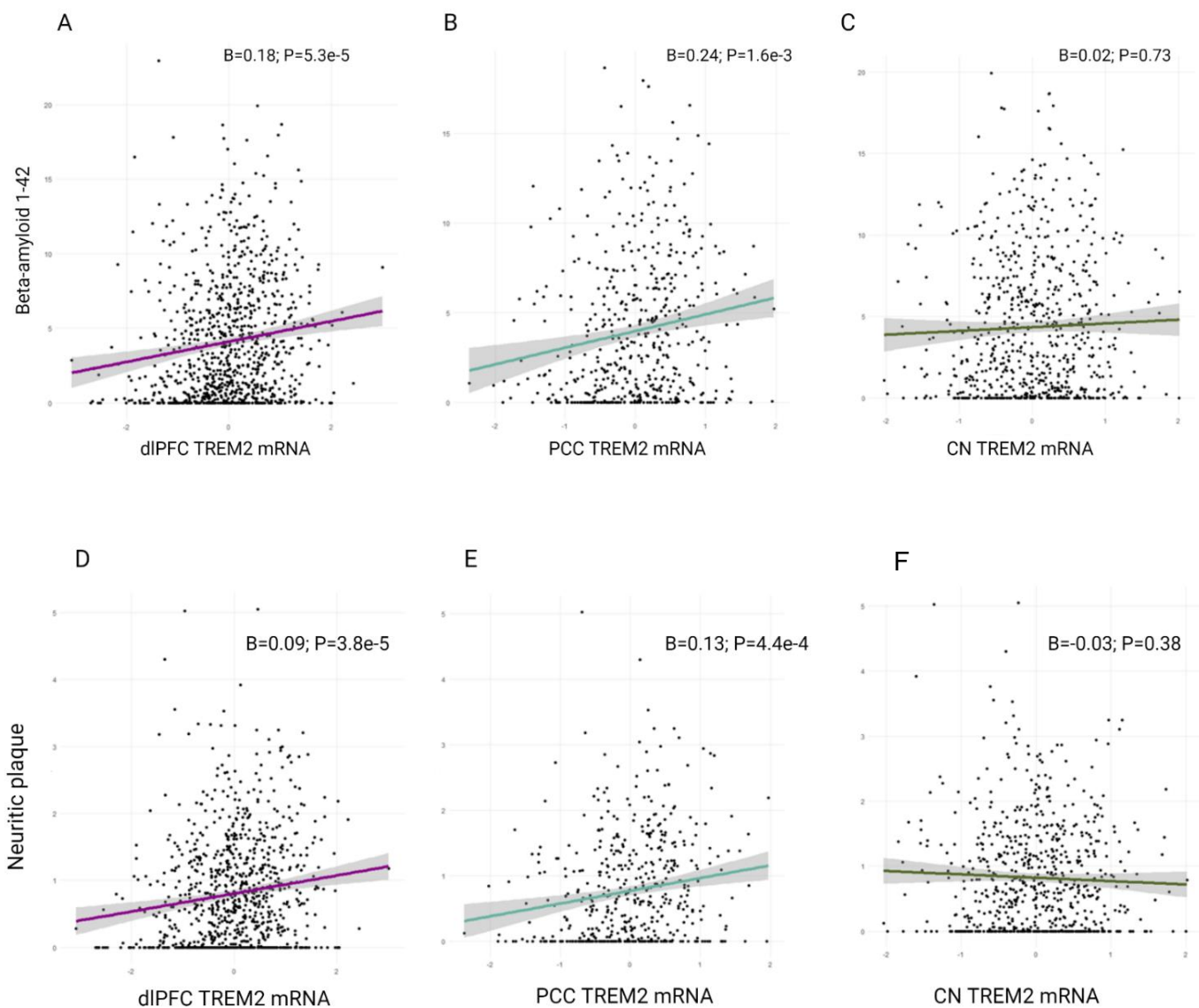


Table 2.2. Main Effects of *TREM2* on Amyloid Outcome Measures

<i>Predictor (Tissue)</i>	<i>Outcome</i>	β	<i>SE</i>	<i>Pvalue</i>	<i>P.fdr</i>
dIPFC	A β_{1-42}	0.182	0.045	5.25 e-05	5.09e-04
dIPFC	neuritic plaque	0.088	0.021	3.77e-05	5.09e-04
PCC	A β_{1-42}	0.236	0.074	0.002	0.014
PCC	neuritic plaque	0.125	0.035	4.39e-04	0.004
CN	A β_{1-42}	0.023	0.066	0.731	0.822
CN	neuritic plaque	-0.027	0.031	0.384	0.494

Table 2.3. Main Effects of *TREM2* on Amyloid Outcome Measures Adjusting for Microglial Fraction

<i>Predictor (Tissue)</i>	<i>Outcome</i>	<i>B</i>	<i>SE</i>	<i>Pvalue</i>	<i>Covariate Inclusion</i>
dIPFC	A β_{42}	0.457	0.090	5.28e-7	Microglial Cell-Type Fraction
dIPFC	neuritic plaque	0.183	0.044	3.79e-5	Microglial Cell-Type Fraction

TREM2 mRNA Associations with Tau

Regression models assessing *TREM2* mRNA expression for association with levels of tau neuropathology were inconsistent across outcome measures and mostly weak. Results showed *TREM2* mRNA negatively associated with tau neuropathology as quantified by IHC in the CN, albeit nominally (**Figure 2.6C**; $\beta=-0.17$; $P=0.02$). Positive signals were found using *TREM2* measurement from the other two cortical regions (**Figure 2.6A-B**; dIPFC; $\beta=-0.12$, $P=0.02$ and PCC; $\beta=0.17$; $P=0.04$). However, **Table 2.4** shows results from the main effects models do not pass significance for multiple corrections. The strength and flipping in the direction of the signal in distinct brain tissues indicates these results may be spurious or otherwise obscured by individual variances in microglial abundance.

To further assess the latter, sensitivity analyses adjusting for microglial cell-type fraction were utilized. The results from models adjusting for microglial cell-type fraction were not significantly different from the main effects after corrections for multiple comparisons using *TREM2* mRNA from the dIPFC (**Table 2.5**).

Figure 2.6. *TREM2* associations with tau. *TREM2* mRNA differentially associates with tau neuropathology depending on brain region. **A-C:** Regional *TREM2* mRNA levels by phosphorylated tau (AT8 epitope, Ser202/Thr305) burden as measured by immunohistochemistry. **D-F:** Regional *TREM2* mRNA levels by neurofibrillary burden as measured by silver stain. Unadjusted scatter plots and statistical results from linear regression models adjusting for age at death, sex, education, and post-mortem interval.

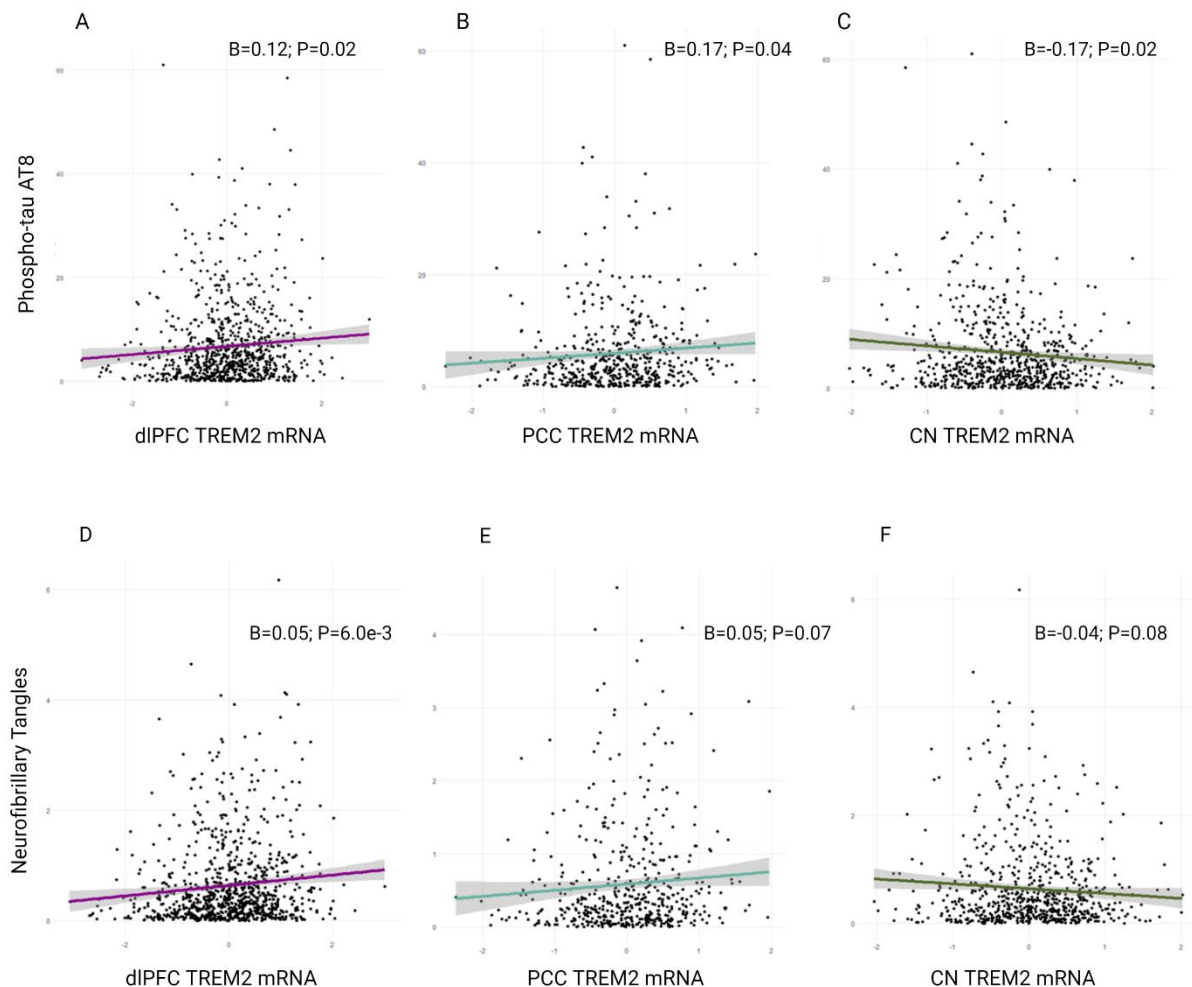


Table 2.4. Main Effects of *TREM2* on Tau Outcome Measures

<i>Predictor (Tissue)</i>	<i>Outcome</i>	<i>B</i>	<i>SE</i>	<i>Pvalue</i>	<i>P.fdr</i>
dIPFC	p-Tau, AT8	0.119	0.052	0.022	0.066
dIPFC	neurofibrillary tangles	0.045	0.016	0.006	0.032
PCC	p-Tau, AT8	0.172	0.084	0.041	0.101
PCC	neurofibrillary tangles	0.048	0.027	0.070	0.142
CN	p-Tau, AT8	-0.169	0.074	0.022	0.066
CN	neurofibrillary tangles	-0.042	0.024	0.075	0.142

Table 2.5. Main Effects of *TREM2* on Tau Outcome Measures Adjusting for Microglial Fraction

<i>Predictor (Tissue)</i>	<i>Outcome</i>	<i>B</i>	<i>SE</i>	<i>Pvalue</i>	<i>Covariate Inclusion</i>
dIPFC	p-Tau, AT8	0.123	0.104	0.234	Microglial Cell-Type Fraction
dIPFC	neurofibrillary tangles	0.100	0.032	0.001	Microglial Cell-Type Fraction

TREM2 mRNA Associations with Cerebrovascular Pathology

Despite the initial hypothesis that upregulation of *TREM2* mRNA at autopsy may reflect concomitant cerebrovascular pathology, this was largely not supported by results using cross-sectional data from ROS/MAP. **Table 2.6** summarizes the main effects, analyses. Interestingly, higher caudal *TREM2* levels were associated with increased severity of arteriolosclerosis ($\beta=0.280$, $p=0.009$). However, it is unknown whether this association withstands adjustment for individual cell-type abundance given a lack of cellular fraction estimates for this brain region. These cell-type sensitivity analyses using dIPFC data yielded insignificant results and are reported below in **Table 2.7**.

Table 2.6. Main Effects of *TREM2* on Cerebrovascular Outcome Measures

<i>TREM2</i> Predictor (Tissue)	<i>Outcome</i>	β	<i>SE</i>	<i>P-value</i>
dIPFC	Cerebral Macro Infarcts	0.161	0.104	0.123
dIPFC	Cerebral Micro Infarcts	-0.098	0.093	0.289
dIPFC	Arteriolosclerosis	-0.040	0.075	0.595
dIPFC	Atherosclerosis	-0.175	0.076	0.022
dIPFC	CAA	0.148	0.075	0.049
PCC	Cerebral Macro Infarcts	0.007	0.172	0.967
PCC	Cerebral Micro Infarcts	-0.007	0.151	0.965
PCC	Arteriolosclerosis	0.112	0.123	0.361
PCC	Atherosclerosis	0.033	0.126	0.795
PCC	CAA	0.214	0.121	0.079
CN	Cerebral Macro Infarcts	0.339	0.152	0.026
CN	Cerebral Micro Infarcts	0.161	0.133	0.228
CN	Arteriolosclerosis	0.280	0.107	0.009*
CN	Atherosclerosis	0.161	0.109	0.139
CN	CAA	-0.067	0.107	0.534

Asterisk * indicates survival for FDR correction across all main effects models.

Table 2.7. Main Effects of *TREM2* on Cerebrovascular Outcome Measures

Adjusting for Microglial Fraction

<i>Predictor (Tissue)</i>	<i>Outcome</i>	β	<i>SE</i>	<i>Pvalue</i>	<i>Covariate Inclusion</i>
dIPFC	Macro Infarcts	0.043	0.227	0.851	Microglial Cell-Type Fraction
dIPFC	Micro Infarcts	-0.156	0.203	0.444	Microglial Cell-Type Fraction
dIPFC	Arteriolosclerosis	-0.178	0.156	0.254	Microglial Cell-Type Fraction
dIPFC	Atherosclerosis	-0.173	0.161	0.283	Microglial Cell-Type Fraction
dIPFC	CAA	0.220	0.159	0.164	Microglial Cell-Type Fraction

TREM2 Associations with Microglial Density and Activation

Next, it was investigated whether or not these associations between *TREM2* and AD neuropathology described above were accompanied by *TREM2* associations with microglial density and/or activation in the same regions. Interestingly, *TREM2* measurements from cortical regions were not correlated with microglial outcome measures as hypothesized (**Figure 2.7**). However, *TREM2* levels were significantly correlated with the activated component of microglial density cis-regionally in the caudate (**Figure 2.7**). This association survived adjustment for covariates in a multiple linear regression model (stage 2-3 caudal microglia ~ age at death + sex + education + pmi, + caudal *TREM2*; $\beta=3.04$, $se= 1.17$, $p=0.011$). Next, it was investigated whether levels or severity of concomitant neuropathology interacted with *TREM2* expression on

Table 2.8. *TREM2* * Neuropathology Interactions on Activated Microglial Density in the Caudate

Interaction Term (neuropathology)	B	SE	P-value
Cerebral Macro Infarcts	3.172	4.100	0.431
Cerebral Micro Infarcts	-2.648	3.474	0.448
Arteriolosclerosis	-1.682	1.514	0.269
Atherosclerosis	-0.607	1.531	0.693
CAA	-3.408	1.779	0.058
A β_{1-42}	0.119	0.861	0.891
neuritic plaque	-1.258	-0.471	0.639
p-Tau, AT8	2.005	1.499	0.137
neurofibrillary tangles	0.629	0.154	0.878

this activated microglial state. There was a lack of evidence that select AD neuropathology including morphological substrates of small vessel disease modified the association between *TREM2* and microglial activation density in the caudate suggesting this signal may

represent a collection of diverse biological processes beyond the scope of individual AD neuropathologies examined herein (**Table 2.8**).

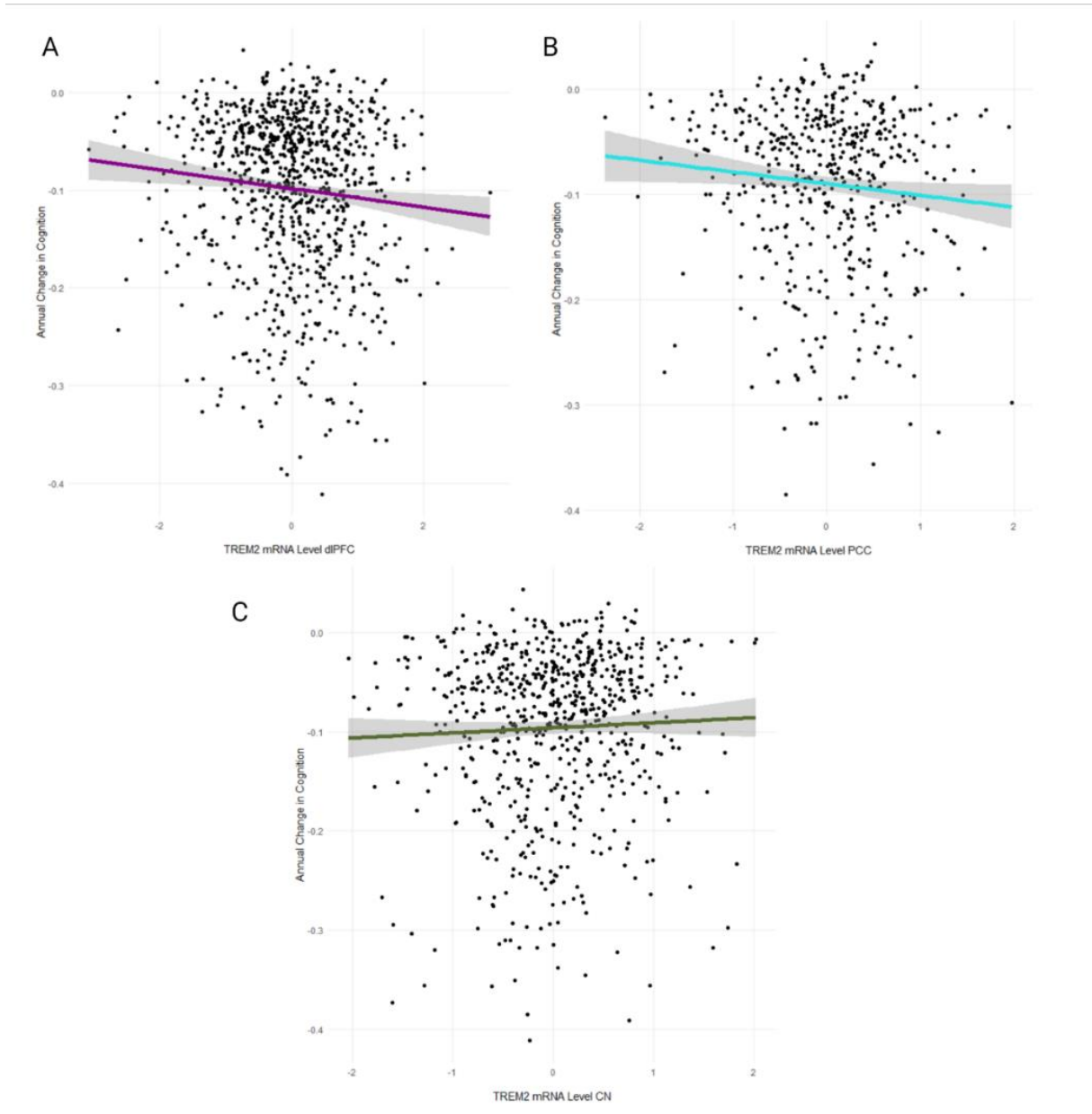
Figure 2.7. *TREM2* correlations with microglial density components. Caudal not cortical *TREM2* mRNA is significantly correlated with several components of microglial density. Midfrontal cortex (mfCx); ventral medial caudate (vmCaudate). A Pearson's correlation coefficient (r) is displayed for each comparison. An asterisk denotes significance set to an *a priori* threshold of $p < 0.05$.



Finally, we explored potential *TREM2* mRNA expression associations with global cognition scores. Cross-sectional results revealed *TREM2* mRNA levels were not significantly associated with global cognition in any brain region ($p > 0.15$). However, *TREM2* mRNA levels did significantly relate to faster decline in global cognitive scores

in longitudinal analysis from the dlPFC (**Figure 2.8A**; $p=0.02$) and trended toward significance using PCC *TREM2* measurement (**Figure 2.8B**; $p=0.07$). *TREM2* mRNA in the CN was not associated with longitudinal global cognition (**Figure 2.8C**; $p=0.37$). Additionally, after adjusting for levels of AD neuropathology as measured by IHC specific to $A\beta_{1-42}$ and p-tau AT8, *TREM2* expression was no longer a significant predictor of global cognition in the dlPFC ($\beta=-4.8e-3$; $p=0.25$) suggesting the main effect of *TREM2* levels on cognition was observed due to variance in levels of AD neuropathology.

Figure 2.8. *TREM2* associations with cognition. *TREM2* cortical but not caudal mRNA at autopsy is a predictor of retrospective cognitive decline. **A:** Dorsolateral prefrontal cortex (dlPFC) *TREM2* mRNA levels by annual change in global cognition. **B:** Posterior cingulate cortex (PCC) *TREM2* mRNA levels and **C:** head of caudate nucleus (CN) *TREM2* mRNA levels by annual change in global cognition.



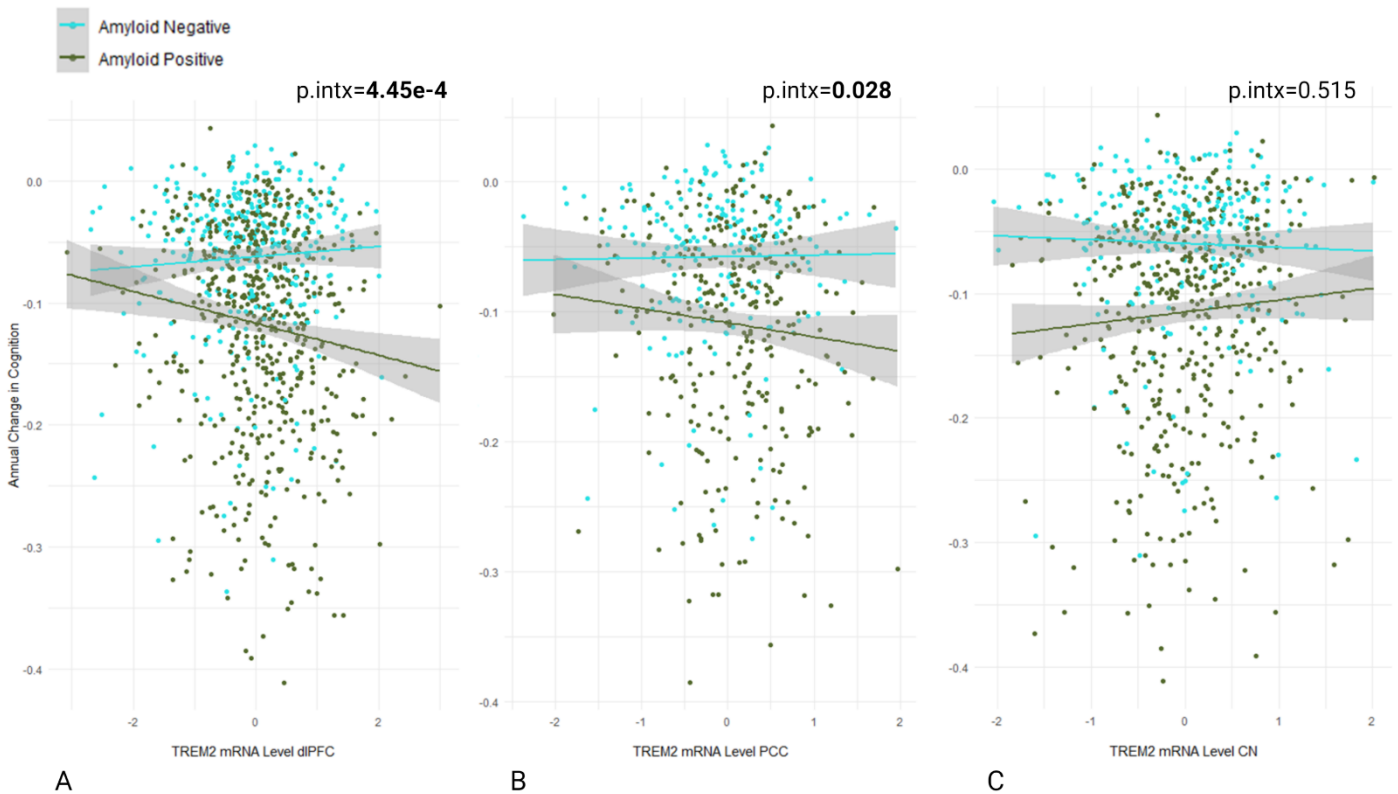
Microglial fraction data was obtained from dlPFC tissue in just under half of the individual participants (N=445) included in the above models. It was next tested whether or not adjusting for variance in microglial fraction modified results. When including microglial fraction as a covariate in the original longitudinal mixed effects model examining *TREM2* mRNA levels and longitudinal global cognition, the result approached but did not reach statistical significance ($\beta=-0.01$; $se=7.0e-3$; $p=0.07$). This could be due to a reduced sample size or microglial cell type fraction variance could indeed be responsible for the original association between *TREM2* and cognition. Additional sensitivity analyses stratifying on *APOE*- $\epsilon 4$ carrier status and sex showed the significant association signal of *TREM2* mRNA expression on longitudinal cognition was driven by females and non-carriers of the $\epsilon 4$ allele (**Table 2.9**).

Table 2.9. Stratified Main Effects of *TREM2* on Global Cognition

<i>Stratification</i>	<i>Predictor TREM2 (Tissue)</i>	<i>Outcome</i>	β	<i>SE</i>	<i>Pvalue</i>
APOE- $\epsilon 4$ carrier	dlPFC	longitudinal cognition	9.0e-4	0.011	0.936
APOE- $\epsilon 4$ non- carrier	dlPFC	longitudinal cognition	-0.010	0.004	0.031
Females	dlPFC	longitudinal cognition	-0.013	0.005	0.018
Males	dlPFC	longitudinal cognition	-0.003	0.007	0.704
APOE- $\epsilon 4$ carrier	PCC	longitudinal cognition	-0.002	0.019	0.913
APOE- $\epsilon 4$ non- carrier	PCC	longitudinal cognition	-0.011	0.006	0.076
Females	PCC	longitudinal cognition	-0.015	0.008	0.076
Males	PCC	longitudinal cognition	-0.007	0.011	0.512
APOE- $\epsilon 4$ carrier	CN	longitudinal cognition	0.027	0.015	0.066
APOE- $\epsilon 4$ non- carrier	CN	longitudinal cognition	0.001	0.006	0.851
Females	CN	longitudinal cognition	-0.007	0.008	0.931
Males	CN	longitudinal cognition	-0.017	0.010	0.098

Next it was tested whether amyloid status interacted with *TREM2* levels on longitudinal global cognition scores (**Figure 2.8**). *TREM2* levels in both the dlPFC and PCC interacted with amyloid positivity on cognitive trajectory whereby the association between higher *TREM2* and a faster rate cognitive decline was driven by individuals who were amyloid positive (**Figure 2.8A-B**; $\beta=-0.18$; $p=4.45e-4$, and $\beta=-0.176$; $p=0.03$, respectively). Interestingly, there was not an interaction of this kind in the caudate (**Figure 2.8C**; $\beta=0.05$; $p=0.52$).

Figure 2.8. *TREM2* X amyloid interactions on cognition. *TREM2* cortical but not caudal mRNA at autopsy interacts with A β positivity on retrospective cognitive decline. **A:** Dorsolateral prefrontal cortex (dlPFC) *TREM2* mRNA levels by annual change in global cognition. **B:** Posterior cingulate cortex (PCC) *TREM2* mRNA levels and **C:** head of caudate nucleus (CN) *TREM2* mRNA levels.



Discussion

The principal aim of this chapter was to evaluate the effects of *TREM2* gene expression on concomitant AD neuropathology at autopsy as well as cognition. Given the hypothesis that *TREM2* upregulation in AD brain likely represents a compensatory microglial response to disease pathology, positive association between increased levels of *TREM2* mRNA and increases in various neuropathological outcomes ($A\beta$, tau, microglial activation, and morphological substrates of small vessel disease), also decreases in cognitive function were expected. Using an aged subset of participants from the ROS/MAP cohort with available autopsy and RNA sequencing data, cross-sectional multiple regression analyses revealed evidence of a stronger association between *TREM2* expression and measures of amyloid neuropathology than those of tau. Additionally, novel associations between *TREM2* expression and longitudinal global cognition in cortical regions as well as with arteriolosclerosis in caudal tissue suggest a broader relationship between this pathway and AD phenotypic heterogeneity than previously recognized.

As expected, *TREM2* mRNA was a significant predictor of cognitive decline, albeit this association was weak and limited to the two cortical brain regions (dlPFC and PCC). To our knowledge, it has been previously unknown whether *TREM2* mRNA levels at autopsy relate to longitudinal cognition. Whereas, CSF sTREM2 has been associated with cognition in the literature, few studies have looked at bulk RNA sequencing quantification of *TREM2* and cognition in human brain. Here we present

such significant results indicating that the magnitude of late-life *TREM2* expression in cortical brain regions, while previously associated with AD cognitive diagnosis, may also be a signifier of cognitive trajectory whereby increases at autopsy are associated with a more rapid cognitive decline regardless of cognitive diagnosis. We expand upon this showing that the association with cognition is likely related to neuropathological tissue status, namely NIA-Reagan tissue diagnosis (**Figure 2.2B**).

As hypothesized, if increases in *TREM2* mRNA reflect a compensatory microglial-mediated response to neuropathology, then the association between *TREM2* and cognition is likely driven by individuals with a higher burden of neuropathology. To determine whether the degree of amyloid pathology modified this association, interaction models utilizing *TREM2* mRNA * A β on longitudinal cognition revealed amyloid burden as a significant modifier in the dlPFC whereas, individuals with higher levels of A β as measured by IHC displayed a stronger negative association between *TREM2* mRNA levels and global cognition driving the original association (**Figure 2.8**). This suggests that some degree of *TREM2* upregulation in late life may be indicative of cognitive functioning as modified by neuropathology. Furthermore, interaction models, *TREM2* * *APOE*- ϵ 4 carrier status on cognition, as well as stratified models, showed the signal of association between *TREM2* levels and cognitive decline is significant only in *APOE*- ϵ 4 non-carriers (**Table 2.9**). This indicates that *TREM2* response to neuropathology on cognition may occur independently of ϵ 4 allele-mediated cognitive decline. Similarly, sex-stratified models revealed a negative association between *TREM2* levels and cognitive decline in females whereas the association in males was non-significant. However, this was not marked and may be attributed to a significantly

smaller sample size of males and *APOE*- ϵ 4 carriers as compared to females and *APOE*- ϵ 4 non-carriers.

Amongst neuropathology outcome measures, perhaps the most notable was a robust association between *TREM2* and A β burden. This is consistent with the fact that the functional responses of microglial to A β plaque has been shown to reflect such increases in transcription of *TREM2* which in turn is vital to the microglial barrier formation and subsequent compaction of the plaque residue. These associations were consistent in cortical brain tissues supported by previous work showing post-mortem immunoreactivity of cortical *TREM2* in microglia, particularly those surrounding A β plaque⁹⁰. Furthermore, in APP23 transgenic mice, microglia surrounding A β plaque increased expression of *TREM2* corresponding with the progression of amyloid pathology¹¹⁵. The head of the caudate nucleus (CN) is also a region shown to be vulnerable to amyloid pathology albeit a subcortical region affected later-on in the spatial-temporal pattern of A β plaque progression in AD as compared to neocortical regions¹²⁹. Yet, *TREM2* mRNA levels from the CN did not relate to A β burden (**Figure 2.5**). This is likely explained by the methods of amyloid quantification which incorporated an average amyloid burden score from mostly cortical subregions without any calculations from the basal ganglia. Therefore, subcortical *TREM2* expression did not predict A β pathology transregionally. Additionally, from sensitivity analysis, accounting for microglial fraction intensified signal from the dlPFC suggesting variance in the model from microglial abundance may have partially obscured the original association signal between *TREM2* and amyloid in the cortex (**Table 2.3**). Sensitivity results using cell-type fraction data suggests the association between the two does not

fully depend on increases in microglial abundance but may be specific to *TREM2* transcription.

In contrast to amyloid, there was weaker evidence of *TREM2* expression association with levels of tau neuropathology. In fact, there is a flip in the direction of association of *TREM2* with tau when *TREM2* is measured from caudal tissue (**Figure 2.6**). This is despite contrasting work showing a positive association of bulk *TREM2* RNA sequencing expression in human temporal cortex and phosphorylated tau, AT8 immunohistochemistry⁹⁰. This may be due to several factors. First, the previous study may not have captured a wide range of phenotypic heterogeneity due to a small sample size (N=11; AD) and additionally, this cohort included a higher percentage of *APOE-ε4* carriers. Second, unlike the direct functional relationship between *TREM2* binding Aβ ligand¹⁰⁵, there is currently a lack of evidence of a direct functional relationship between *TREM2* and phosphorylated tau or other intraneuronal pathological process leading to dystrophic neurite formation. Rather, it is thought to be the case that *TREM2* regulation of microglial activity and subsequent immune dysfunction are external triggers of neuronal tau pathology via microgliosis and excessive neuroinflammation¹³⁰. In other words, *TREM2* signaling has been indirectly link to tau via neuroinflammation but no direct functional relationship between the proteins has yet to be discovered. This, however, is an active area of exploration. Furthermore, the dynamic between *TREM2* transcriptional upregulation and Aβ deposition is thought to be deleterious to microglia and the immune landscape, whereas the development of tau pathology downstream has been shown to be dependent to some extent on the *a priori* amyloid accumulation

¹³¹. Therefore, transcriptional upregulation of *TREM2* expression itself may not be as closely coupled to the development of tau pathology.

Sensitivity models suggest a potential positive relationship between *TREM2* expression and neurofibrillary tangle pathology as measured by silver staining method after accounting for microglial cell-type fraction variance (**Table 2.5**). Suggesting a potential positive relationship between dlPFC *TREM2* levels and neurofibrillary tangles after accounting for sample variance in microglial cell-type abundance.

We provide modest evidence that cortical *TREM2* expression relates to classical AD pathology while caudal *TREM2* expression, instead, relates to markers of cerebrovascular disease and microglial reactivity. This is interesting given it is not explicitly clear whether microglia derived from these distinct brain regions harbor distinct functions. There is precedence for this since other cell types such as neurons exist in disparate phenotypic and functional forms, and these tend to aggregate in their own regionally distinct territories. Evidence from transcriptomic- and other omic-profiling has revealed distinctive spatial and molecular patterns of microglia across the brain ¹³²⁻¹³⁴. Our data highlight the importance of this regional heterogeneity in microglial function. The association of high *TREM2* levels with increased arteriolosclerosis (**Table 2.6**) is an interesting novel take-away from this work, suggesting transcription of *TREM2* may be relevant to the etiology and/or progression of this pathology or otherwise linked by an unmeasured third variable. *TREM2* function has been implicated in mechanisms relating to the integrity of the vascular endothelial luminal wall. This includes several studies linking *TREM2* signaling to the progression of atherosclerosis. *TREM2* is highly expressed in foamy macrophages and seems to be associated with atherogenesis in

the aorta ¹³⁵ and important for their expression in brain under ischemic conditions ¹³⁶. However, the association with arteriolosclerosis did not generalize to atherosclerosis in our dataset. One possibility for this may be the difference in quantification between the two outcome variables. For instance, the arteriosclerosis rating relied on semi-quantitative grading of anterior basal ganglia vessels which correspond more closely with *TREM2* sampled from the head of the caudate. Whereas the atherosclerosis grading relied on a more global inspection of vertebral, basilar, posterior cerebral, middle cerebral, anterior cerebral arteries as well as their proximal branches. Alternatively, our analysis may be picking up on an association of *TREM2* mRNA levels with arteriole degeneration that is distinct from *TREM2*'s proposed function in the pathogenesis of vessel plaque formation in macrophages. Adding to the evidence potentially linking *TREM2* function to vessel dysfunction is recent work showing *TREM2* may be necessary for endothelial cell homeostasis ¹⁰⁹. This remains an interesting topic for future studies and further work clarifying the mechanisms of *TREM2* and cerebrovascular dysregulation is needed, particularly given recent single cell RNA sequencing data of the human microvasculature highlights enrichment of *TREM2* in perivascular macrophages and microglia in AD, while in age-matched controls *TREM2* is mostly enriched in capillary, venous, and vascular smooth muscle cell types ¹³⁷. *TREM2* protein is also thought to be a marker of monocyte recruitment to vascular lumens in aged individuals ¹³⁸; perhaps the relationship between *TREM2*-expressing monocytes and vascularly deposited A β regulates pathophysiology underlying the development of arteriolosclerosis. However, the relationship of *TREM2* expression dysregulation and function to arteriolosclerosis remains underexplored.

Due to the finding that increases in caudal *TREM2* relates to the PAM cis-regionally we are left to speculate as to why this relationship does not extend to the cortex (**Figure 2.7**). There are several possibilities for this including limitations to using bulk RNA sequencing measurement of *TREM2* transcript abundance which may obscure single-cell or transcript-specific resolutions. The lack of association signal in the cortex between microglial activation and *TREM2* could otherwise be due to a window of late-life measurement when *TREM2* transcription may no longer reflect compensatory microglial activation as is believed to be true in the face of earlier stages of neuropathologic progression. For example, A β plaque deposits more abundantly in the cortex of AD patients¹³⁹ and previous studies have shown microglial metabolism may become inefficient or fail given a high amyloid burden¹⁴⁰ which paves the possibility that the lack of association in this region may be due to loss of function. This is particularly interesting given the recent links between microglial metabolic fitness, glucose metabolism and *TREM2* function^{64, 141}.

There are several strengths and limitations to the present analyses. First, ROS/MAP is a well-characterized cohort detailing multiple measures of cerebrovascular neuropathology. Second, the availability of cellular fraction data as well as genotype and multiple measures of diagnosis permitted the exploration of potential interactions and statistical variation in models. Additionally, the availability of longitudinal cognitive data and *TREM2* measurement in multiple brain regions bolstered characterizations. However, analyses herein are limited to a late-life window of neuropathology at autopsy, therefore investigation of *TREM2* expression changes in brain throughout the course of normal aging and/or disease in humans remain unknown begging the advent and

development of a TREM2-specific PET radioligand assay. Moreover, measurement of RNA transcript does not necessarily translate to protein expression or signaling competent membranous TREM2. Finally, the lack of racial diversity precludes generalization of results to more diverse populations. Future work, looking at whether caudal *TREM2* associations with A β and or tau are present if measured cis-regionally are needed to clarify disparate regional results herein.

Taken together, data support previous preclinical demonstrations of a strong functional relationship between TREM2 protein expression and amyloid which is evident in the present cohort at autopsy. We find weak evidence of *TREM2* mRNA expression association with tau neuropathology suggesting transcriptional upregulation of *TREM2* may not be a sensitive measure of abnormally phosphorylated tau or dystrophic neurites. A more novel association was drawn between *TREM2* and arteriolosclerosis, further implicating this pathway in the pathogenesis of yet another vascular feature at the intersection of neurodegenerative disease and immune dysregulation. Finally, we draw attention to a previously unrecognized disparity between cortical and caudal TREM2 expression associations; the former, with classical AD neuropathology and cognitive decline, the later, with PAM and arteriolosclerosis.

CHAPTER 3

BIOLOGICAL CORRELATES OF ELEVATED STREM2 IN CSF

Portions of this chapter are published under the title, “*Biological Correlates of Elevated Soluble TREM2 in Cerebrospinal Fluid*” in *Neurobiology of Aging*

Introduction

Alzheimer’s disease (AD) is a devastating neurodegenerative disease and the most common cause of dementia, affecting more than one in nine seniors in the U.S.⁴. Nosologically-defined AD pathology consists of amyloid- β ($A\beta$) plaques and neurofibrillary tangles that are thought to drive neuroinflammation, blood-brain barrier (BBB) dysfunction, and neurodegeneration resulting in cognitive decline and clinical disease^{11, 27}. The prodrome of AD can be 20+ years, whereby neuropathology begins to deposit and brain changes occur years prior to the onset of clinical symptoms. For that reason, there has been an incredible focus on the development of biomarkers in AD, including both fluid and imaging biomarkers of AD neuropathology, neurodegeneration^{142, 143}, and more recently neuroinflammation and BBB dysfunction¹⁴⁴⁻¹⁴⁶. While cerebrospinal fluid (CSF) biomarkers of amyloid and tau are well-established, there is a pressing need to better characterize emerging biomarkers to understand their temporal dynamics and biological correlates.

One promising biomarker with a strong genetic and molecular basis is soluble triggering receptor expressed on myeloid cells-2 (sTREM2) measured in CSF. *TREM2*, encoding its transmembrane parent, was originally implicated as an AD risk gene

through two large genome-wide association studies (GWAS), including the identification of the R47H missense mutation that confers an increased risk similar in magnitude to a single copy of the *APOE-ε4* allele^{76, 77}. TREM2 is expressed preferentially on microglia in the brain and plays a critical role in the neuroinflammatory response to AD. More specifically, functional studies of TREM2 have revealed roles in the regulation of parenchymal Aβ plaque deposition^{55, 64, 87, 96, 103, 147, 148}, progression of tau pathology^{86, 130, 149-151}, and BBB dysfunction^{63, 152, 153}. Beyond these roles in AD, TREM2 is also involved more generally in microglial activation^{154, 155}, ischemia/hypoxia⁶³, oxidative stress responses^{62, 156}, and transcriptional regulation of brain endothelial cells¹⁰⁹, providing numerous potential avenues that could contribute to risk and progression in AD.

Cleavage of TREM2 ectodomain produces a soluble fragment (sTREM2), considered a biomarker of microglial activation, whereby increased protein levels have been reported to coincide with the transition of mild cognitive impairment (MCI) to AD dementia^{157, 158}. Additionally, sTREM2 is signaling competent, thought to modulate inflammatory and phagocytic responses from microglia, and has also been shown in this manner to promote Aβ clearance in 5XFAD mice⁸⁴. Increases in sTREM2 levels during AD may mark a transition in the neuroinflammatory state that correlates with neurodegeneration and clinical progression. Thus, it is not surprising that CSF sTREM2 is strongly correlated with CSF biomarkers of tau pathology that track closely with the neurodegenerative processes in AD^{144, 158-160}. In contrast, CSF sTREM2 associations with Aβ and BBB dysfunction have been inconsistent^{110, 144, 158-160} and remain poorly understood. There is a need to fully characterize the biological correlates of CSF

sTREM2, particularly a need to deconvolve the variance in sTREM2 levels that are explained by biomarkers of A β , tau, neurodegeneration, and BBB dysfunction, which are all thought to contribute to the neuroinflammatory milieu in AD.

It has been hypothesized that sTREM2 may be a complementary biomarker that could be useful in the context of aging and disease. Moreover, therapeutics targeting TREM2 are in active development, yet there is limited knowledge of the types of related biological processes and functions of sTREM2 itself. The goal of this chapter is to clarify the biological correlates and thus types of biological processes that coincide with elevated sTREM2 in CSF. A comprehensive characterization of biomarkers in the CSF compartment and neuroimaging measures of cerebrovascular injury related to sTREM2 elevation and therefore microglial activation will build understanding of potential early neuroimmune dynamics relevant to AD. First, we fully characterize the associations between CSF sTREM2 levels and well-established biomarkers of AD pathology, neurodegeneration, and BBB dysfunction. Second, we evaluate the unique contribution of each of these biomarkers to sTREM2 levels in competitive models, evaluating whether biomarkers of BBB and A β explain variance in sTREM2 levels above and beyond the well-established associations with CSF tau. Third, we relate residual variance in sTREM2 levels to measurements of longitudinal cognition evaluating potential clinical relevance of sTREM2 associations in CSF. Together, these analyses provide a more comprehensive picture of the biological underpinnings of elevated CSF sTREM2 in aging and disease and provide critical information for the application and interpretation of CSF sTREM2 levels in future biomarker studies.

Methods

Study cohort

Participants were drawn from the Vanderbilt Memory and Aging Project (VMAP) launched in 2012 in Nashville, TN. VMAP is a longitudinal study of vascular health and brain aging ¹⁶¹. A total of 335 participants, 60-92 years of age, were enrolled. This included 168 with mild cognitive impairment (MCI) and 167 age-, sex-, and race-matched cognitively normal controls (NC). MCI diagnosis was determined by the National Institute on Aging/Alzheimer's Association Workgroup core clinical criteria ⁸. Briefly, this includes a CDR score $0 \geq 0.5$, concern of changes in cognition (reported by the participant, informant, or clinician), absence of dementia, relatively spared daily functioning, and neuropsychological functioning indicating objective impairment outside age-adjusted mean performance in one or more cognitive domains. Inclusion criteria required participants to speak English, have adequate auditory and visual acuity, and have a reliable study partner. Exclusion criteria included MRI contraindications, history of neurological disease or major psychiatric illness, heart failure, head injury with loss of consciousness >5 min, or a systemic or terminal illness. A subset of participants underwent fasting lumbar puncture for CSF collection at baseline. Written informed consent was obtained from all participants prior to data collection, and all protocols were approved by the Vanderbilt University Medical Center Institutional Review Board.

Neuropsychological composites

Participants underwent detailed neuropsychological assessment of various domains of cognitive performance at baseline and every 18 months. An episodic memory composite was calculated as a z-score from the following independent tests: California Verbal Learning Test Second Edition (CVLT-II) Total Immediate Recall, CVLT-II Delayed Recall, CVLT-II Recognition, Biber Figure Learning Test (BFLT) Total Immediate Recall, BFLT Delayed Recall, and BFLT Recognition. An executive functioning composite was calculated as a z-score from the following: Delis–Kaplan Executive Function System (D-KEFS) Number-Letter Switching Test, D-KEFS Color-Word Inhibition Test, and Letter Fluency Test (FAS). Assessments were reviewed to avoid floor and ceiling effects and composites were calculated from a latent variable model where each item was treated as a raw continuous variable loaded on a general factor, also as on a test-specific factor to reduce potential confounds^{161, 162}. Participants with longitudinal cognition data had up to five measurement timepoints (mean±sd=2.6±1.3 visits) and a mean follow-up period of (mean±sd=4.6±1.7 years).

Blood draw and albumin measurement

Participants underwent morning fasting venous blood draw and samples were immediately stored at -80°C. Whole blood was centrifuged at 2000g and 4°C for 15 min and plasma was extracted and stored in ten 0.5mL aliquots. Albumin levels (plasma and CSF) were measured by immunonephelometry on a Beckman Immage Immunochemistry system (Beckman Instruments, Beckman Coulter, Brea, CA, USA). The albumin ratio was calculated as CSF albumin (mg/L)/plasma albumin (g/L).

APOE genotyping

White blood cell extraction was performed on frozen whole blood. The TaqMan single nucleotide polymorphism genotyping assay from Applied Biosystems (Foster City, CA) was applied to determine *APOE* genotypes by identifying the two single-nucleotide polymorphisms that characterize alleles $\epsilon 2$, $\epsilon 3$, and $\epsilon 4$. Polymerase chain reaction (PCR) was performed as previously described¹⁶¹. Genotyping efficiency was >99%.

Lumbar puncture and biochemical analyses

A maximum of 25mLs of CSF was drawn from a baseline, optional, fasting lumbar puncture procedure and collected with polypropylene syringes using a Sprotte 25-gauge spinal needle from an intervertebral lumbar space. CSF supernatant was immediately extracted and aliquoted in 0.5mL polypropylene tubes and stored at -80°C. Analysis of CSF total tau, p-tau₁₈₁, A β _{x-40}, A β _{x-42}, A β ₁₋₄₂, and neurofilament light (NfL) was performed in batch using commercially available enzyme-linked immunosorbent assays (carboxy-terminal specific antibodies aided in quantification of A β _{x-40} and A β _{x-42} species with varying amino-terminal lengths). CSF sTREM2 concentration was measured using an in-house Meso Scale Discovery (MSD) assay (Rockville, MD), as previously described in detail¹⁶³. Samples were processed in one round of experiments using one batch of reagents by board-certified laboratory technicians blinded to clinical information. Coefficients of variation for duplicate samples were <10% (mean 2.4%).

Supplemental Table 3.1 contains assay kit information. CSF and plasma albumin

measurements were conducted at the Clinical Neurochemistry Laboratory, University of Gothenburg under Drs. Henrik Zetterberg and Kaj Blennow.

Replication of amyloid- β results using ADNI data

The Alzheimer's Disease Neuroimaging Initiative (ADNI) is a longitudinal multisite study launched in 2004 focused on the development of biomarkers for AD early detection. Participant demographics are provided in **Supplemental Table 3.2**. Baseline CSF biomarker measurement of $A\beta_{1-42}$, $A\beta_{1-40}$, and $A\beta_{1-38}$ were acquired utilizing 2D-UPLC tandem mass spectrometry. Each data point represents the average of duplicate 0.1 mL aliquots from a single CSF sample. Methodology was previously validated for analysis of $A\beta_{1-42}$ ¹⁶⁴ and then adapted for the additional peptides by including their internal standards and re-validation of the protocol ¹⁶⁵. A detailed summary of the analytical method including sample preparation, parameters, and standards is publicly available for download on the ADNI database (adni.loni.usc.edu). Tau positivity was determined by the previously defined cut-off value of 23pg/mL ¹⁶⁶.

An MSD platform-based assay was used for CSF sTREM2 measurement which has been previously established and validated by Christian Haass' group and reported ^{61, 158, 160, 167}.

Neuroimaging

Cerebral blood flow (CBF) in microvasculature (rate of blood delivery to tissue, mL/g/min) was measured using vessel-encoded pseudo-continuous arterial spin labeling (VE-pCASL), allowing total CBF quantification as well as regional measurement

in separate flow territories. Hypercapnic VE-pCASL using identical scan parameters and a non-rebreathing facemask delivering 5% CO₂ and 95% normoxic, normocapnic medical-grade air measured cerebrovascular reactivity (CVR) by quantifying percentage change in CBF normalized by the end-tidal CO₂ measurement. Both CBF and CVR methods have previously been described in detail¹⁶¹.

Brain MRI (3T Philips Achieva system with 8-channel SENSE reception) was performed to collect the following cerebrovascular outcome measures: cerebral microbleeds, lacunar infarcts and white matter hyperintensities. Descriptions of the measurement of each biomarker has been described in detail previously¹⁶¹. Briefly, a board-certified neuroradiologist blinded to clinical information oversaw postprocessing quantification. This included counting of cerebral microbleeds (1-10mm in diameter) measured using susceptibility weighted imaging (SWI) scans with high resolution 3D GRE T2* weighted gradient echo. Lacunar infarcts were identified as lesions on T1 images showing signal intensity approaching the threshold of CSF while also fulfilling hypo/hyper-intensity criteria on fluid-attenuated inversion recovery (FLAIR) images. These features, in combination with size (ranging 2-20mm in diameter), were used to distinguish lacunar infarcts from other small vessel disease markers following previously established standards¹⁶⁸. T2-weighted FLAIR data was utilized to quantify white matter hyperintensity lesion volumes in conjunction with an automated pipeline (Lesion Segmentation Tool toolbox for Statistical Parametric Mapping 8) with manual edits performed using MIPAV.

Statistical analyses

Statistical analyses were performed in R v.4.1.2 using R Studio IDE (<https://www.rstudio.com/>). Linear regression models were leveraged using CSF protein levels of AD biomarkers to predict CSF sTREM2 measures at baseline. Covariates included age, sex, education, and clinical diagnosis (MCI vs. NC). For neuroimaging outcome variables, additional covariates included intracranial volume and Framingham Stroke Risk Profile (FSRP) score. Following independent models for each biomarker, we performed competitive models leveraging a hierarchical linear regression approach to evaluate the unique contribution and variance explained by each significant predictor from the independent analyses. Model selection, aided by Akaike information criterion (AIC) and Bayesian information criterion (BIC) calculations, was performed using R packages *AICcmodave* and *flemix*, respectively. Residuals were then calculated from the cross-sectional models assessing variance in baseline CSF sTREM2 measurements and used to predict future cognitive performance using either a memory or executive functioning composite score as the outcome variable within a longitudinal linear mixed-effects regression.

Given the established association between CSF tau and CSF sTREM2, we performed post-hoc interaction analyses for the biomarkers that remained statistically significant in competitive hierarchical linear regression models to better understand whether the novel biomarker associations were modified according to tau status. All covariates remained the same as in our primary models above.

Sensitivity analyses included interaction models with sex, *APOE*- ϵ 4 carrier status, and MCI diagnosis (**Supplemental Table 3.3**). Additional analyses included the date of CSF collection as a covariate to account for potential protein

storage/degradation effects; however, accounting for this added variable did not have a significant impact on the main effects results (**Supplemental Table 3.4**) or competitive models (**Supplemental Table 3.5**). Further sensitivity analyses explored potential variation in results due to statistical and visual outliers as well as adjusting MCI diagnosis criteria to align with ADNI (**Supplemental Tables 3.6-3.9**). Scatter plots showing sTREM2 by additional biomarkers after outlier removal are provided in **Supplementary Figures 3.1A-D**.

All models were corrected for multiple comparisons using the Benjamini & Hochberg (1995) false discovery rate.

Results

3.1 Participant characteristics VMAP

The VMAP discovery cohort is divided fairly equally among individuals with MCI (46%) and NC (54%), comprised mostly of males (67%), also non-Hispanic White participants (94%), and is highly educated (mean: 16 years). Baseline age and *APOE-ε4* carrier status was similar across diagnostic groups, but years of education differed with lower levels in MCI (mean: 15 years) compared to NC (mean: 17 years) shown in **Table 3.1**.

Table 3.1. VMAP Cohort Demographics

Characteristic	Clinical Diagnosis		Total (N=155)	P-value
	Normal Cognition (N=83)	Mild Cognitive Impairment (N=72)		
Male, no. (%)	58 (70)	46 (63)	104 (67)	0.535
Age (baseline)	72±6.50	72±6.18	72±6.33	0.458
Education	17±2.41	15±2.94	16±2.80	0.001
APOE-ε4 carriers, no. (%)	24 (29)	27 (38)	51 (33)	0.334
sTREM2 CSF pg/mL	3530±1867.29	3817±1759.49	3667±1812.50	0.327
p-tau ₁₈₁ CSF pg/mL (% p-tau positive) †	56±21.92 (17)	67±28.59 (26)	61±25.70 (21)	0.212
Aβ ₁₋₄₂ CSF pg/mL (% Aβ positive) ††	760±229.54 (20)	662±254.02 (40)	714±245.40 (30)	0.012

Values are presented as mean±standard deviation, unless otherwise indicated. A student's t-test or a Pearson's chi-squared test was used to compare continuous or categorical variables, respectively, between cognitive diagnoses. Bold represents statistical significance set to a *priori* threshold $P < 0.05$. 6 participants are Black/African American; 2 American Indian/Alaska Native; 2 Asian. † p-tau positive ≥ 80 pg/mL and †† Aβ positive ≤ 530 pg/mL.

Interestingly, we also find decreases in mean CSF sTREM2 levels in amyloid positive, tau negative (A+/T-) individuals utilizing VMAP cut-offs for amyloid and tau_{181P}

positivity (≤ 530 pg/mL and ≥ 80 pg/mL, respectively). Few individuals (N=16) were A+/T- and the difference between sTREM2 levels in these individuals compared to A-/T- individuals does not reach statistical significance (**Supplementary Figure 3.2**; $p=0.18$).

3.2 Biomarker associations with CSF sTREM2

Main effects of AD biomarkers on sTREM2 levels (sTREM2 ~ biomarker + base covariates) were examined. First, sTREM2 associations were characterized with respect to biomarkers of A β peptide abundance. CSF sTREM2 did not relate to A β_{1-42} ($p=2.59e-01$; **Table 3.2**; **Figure 3.1A**), consistent with previous work showing weak¹⁵⁸ or no association^{144, 160}. In contrast, higher levels of sTREM2 robustly related to higher CSF A β_{x-40} ($p=1.53e-09$; **Table 3.2**; **Figure 3.1B**), and to a lesser degree related to higher levels of N-truncated A β_{x-42} species ($p=7.72e-03$; **Table 3.2**; **Figure 3.1C**). Second, associations with biomarkers of tau pathology and axonal injury (NfL) were assessed. As expected, higher CSF sTREM2 was associated with higher levels of both total and phosphorylated tau ($p=6.13e-07$ and $1.81e-08$, respectively; **Table 3.2**; **Figures 3.1D-E**). High levels of sTREM2 also associated with high NfL ($p=3.18e-04$; **Table 3.2**; **Figure 3.1F**). Next, associations of sTREM2 levels with a CSF biomarker of BBB integrity were investigated. Higher levels of sTREM2 protein in CSF associated with an increased CSF/plasma albumin ratio, indicating decreased BBB integrity ($p=1.35e-07$; **Figure 3.2A**). This association remained regardless of *APOE*- $\epsilon 4$ carrier status, an independent predictor of BBB permeability (**Figure 3.2B**) and interaction models between the CSF/plasma albumin ratio and *APOE*- $\epsilon 4$ carrier status on sTREM2

levels (sTREM2 ~ CSF/plasma albumin ratio**APOE*- ϵ 4 + base covariates) were insignificant ($p=0.29$; **Supplemental Table 3.3**). A correlation matrix of sTREM2 and additional biomarkers is provided in **Supplemental Figure 3.3**.

Due to the novelty of the A β species results, we replicated associations of sTREM2 with both A β ₁₋₄₀ and A β ₁₋₃₈ in ADNI ($\beta=0.37$, $p=6.37e-38$ and $\beta=1.50$, $p=4.09e-34$, respectively; **Figures 3.3A-B**), indicating broad elevations of A β peptide species concurrent with rises in sTREM2.

Figure 3.1. Main effects of AD CSF biomarkers on sTREM2 levels. Unadjusted scatter plots showing the main effects of AD CSF Biomarkers (x axis) on CSF sTREM2 (y axis). Higher sTREM2 levels relate to increases in AD biomarkers of shorter amyloid- β peptides and neurodegeneration: (A) sTREM2 levels do not significantly relate to levels of full-length $A\beta_{1-42}$, $p=2.59e-1$. Higher sTREM2 levels significantly relate to increases in (B) $A\beta_{x-40}$, $p=1.53e-9$; (C) $A\beta_{x-42}$, $p=7.72e-3$; (D) total tau, $p=6.13e-7$; (E) phosphorylated tau, $p=1.81e-8$, and (F) NfL, $p=3.18e-4$. Protein measurements given in pg/mL.

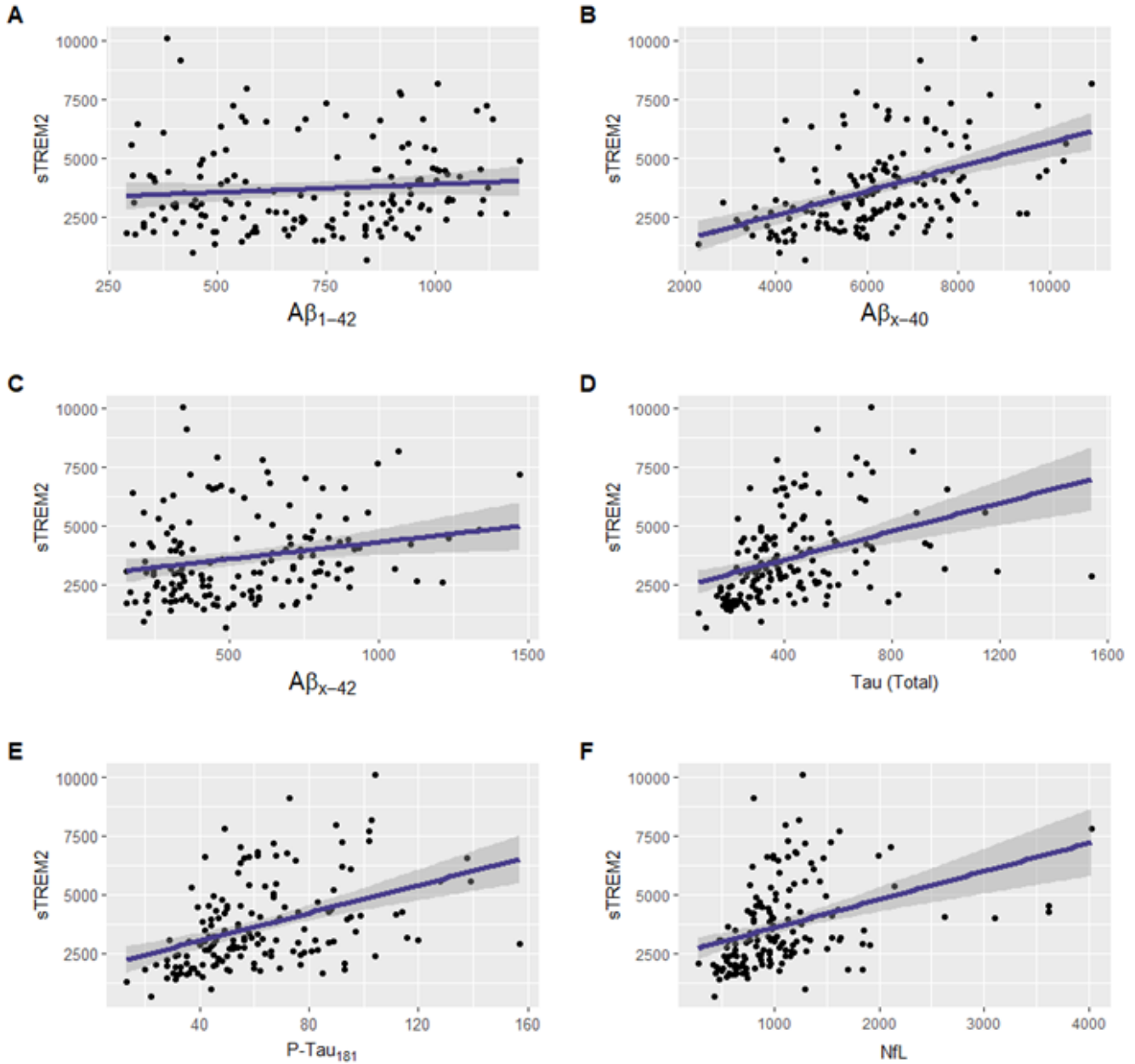


Table 3.2. Main Effects of Baseline CSF Biomarkers on sTREM2 Measurement

Predictor	β	SE	DF	P
$A\beta_{x-40}$	0.490	0.076	149	1.532e-09*
p-tau ₁₈₁	30.513	5.126	149	1.818e-08*
CSF/plasma albumin ratio	327.552	59.077	145	1.355e-07*
t-tau	3.146	0.604	149	6.137e-07*
NfL	0.969	0.263	144	3.185e-04*
$A\beta_{x-42}$	1.448	0.536	149	7.728e-03*
$A\beta_{1-42}$	0.678	0.599	149	2.599e-01

Bold represents statistical significance set to a *priori* threshold $P < 0.05$. An asterisk indicates survival for multiple comparisons by FDR correction across each primary model (Benjamini & Hochberg 1995). Significance value (P), degrees of freedom (DF), standard error (SE) and estimate of coefficient (β) represented for each model.

Figure 3.2. CSF/plasma albumin X APOE- ϵ 4 status on sTREM2. Unadjusted plots showing higher CSF sTREM2 levels relate to an increased CSF/plasma albumin ratio independent of APOE- ϵ 4 carrier status: (A) Main effect of the CSF/plasma albumin ratio on sTREM2 ($p = 1.35e-07$). (B) Interaction of CSF/plasma albumin* APOE- ϵ 4 carrier status on sTREM2 ($p.int. = 0.28$). sTREM2 protein measurements given in pg/mL.

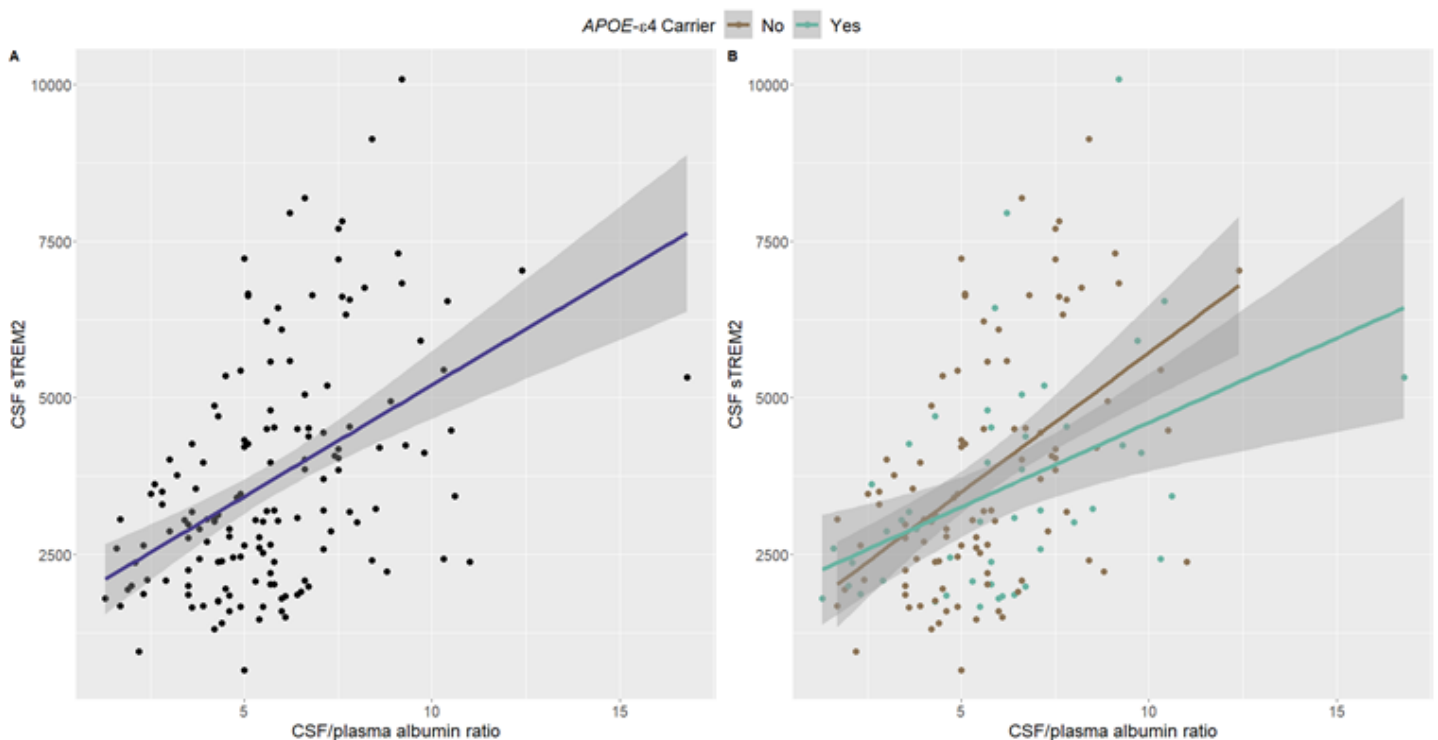
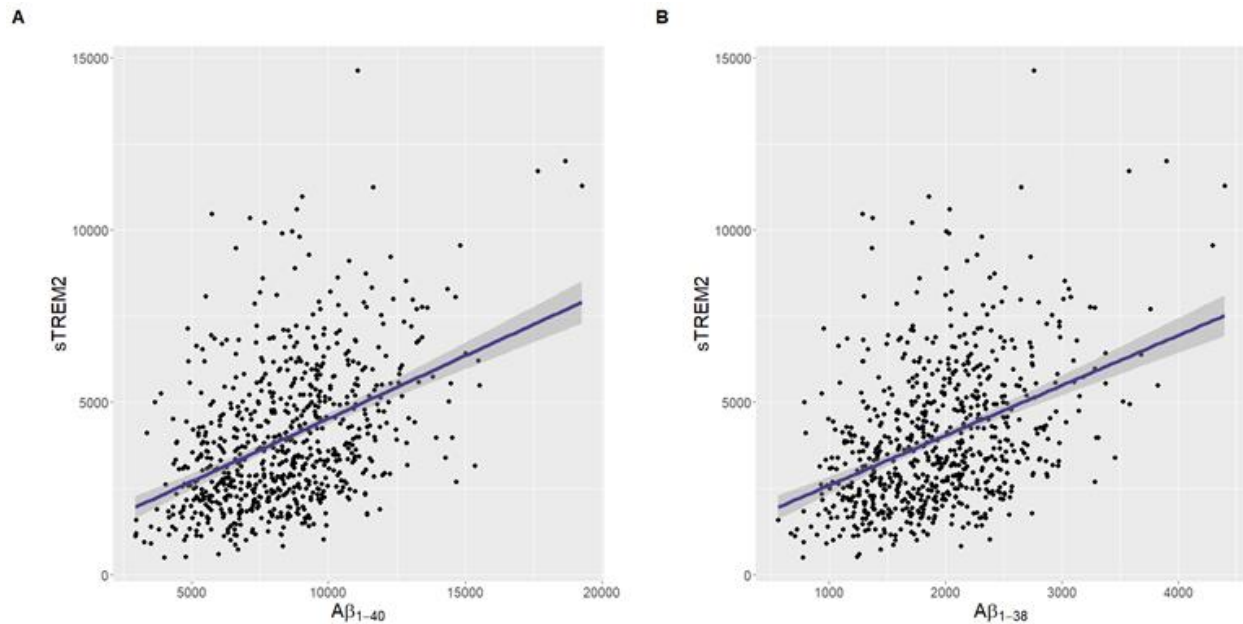


Figure 3.3. Main effects of AD CSF biomarkers on sTREM2 ADNI replication.

Unadjusted plots demonstrating main effects of shorter A β species on sTREM2 using ADNI data. Higher CSF sTREM2 levels relate to increases in CSF (A) A β 1-40 and (B) A β 1-38 ($\beta=0.37$, $p=6.37e-38$ and $\beta=1.50$, $p=4.09e-34$, respectively). Protein measurements given in pg/mL.



3.3 Competitive models highlight sTREM2 relationships beyond tau

To further deconvolve components of CSF sTREM2 signal in VMAP, competitive hierarchical linear regression models were utilized (**Table 3.3**). The base model (CSF sTREM2 ~ age + sex + education + cognitive diagnosis) explained 11.8% of variance in sTREM2 protein measurement. Independently, p-tau₁₈₁ explained 17.7%, A β _{x-40} explained 21.2% and the CSF/plasma albumin ratio explained 21.2% of variance in sTREM2 levels. For the purpose of model selection, p-tau was inputted first given the association is well-established in the literature. This allowed use of the hierarchical model to evaluate variance explained above and beyond p-tau and covariates. Model 1

includes p-tau₁₈₁ as a predictor explaining an additional 16.9% of variance in sTREM2 levels above and beyond the base model. The addition of Aβ_{x-40} in Model 2 explains an additional 4.6% of variance above and beyond Model 1. And the inclusion of the BBB marker in Model 3 explains 14.8% of variance above and beyond Model 2 (R²=0.4813). When including biomarkers (p-tau, Aβ, and the CSF/plasma albumin ratio) in Model 3 all three remained statistically significant. Together, p-tau₁₈₁, Aβ_{x-40}, and the CSF/plasma albumin ratio explain 36% of the variance in CSF sTREM2 levels.

Table 3.3. Competitive Hierarchical Linear Regression Results

Model	Formula	DF	AIC	BIC	R ²	Adjusted R ²	ΔR ²
base	CSF sTREM2 ~ age + sex + education + cognitive diagnosis	150	2778	2798	0.118	0.089	N/A
1	CSF sTREM2 ~ base covariates + p-tau ₁₈₁	149	2747	2770	0.288	0.259	0.169
2	CSF sTREM2 ~ base covariates + p-tau ₁₈₁ + Aβ _{x-40}	148	2738	2765	0.333	0.302	0.046
3	CSF sTREM2 ~ base covariates + p-tau ₁₈₁ + Aβ _{x-40} + CSF/plasma Albumin ratio	143	2636	2664	0.481	0.452	0.148

ΔR² = change in R² from previous nested model. Akaike information criterion (AIC) and Bayesian information criterion (BIC) calculations derived as follows: AIC = 2K – 2ln(L); where K = number of model parameters, and ln(L) = model log-likelihood. BIC = (RSS+log(n)dσ²) / n; where RSS = residual sum of squares, n = total observations, d = number of predictors, and σ² = estimate of variance of the error associated with each response

3.4 Deconvolving tau, Aβ, and BBB associations with post-hoc interaction models

Given the known association between CSF tau and CSF sTREM2, we sought to better understand if the novel sTREM2 associations with A β and BBB differed by tau status. We did not observe statistically significant interactions between A β_{x-40} and p-tau₁₈₁ on sTREM2 ($p=0.64$) or between the CSF/plasma albumin ratio and p-tau₁₈₁ ($p=0.25$), demonstrating associations were present regardless of tau status (**Supplemental Figures 3.4A-B**). Similarly, no significant interaction between A β_{1-40} and p-tau₁₈₁ positivity on sTREM2 in the larger ADNI dataset was observed ($\beta=0.07$, $se=0.06$, $p=0.22$; **Supplemental Figure 3.5**).

Sensitivity analyses

Interactions between tau markers with cognitive diagnosis, as well as *APOE- ϵ 4* carrier status on sTREM2, survived correction for multiple comparisons suggesting a stronger association between sTREM2 and biomarkers of tau pathology amongst *APOE- ϵ 4* non-carriers compared to carriers, and among individuals with NC compared to those with MCI (**Figures 3.4A-D**). Additionally, nominal interactions between tau and sex (**Supplemental Table 3.3**) were observed. In contrast, neither interactions between A β_{x-40} nor the CSF/plasma albumin ratio with sex, *APOE- ϵ 4* carrier status, or diagnosis (**Figures 3.5A-D** and **Supplemental Table 3.3**) were observed. In replication analyses using ADNI data we observed similar *APOE- ϵ 4* ($p<0.02$) and diagnosis interactions ($p<2.0e-05$; **Supplemental Figure 3.6**) with tau on sTREM2 levels and did not observe such interactions with A β species ($p>0.16$).

Figure 3.4. Tau interactions with diagnosis and *APOE*- ϵ 4 status on sTREM2.

Unadjusted plots showing tau biomarkers interact with cognitive diagnosis as well as *APOE*- ϵ 4 carrier status on sTREM2 levels in CSF: (A) phosphorylated tau*diagnosis, $p.int.=0.033$, (B) phosphorylated tau**APOE*- ϵ 4, $p.int.=0.006$, (C) total tau*diagnosis, $p.int.=0.003$, and (D) total tau* *APOE*- ϵ 4, $p.int.=0.002$. Protein measurements given in pg/mL.

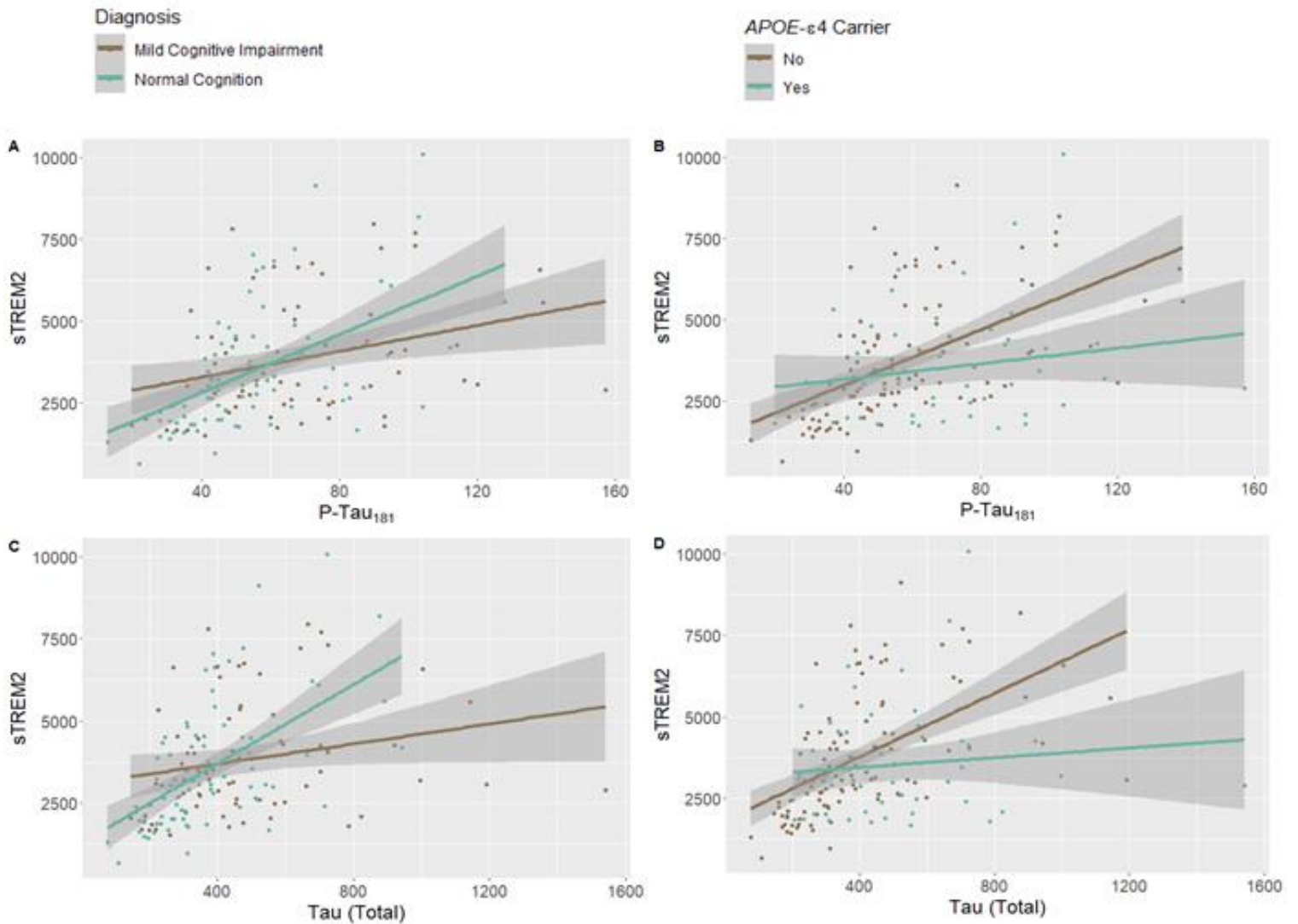
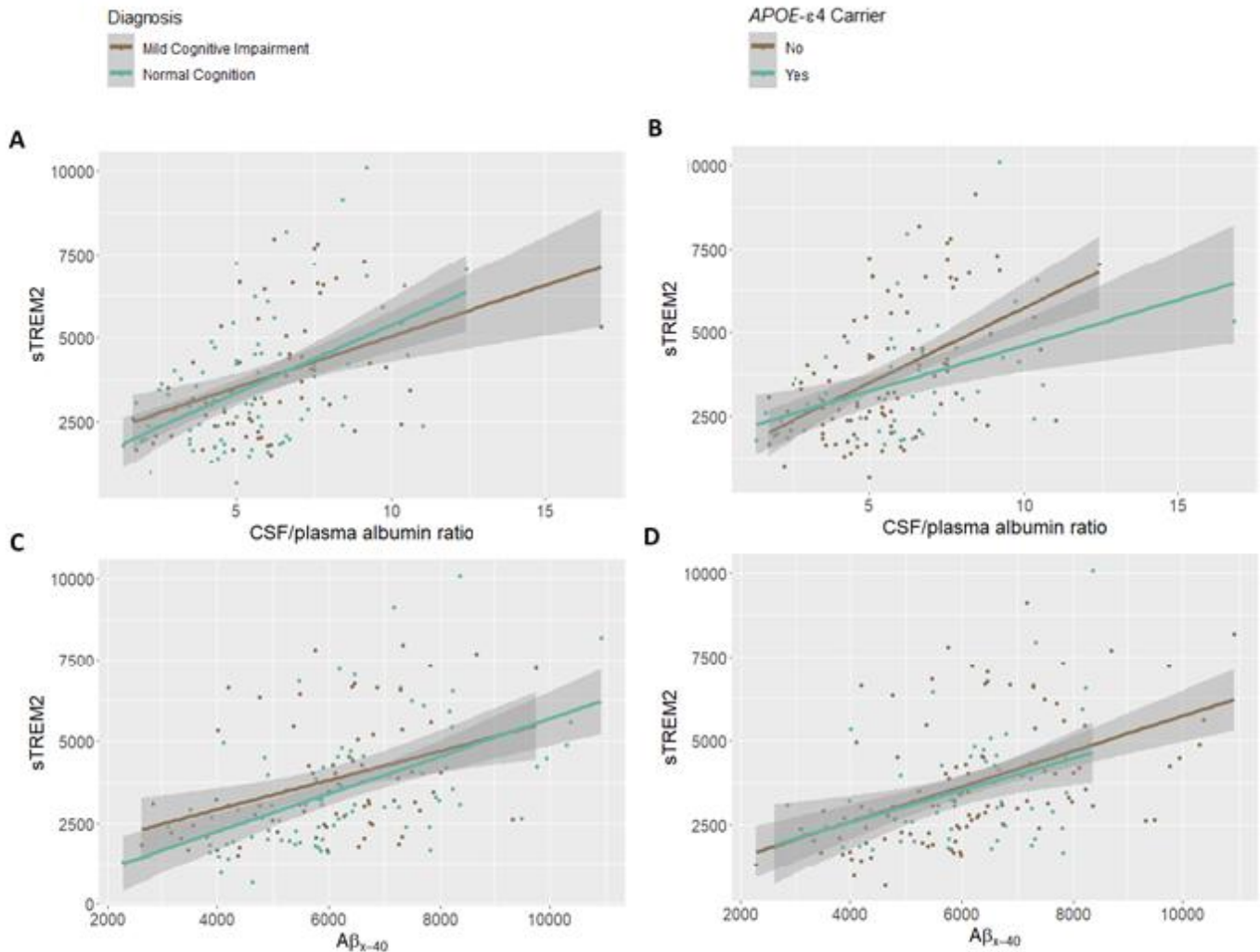


Figure 3.5. A β and BBB interactions with diagnosis and APOE- ϵ 4 status on sTREM2.

Unadjusted plot demonstrating A β , and BBB biomarkers do not significantly interact with cognitive diagnosis nor APOE- ϵ 4 carrier status on sTREM2 levels in CSF: (A) CSF/plasma albumin ratio * diagnosis, p.int.=0.62, (B) CSF/plasma albumin ratio * APOE- ϵ 4, p.int.=0.28, (C) A β_{x-40} * diagnosis, p.int. =0.36, and (D) A β_{x-40} * APOE- ϵ 4, p.int.=0.78. Protein measurements given in pg/mL.



Lastly, sensitivity analyses assessed the impact of MCI diagnosis criteria between VMAP and ADNI as well as statistical and visual outliers. Specifically, VMAP MCI diagnosis criteria was updated to resemble more closely that of ADNI. This included the removal of 13 individuals with a Clinical Dementia Rating (CDR) of 0 or a Montreal Cognitive Assessment (MoCA) score of 17 or less (a MoCA score of 18 corresponds to an MMSE score of 24) ¹⁶⁹. These analyses yielded similar results and are provided in **Supplemental Tables 3.6-3.9**.

3.5 Associations with cognition and clinical progression

Given that CSF p-tau₁₈₁, CSF A β _{x-40}, and the CSF/plasma album ratio all explain independent variance in sTREM2, next, it was explored which component of the sTREM2 variance is also associated with cognitive performance. This was evaluated by regressing out variance in sTREM2 associated with each biomarker sequentially and assessing the association between sTREM2 residual variance (when accounting for a given biomarker) with cognition. If regressing out a biomarker alters the association with cognition, it was concluded that the variance in sTREM2 associated with that particular biomarker is also relevant to cognitive performance. Baseline CSF sTREM2 levels predicted longitudinal memory in VMAP ($\beta=1.44e-05$, $se=6.80e-06$, $p=0.03$), similar to previous reports ^{170, 171} but not longitudinal executive functioning ($\beta= -3.22e-06$, $se=7.32e-06$, $p=0.66$). Due to the well-established association between tau levels and cognitive decline, we wanted to determine whether this association was due simply to covariance with tau. When regressing out the variance in sTREM2 associated with p-tau₁₈₁, the residual variance in sTREM2 remained associated with longitudinal memory decline ($\beta=1.68e-05$, $se=7.28e-$

06, $p=0.02$). Similarly, when regressing out the variance in sTREM2 associated with both the CSF/plasma albumin ratio and $p\text{-tau}_{181}$ the residual variance remained significantly associated with longitudinal memory decline ($\beta=2.21e-05$, $se=8.15e-06$, $p=6.83e-03$). In contrast, when regressing out the variance in sTREM2 associated with CSF $A\beta_{x-40}$, the residual variance was not associated with longitudinal cognitive performance ($\beta=1.37e-05$, $se=7.41e-06$, $p=0.06$). These results suggest that variance in sTREM2 that is related to $A\beta$ species may indeed be relevant to cognitive trajectory.

3.6 CSF sTREM2 does not relate to neuroimaging measures of cerebral small vessel disease

Due to the association between sTREM2 and BBB permeability it was sought to examine sTREM2 levels in relation to additional measures of vascular integrity using VMAP data. Hemodynamic and structural neuroimaging measures of cerebrovascular health and small vessel disease, including whole-brain CBF and CVR, cerebral microbleeds, lacunar infarcts, and global white matter lesion volume were utilized as outcome variables in these models. sTREM2 protein levels in CSF at baseline in VMAP were not associated with any of the neuroimaging measures of cerebrovascular health and disease (**Table 3.4**; $p>0.389$).

Table 3.4. Main Effects of Baseline CSF sTREM2 Measurement on Neuroimaging Measures of Cerebrovascular Injury

Outcome	β	P
Presence of cerebral microbleeds	-4.358e-05	0.669
Presence of lacunar infarcts	-4.522e-05	0.673
Global white matter lesion volume	3.026e-06	0.971
Grey matter cerebrovascular blood flow (CBF)	3.128e-04	0.389
Grey matter cerebrovascular reactivity (CVR)	3.045e-05	0.754

Furthermore, sex, MCI diagnosis as well as *APOE*- ϵ 4 carrier status did not interact with sTREM2 levels on these outcome measures (**Table 3.5**).

Table 3.5. CSF sTREM2 Interactions on Cerebrovascular Neuroimaging Measures

CSF sTREM2 Interactions on Cerebrovascular Neuroimaging Measures									
Outcome	sTREM2 x APOE-ε4 carrier status			sTREM2 x Sex			sTREM2 x MCI diagnosis		
	β	P	P.fdr	β	P	P.fdr	B	P	P.fdr
Hemodynamic									
Grey matter cerebrovascular blood flow (CBF)	1.720e-04	0.822	0.822	1.232e-03	0.271	0.541	3.246e-04	0.643	0.643
Grey matter cerebrovascular reactivity (CVR)	-2.226e-04	0.265	0.529	-1.298e-04	0.568	0.568	-1.661e-04	0.386	0.643
Structural									
Presence of cerebral microbleeds	-1.263e-04	0.556	0.647	1.878e-04	0.464	0.464	-7.920e-05	0.684	0.684
Lacunar infarcts	-1.059e-04	0.647	0.647	5.837e-04	0.045	0.134	-1.962e-04	0.332	0.498
Global white matter lesion volume	-2.845e-04	0.100	0.301	3.297e-04	0.119	0.179	-1.856e-04	0.243	0.498

Bold represents statistical significance set to a *priori* threshold $P/P.fdr < 0.05$ (Benjamini & Hochberg 1995).

Discussion

The present results provide an in-depth characterization of CSF sTREM2 expression in non-demented older adults. We provide strong evidence that fluid biomarkers of tau pathology, A β abundance, and BBB dysfunction independently relate to sTREM2 levels, and that together these biomarkers explain substantial variance in CSF sTREM2. Specifically, we recapitulate previously reported associations between CSF sTREM2 and both biomarkers of BBB integrity and tau pathology demonstrating for the first time that all three biomarkers (A β_{x-40} , the CSF/plasma albumin ratio, and p-tau) explain unique variance in sTREM2 using competitive models. Importantly, our results provide novel evidence that sTREM2 relates to elevated CSF A β species and that the variance in baseline CSF sTREM2 levels associated with A β_{x-40} predicts future cognitive performance. Together, our results highlight the need to better understand sTREM2 in relation to the complex intersection of AD neuropathology, microglial activation, and BBB dysfunction to characterize its utility as both a dynamic biomarker of disease and therapeutic target.

4.1 Unique contribution of tau, BBB dysfunction, and A β abundance to sTREM2 levels

Together, findings suggest that a heterogeneous set of biological correlates in the aging brain likely contributes to sTREM2 changes in CSF, including independent associations with tau, BBB dysfunction, and the most abundant A β species (**Table 3.2; Figures 3.1-3.2**). Given the previously described associations between CSF biomarkers of tau pathology and CSF sTREM2, it is not surprising that CSF p-tau₁₈₁ explained significant variance in sTREM2 levels. Previous work has demonstrated not only that

sTREM2 relates to CSF p-tau, but also that the ratio of sTREM2 to p-tau is predictive of future cognitive decline¹⁷⁰. Although this was not recapitulated in our smaller cohort, we do see a significant interaction between total tau and cognitive diagnosis on sTREM2 levels (sTREM2 ~ t-tau*diagnosis + base covariates) while p-tau performs similarly but does not reach statistical significance (**Figure 3.4**), demonstrating a stronger association between tau biomarkers and sTREM2 in cognitively normal individuals compared to those with MCI. Likewise, using ADNI data, the association between p-tau₁₈₁ and sTREM2 differs by diagnosis where tight coupling is attenuated in both MCI and AD compared to cognitively normal individuals (**Supplemental Figure 3.6**). Therefore, the sTREM2/p-tau ratio likely predicts longitudinal cognitive outcomes because of this decoupling of sTREM2 and tau as the disease progresses. In contrast to p-tau, A β _{x-40} explains a slightly larger percentage of variance in sTREM2, but this association does not differ by diagnosis. Interestingly, even when removing the variance in sTREM2 that is due to p-tau, the variance in sTREM2 that is associated with A β _{x-40} remains associated with future cognitive decline, suggesting that the complex interplay between A β abundance, tau pathology, and sTREM2 is needed to properly interpret the clinical relevance of this emerging biomarker. Finally, the CSF/plasma albumin ratio explained an additional 14.8% of variance in CSF sTREM2 beyond covariates, CSF p-tau₁₈₁, and A β _{x-40}, highlighting the potential importance of the neurovascular unit (NVU) to changing CSF sTREM2 levels (**Table 3.3**). While previous work has discussed the potential drivers of tau associations with sTREM2^{107, 149, 160}, less is known about the independent associations with BBB and A β abundance, so we expand our discussion of those two relationships below.

CSF sTREM2 relates to broad peptide species of CSF amyloid- β

CSF sTREM2 associations with A β have been inconsistent and focused on A β ₁₋₄₂^{144, 158-160}. However, we observed a robust, novel association between CSF sTREM2 and shorter species including truncated CSF A β (**Figure 3.1B-C; Table 3.2**) as well as A β ₁₋₄₀ and A β ₁₋₃₈ using ADNI data (**Figure 3.3**) that may explain some of the discrepant reports in the literature. One possibility is that the positive correlation between A β _{x-40} and sTREM2 concentration reflects a direct beneficial role of sTREM2 in facilitating amyloid clearance described in the animal model literature. Specifically, injection of recombinant sTREM2 in Trem2-knockout and wild-type mice, as well as in culture, induced inflammatory responses in microglia, significantly increasing IL-1 β , IL-10, IL-6, and TNF cytokine production and enhancing microglial survival⁷⁴. Additionally, sTREM2 stereotaxic injection in the hippocampus has been shown to ameliorate A β plaque load in 5XFAD mice, suggesting a beneficial role for sTREM2 in AD⁸⁴. However, we did not observe associations with A β ₁₋₄₂ or the A β _{42/40} ratio (**Supplemental Figure 3.3**), both of which are thought to be the most sensitive markers of AD neuropathology, suggesting the associations with other A β species may not reflect brain amyloidosis. This is particularly interesting given previous evidence that sTREM2 levels decline in the early preclinical stages of AD in amyloid positive individuals before elevating later in the disease cascade¹⁶⁰, a pattern recapitulated in the present cohort. It may be that the tau association masks an independent A β ₁₋₄₂ association as pathology begins to emerge, but the data presented cannot speak to such a possibility.

Beyond a direct role in A β processing or clearance, it is also possible that the association between sTREM2 and A β reflects a compensatory alteration in A β abundance in response to glial activation and/or altered neuronal activity. Synaptic activity has indeed been linked to the regulation of soluble A β abundance in interstitial fluid (ISF) in vivo and in vitro ^{172, 173}. And this activity-dependent modulation of A β production has been proposed as a compensation to neuronal hyperactivity ^{174, 175}. This compensation hypothesis aligns with our data suggesting the relationship of A β_{x-40} to sTREM2 may indeed be important to cognitive functioning. It is possible that prior to the onset of neurodegeneration, sTREM2 is elevated concurrently with an inflammatory response that promotes glymphatic trafficking of free and abundant A β peptide. As A β_{40} is the most abundant species, this provides for a more sensitive window in which it is possible to detect alterations of abundance in the CSF compartment by regulators of ISF/CSF flow. Functional studies will be needed to evaluate these mechanistic hypotheses and understand the interplay more thoroughly between A β species and TREM2 proteins. Finally, it is also possible that sTREM2 levels rise concurrently with a parallel mechanism of A β abundance that is causally unrelated or driven by a third unmeasured variable. Regardless of the mechanism, our results provide strong evidence that sTREM2 levels are correlated with the abundance of A β species in a manner that does not appear to be specific to plaque deposition and that does not change with clinical disease.

CSF sTREM2 relates to BBB integrity

We also identified an association of the TREM2 axis with BBB permeability, recapitulating one other report in the literature ¹¹⁰ whereby higher levels of CSF sTREM2 were associated with greater BBB permeability as indicated by the CSF/plasma albumin ratio (**Figure 3.2A; Table 3.2**). This association was independent of *APOE-ε4* carrier status (**Figure 3.2B**), suggesting an alternative pathway of cerebrovascular injury coincides with elevations in CSF sTREM2. Notably, our analyses revealed that BBB integrity, as measured by the CSF/plasma albumin ratio, explained a substantial proportion of variance in CSF sTREM2 levels (**Table 3.3**). BBB breakdown allows blood-derived accumulation of toxic proteins (i.e., fibrin and thrombin), microbial agents, as well as peripheral immune cells within the brain parenchyma ²⁷. In turn, this remodeling drives microglial alterations associated with elevated sTREM2. Moreover, it is possible that the high levels of CSF/plasma albumin and sTREM2 reflect a compensatory change in barrier permeability in response to deposition of amyloid as early neuroinflammation may also serve to stave off plaque formation. Similarly, the pro-inflammatory role of sTREM2 in activating microglia may drive cerebrovascular dysregulation as microglia are known to regulate critical NVU mechanisms such as the recruitment of peripheral immune cells and the integrity of tight junction proteins ¹⁷⁶. This balance of neuronal-glia-vascular communication is a critical component of AD pathophysiology and subsequent heterogeneity. A better understanding of the role of sTREM2 and BBB function is critical, particularly as modulation of TREM2 is being actively pursued as a treatment target for AD pathogenesis ⁵¹. Future studies including longitudinal measurement of sTREM2, and markers of cerebrovascular injury are

needed to determine whether early elevations of sTREM2 predict changes in other NVU processes over the course of disease.

CSF sTREM2 expression was additionally characterized in relation to neuroimaging biomarkers of cerebrovascular health and disease. Results show baseline CSF sTREM2 did not associate with grey matter measurement of CBF nor CVR indicating sTREM2 protein levels may not be an efficacious predictor of hemodynamic changes during the preclinical or prodromal stages of AD. Similarly, CSF sTREM2 did not associate with structural measurements of morphological substrates of small vessel disease, further suggesting that CSF sTREM2 does not correlate with cerebrovascular neuropathology during an early window of disease. Conversely, very few individuals in VMAP were diagnosed with CVD (n=5/155) and exclusion criteria included a diagnosis of dementia. Therefore, it is possible that results may differ in a setting of more severe disease or vascular dementia. In summary, elevated CSF sTREM2 appears to occur in the absence of neuroimaging evidence of overt cerebrovascular disease, suggesting associations may be specific to the BBB. Despite many sensitive neuroimaging outcome measures, one important limitation to note was the lack of a neuroimaging marker of BBB integrity, which precludes the confirmation of a structural correlation of sTREM2 and BBB permeability. Future studies will be needed to determine this as well as the exact relationship between concurrent elevations in CSF sTREM2 and the CSF/plasma albumin ratio.

Strengths and limitations

Our deeply characterized cohort provides rich timepoints early in the disease process providing a unique opportunity to understand changes in sTREM2 within the preclinical period. Moreover, we were able to replicate previous associations and provide independent replication for the novel associations reported herein. Despite these strengths, our focus on baseline biomarker measurements precludes the temporal resolution and experimental control needed to determine cause and effect. Finally, it should be noted that our sample is enriched for highly educated, non-Hispanic White individuals, limiting our ability to generalize to other populations.

Conclusions

Taken together, we demonstrate that CSF sTREM2 relates to biomarkers of concomitant pathological processes in AD including A β peptide abundance, tau pathology, and BBB dysfunction. We highlight multiple novel and independent pathways that are relevant to sTREM2 levels in aging and AD, enhancing its characterization as a biomarker and therapeutic target. Results suggest sTREM2 is relevant to cognitive progression with a heterogeneous etiology that must be further explored if it is going to have future clinical utility.

CHAPTER 4

“MS4A-ASSOCIATED SNP INTERACTIONS WITH *TREM2* & *STREM2* EXPRESSION ON ALZHEIMER’S DISEASE PATHOLOGY”

Introduction

Variants in the membrane-spanning 4-domains subfamily A (MS4A) gene cluster have been previously linked to late-onset AD risk modulation in several large GWAS^{93, 94, 177-180}, implicating the 12.2 region on chromosome 11q spanning roughly 800kb and including genes *MS4A6A*, *MS4A4E* and *MS4A4A*. Since that initial discovery, the same *MS4A6A* and *MS4A4A* associated variants have also been associated with CSF sTREM2 levels in humans^{92, 95}. MS4A proteins belongs to the tetraspanin superfamily of cellular membrane proteins which are enriched primarily in hematopoietic cells with immunomodulatory functions, such as monocytes and dendritic cells. Several tetraspanin superfamily members are expressed in microglia in brain, including *MS4A4A* and *MS4A6A*^{92, 181, 182}. Although this family of proteins is largely uncharacterized, MS4A proteins are known to be involved in calcium signaling, mast cell degranulation, as well as activation and regulation of both B and T cells. Therefore, several anti-MS4A antibodies have proven effective for autoimmune diseases including multiple sclerosis^{183, 184} and experimental autoimmune encephalomyelitis¹⁸⁵ wherein there is immune hyperactivity . However, to-date, there is no clear link between the MS4A AD-associated SNPs and AD progression¹⁸⁶.

Despite this gap in knowledge, MS4A proteins have several important documented functions in the regulation of AD-relevant immunopathology. For example, members of

the MS4A gene family regulate the of activation and function of T cells. MS4A4B knockdown was found to induce apoptosis whereas overexpression attenuated apoptosis of activated T cells. Another member, MS4A2, is expressed on mast cells in the brain localized to the BBB which undergo cell-cell communication with surrounding components of the neurovascular unit including microglia, vascular endothelial cells, and astrocytes¹⁸⁷. MS4A2 demonstrates the ability to promote T cell infiltration. Its expression promotes inflammation and leads to an increase in T cell activation, survival, as well as infiltration across the BBB¹⁸⁶. Although the exact mechanisms and extent of contribution from peripheral and central immune systems crosstalk to AD pathogenesis is debated, previous research shows increases in T cell infiltration in AD and expression in brain cause microglial activation, subsequent inflammation, and neuronal damage^{43, 188, 189}. Therefore, it is hypothesized that MS4A cluster proteins contribute to AD pathogenesis via immune dysregulation that may involve a complex interplay between peripheral and central immune cell types.

Strikingly, two variants in the MS4A gene cluster were found to be independent genome-wide significant modifiers of CSF sTREM2 expression levels⁹². The main signal, rs1582763, was associated with increased CSF sTREM2 expression and previously linked to decreased risk and slower onset of AD. This SNP explains 6% of CSF sTREM2 expression while another independent signal, rs6591561 helped explain another 1%. In contrast to rs1582763, rs6591561 was associated with decreased CSF sTREM2 levels, but increased risk of AD. Higher levels of CSF sTREM2 have indeed been associated with better cognitive and neuropathological outcomes in AD^{84, 170, 171,}

^{190, 191}. Therefore, we can hypothesize that genetic regulation of sTREM2 production via MS4A SNPs may gate progression of the disease.

Functional annotation of these SNPs by Deming et. al.⁹² revealed a cis-acting eQTL effect using Brainiac and GTEx data. Intergenic rs1582763 increased cortical and decreased peripheral blood expression of MS4A4A and MS4A6A. No trans-eQTL effect on TREM2 expression in brain was found suggesting MS4A4A and/or MS4A6A are responsible for modulating sTREM2 levels. Further supporting this idea were analyses performed by Deming and colleagues using human macrophage culture demonstrating TREM2 and MS4A4A colocalize in the membrane on lipid rafts. Additionally, sTREM2 mRNA expression was significantly higher in macrophages with lentiviral-induced overexpression of MS4A4A as well as with decreasing concentrations of anti-MS4A4A antibody suggesting MS4A4A expression leads to increased sTREM2 production. Finally, results from these same authors utilizing mendelian randomization models highlight variation in sTREM2 levels mediated by these opposing tool SNPs as causal as opposed to being associated with AD risk by means of reverse causality or a confounding variable. Together genetic and functional studies indicate a possible role of MS4A4A and/or MS4A6A upstream TREM2, and, specifically, a potential causal role of sTREM2 in AD pathogenesis^{92, 95, 186}. Additionally, the discovery of genetic regulators of constitutive sTREM2 expression and association with AD bolsters existing evidence for a central role of TREM2/sTREM2 expression contributions to disease beyond that of rare *TREM2* risk variants. A crucial step remains to establish a potential association between genetic regulation of the MS4A gene cluster and AD neuropathology. Fortunately, these two MS4A SNPs with opposing profiles for AD risk modulation, onset,

as well as sTREM2 abundance makes them a great pair of variant tools for further interrogating the associations of MS4A genes with AD phenotypes. Furthermore, since they are both common SNPs found in over 30% of the population^{92, 93}, this indicates that the MS4A cluster regulates constitutive sTREM2 production whereby, a large portion of the population has higher or lower basal levels of sTREM2. Despite natural variation in sTREM2 levels among individuals, possible differences in the levels of A β , tau, or cerebrovascular pathology remain to be determined in relation to MS4A AD-associated SNP status.

Therefore, we sought to determine whether rs1582763 and or rs6591561 interact with sTREM2 levels on multiple markers of AD pathology in VMAP. As per rationale in previous chapters (1-3), the intent was to examine these interactions across markers of A β , tau, and cerebrovascular neuropathology. Due to the proposed role of sTREM2 fragment in regulating microglial response to A β plaques⁸⁴ as well as additional studies showing sTREM2 levels associated with BBB permeability¹¹⁰, also changes in expression of sTREM2 related to α 4 β 1-mediated T cell migration across this barrier¹⁹², CSF sTREM2 levels may be at least partially dependent on peripheral-central inflammatory communication. For these reasons, it was hypothesized that genetic regulation by MS4A variants of CSF sTREM2 levels modify critical sTREM2-mediated neuroinflammatory responses during early A β deposition. It is clear that CSF sTREM2 levels increase with the onset of neurodegeneration in AD^{158, 167}, but because of a lack of functional relationship between sTREM2 and tau itself, it was less certain whether this relationship would extend to a subsequent immunological response to tau.

Specifically, whether genetic regulation of sTREM2 by MS4A variants would modify this later outcome.

Because several previous results indicated a stronger coupling between the TREM2 pathway and amyloid rather than tau (see chapters 2 and 3) and the preclinical animal model literature implicates sTREM2 in early amyloid clearance⁸⁴ – we hypothesized both rs1582763 and rs6591561 would interact with sTREM2 levels on amyloid outcomes but in opposite directions. Specifically, the AD-protective rs1582763 minor allele (MAF = 0.368) may interact with CSF sTREM2 levels to drive established positive associations with shorter CSF A β species which potentially mark processing of A β species not preferentially allocated to parenchymal plaques. MS4A4A missense mutation and AD risk variant, rs6591561_G (p.M159V, MAF = 0.316), was thus hypothesized to attenuate the known positive association between sTREM2 levels and truncated A β species in CSF, indicating reduced processing of trafficable species and potentially a reduced ability to mount a proper sTREM2-mediated immune response against AD neuropathology. These interactions were hypothesized to extend to the previously established main effect of sTREM2 levels on BBB permeability, whereas sTREM2's response to amyloid may be accompanied by early neuroinflammation and hence increases in barrier permeability as measured by the CSF/plasma albumin ratio. However, the directional hypothesis we make *a priori* is difficult given the lack of molecular etiology surrounding the coupling between sTREM2 and AD pathology.

Methods

Participant data was acquired from four separate cohort studies of aging and dementia. VMAP methods including lumbar puncture and biochemical quantification of CSF biomarkers, cognitive diagnosis, neuropsychological composites of memory and executive functioning, and blood draw and albumin measurement are included in Chapter 3 (pages 60-63). ADNI methods of CSF sTREM2 biomarker quantification as well as 2D-UPLC-tandem mass spectrometry measurements of A β ₁₋₄₂, A β ₁₋₄₀, and A β ₁₋₃₈ CSF peptides are also included in Chapter 3 (page 63). ROS/MAP autopsy measures of AD neuropathology, *TREM2* mRNA quantification, and cohort demographics are described in Chapter 2 (pages 25-30). Additional methods included in this present chapter are specified as follows:

Genotyping and Quality Control

Genotyping was performed using whole blood (VMAP and ADNI) or brain tissue extracted DNA (ROS/MAP) on the following genotyping arrays: Illumina MEGA^{EX} (VMAP); three Illumina platforms were used in ADNI: Human610-Quad, HumanOmniExpress, and Omni 2.5M. ROS/MAP genotypes were also obtained on multiple platforms: Affymetrix Genechip 6.0, Illumina Human1M, and Illumina Global Screening Array. Sample sets genotyped on different arrays were processed and imputed in parallel and merged after imputation.

Standard QC was performed in accordance with the Computational Neurogenomics GWAS pipeline (Vanderbilt Memory and Alzheimer's Center) which excluded variants with genotyping efficiency <95% or minor allele frequency (MAF) <1.

Additionally, samples with call rates <99%, who exhibited an inconsistency between reported and genetic sex (i.e., assigned females with an X chromosome homozygosity estimate >0.8 or assigned males with a value <0.2), who displayed excess relatedness (i.e., π -hat >0.25) or excessively high or low rates of heterozygosity (i.e., >5 SD) were removed. In order to detect samples with large-scale differences in ancestry, principal components (PCs) were calculated using 1000 Genomes (<http://ftp.1000genomes.ebi.ac.uk/vol1/ftp/release/20130502/>) as reference populations. Individuals who self-reported as non-Hispanic White were kept. PLINK, versions 1.9 and 2.0 (<https://www.cog-genomics.org/plink/>) were used. Prior to imputation, all palindromic, multi-allelic or duplicated variants were removed. Then, variant positions were lifted over to genome build 38 (when appropriate) and compared to the TOPMed reference panel. Variant strand, position, and reference allele assignment were updated, where necessary. Variants were excluded if they failed lift-over or did not match the reference panel.

Imputation was performed on the TOPMed Imputation Server version 1.5.7 (<https://imputation.biodatacatalyst.nhlbi.nih.gov/>), using Minimac4, and Eagle for phasing. The genetic data was then filtered for imputation quality ($R^2 > 0.8$) and multiallelic SNPs. Finally, variants were filtered for $MAF > 0.01$, and Hardy-Weinberg Equilibrium $p > 1E-06$. Genetic ancestry was assessed using PCs and sample outliers were identified and removed.

ROS/MAP SRM Proteomic Measures of A β and Tau

Frozen dIPFC tissue samples were utilized for single reaction monitoring mass spectrometry (SRM) proteomic analysis. Sample preparation and standard protocols are previously described^{193, 194}. Experiments were carried out using a nano ACQUITY UPLC coupled to TSQ Vantage MS instrument where 2 μ L of sample was injected for each measurement. Peptide separations were performed by an ACQUITY UPLC BEH 1.7 μ m C18 column (75 μ m i.d. \times 25cm) at a flow rate of 350nL/min using a gradient of 0.5% buffer (0.1% FA in 90% ACN) in 0-14.5min, 0.5-15% in 14.5-15.0min, 15-40% in 15-30min and 45-90% in 30-32min. The heated capillary temperature and spray voltage was set at 350 °C and 2.4kV, respectively. Both the Q1 and Q3 were set as 0.7FWHM (full width at half maximum). A scan width of 0.002m/z and a dwell time of 10ms were used. Data were analyzed by Skyline software¹⁹⁵. Accuracy of peak assignments and boundaries were inspected manually. The peak area ratios of endogenous light peptides and their labeled internal standards were automatically calculated by Skyline. Endogenous peptide quantification was assessed as a ratio of spiked-in synthetic heavy isotope-labeled peptides (“light”/”heavy”). Relative abundance of each peptide was normalized yielding a median log₂-transformed ratio of zero to adjust for differences in protein expression between samples. Quality control of signal to noise ratio was assessed as the ratio of variance across subject samples to that of technical controls. This involved a scattering of pooled control samples throughout the experiment (8 samples/96-well plate) allowing for capture of technical variance from sample preparation or instrumental measurement. Peptides measurements with a signal to noise ratio of less than 2, >10% missingness and/or >4 standard deviations from the mean were removed prior to model analyses.

Statistical Analysis

Statistical analyses were performed in R v3.6.1 using R Studio IDE (<https://www.rstudio.com/>). To evaluate the data, a multiple linear regression models (for cross-sectional cognition and AD-related pathology outcomes) were used. Linear regression models covaried for age (or age at death), sex, post-mortem interval (when appropriate), and education. Models assessed MS4A SNP interaction with CSF sTREM2 protein or *TREM2* mRNA expression levels on the following AD clinical and neuropathological outcome measures: cross-sectional baseline cognition (VMAP/ADNI), CSF biomarkers A β ₁₋₄₂, A β _{x-42}, A β _{x-40}, p-tau, t-tau, CSF/plasma albumin ratio (VMAP), mass spectrometry measurement of A β ₁₋₄₂, A β ₁₋₄₀, A β ₁₋₃₈, (ADNI), and mass spectrometry measurement (SRM) of tau AT8, total A β , and A β ₁₋₃₈ peptides (ROS/MAP). ADNI and ROS/MAP data allowed for replication of SNP interactions from initial findings using the VMAP discovery cohort including outcome measures of cognition, and A β .

Sensitivity analyses were conducted to account for possible variation in model predictions due population structure/ancestry by the adding the first five principal components of the genetic data as covariates in the SNP interaction models. Similarly, additional models included race as a covariate. These sensitivity analyses yielded similar results.

All models were corrected for multiple comparisons using the Benjamini & Hochberg (1995) false discovery rate based on the total number of tests completed,

accounting for all interaction analyses. Statistical outliers of *TREM2* mRNA or sTREM2 protein outside four standard deviations from the mean were removed.

Results

Participant Demographics

For detailed cohort demographics in VMAP please see “Participant Demographics” Chapter 3 (pages 66-67) utilizing the same discovery cohort of 155 individuals with CSF sTREM2 measurement. Non-Hispanic white data was used for MS4A-associated SNP interaction analyses in VMAP filtering our sample size for individuals with sTREM2 measurement in CSF and genotype information to N=127 and N=128, respectively, for rs1582763 and rs6591561.

Minor Allele of rs1582763 is Associated with Increased CSF sTREM2 Levels

As expected, individuals carrying the minor allele (A<G) of rs1582763 had higher concentrations of sTREM2 in CSF as compared to non-carriers (**Figure 4.1**; $p=0.004$). There was a dose-dependent response of CSF sTREM2 concentration to minor allele dosage. However, few individuals in this cohort were homozygous for rs1582763_A (**Figure 4.1B**; N=15). Additionally, these increased levels of sTREM2 in minor allele carriers were not specific to cognitive diagnosis, suggesting this SNP contributes to constitutive levels of sTREM2 in CSF (**Figure 4.1C**). In contrast to rs1582763 minor allele carriers, there was no association between sTREM2 levels and rs6591561 genotype (**Figure 4.2**). We expected this risk allele, rs6591561_G, to be associated with decreased CSF sTREM2, supporting results from Deming et. al. 2019⁹². The lack of

significant association may be due to our smaller sample size (N=155) as compared to the initial report concerning 813 individuals in ADNI. Furthermore, these individuals in ADNI included those with clinical AD diagnosis. Whereas this VMAP cohort does not include AD participants and the lack of association between sTREM2 levels and rs6591561 genotype holds true across cognitive diagnosis of either NC or MCI (**Figure 4.2C**).

Figure 4.1. CSF sTREM2 characterization across rs1582763 genotype. (A) CSF sTREM2 levels are increased in minor allele (A) carriers compared to non-carriers **(B)** Increases in CSF sTREM2 are seen in heterozygote carriers compared to non-carriers. P-values reported by a student's t-test. **(C)** sTREM2 increases according to the presence of minor allele by cognitive diagnosis. sTREM2 measurement in pg/mL.

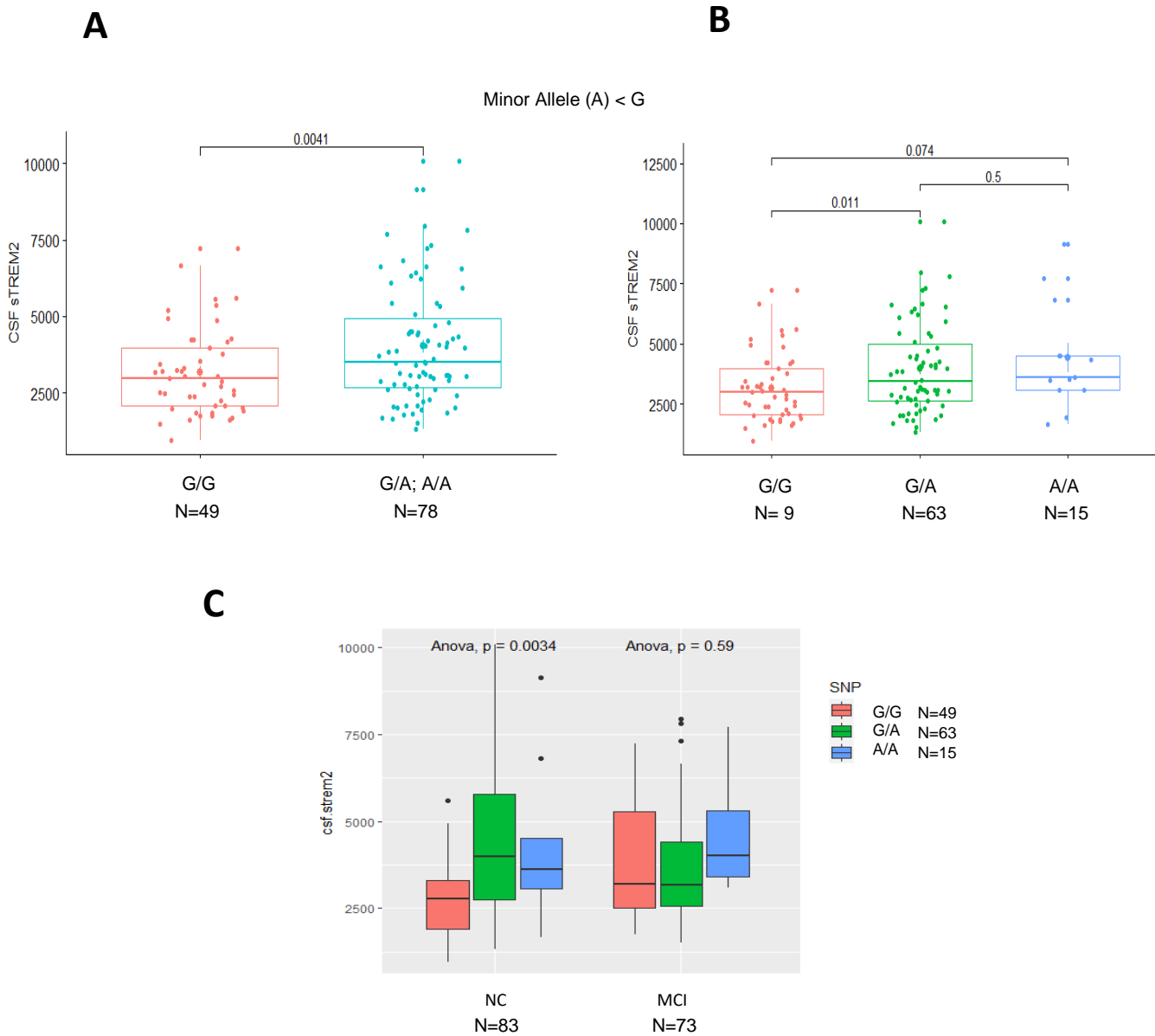
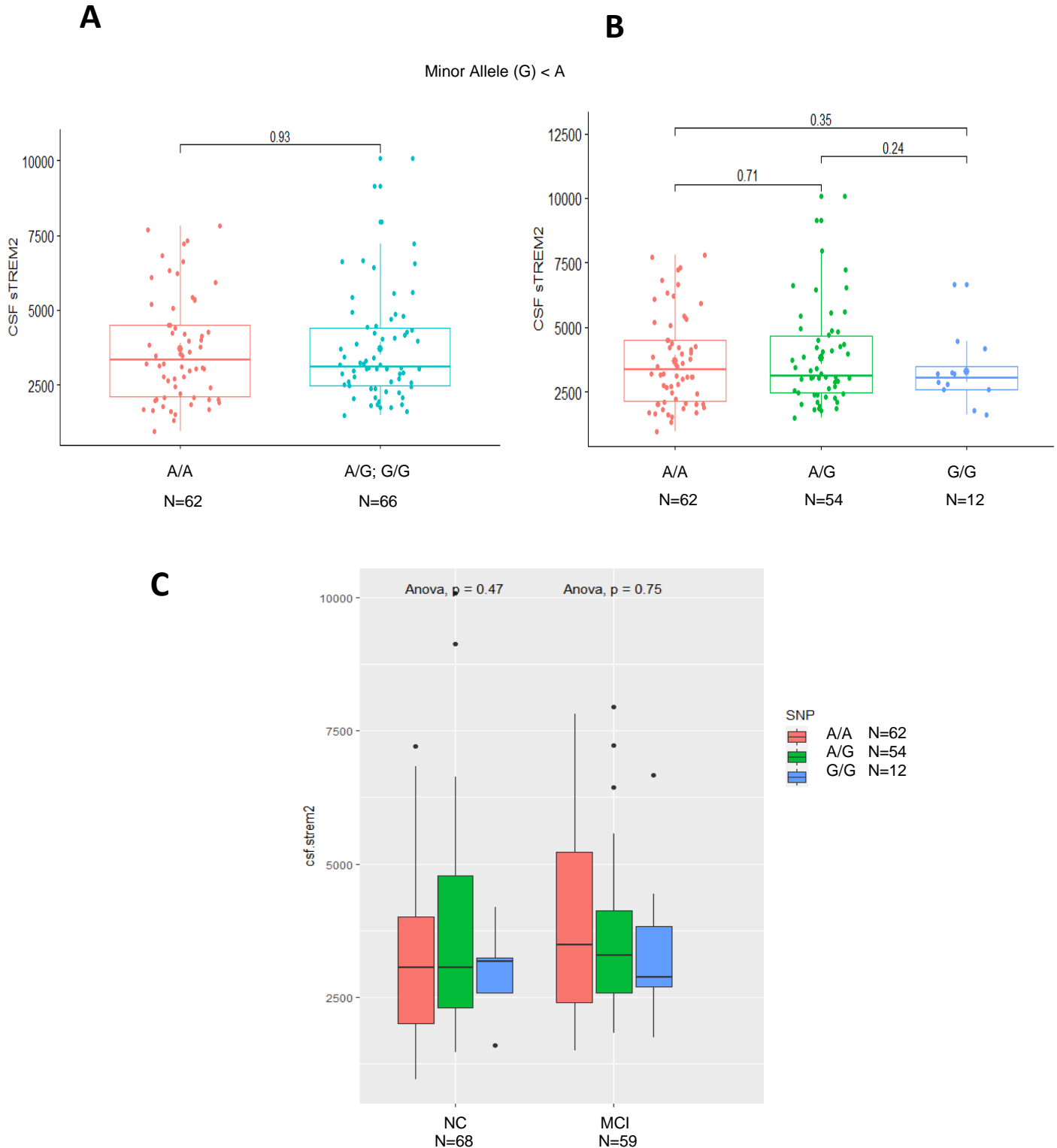


Figure 4.2. CSF sTREM2 characterization across rs6591561 genotype. (A-B) sTREM2 levels were not associated with rs6591561 genotype. P-values reported by a student's t-test. **(C)** sTREM2 levels were not associated with rs6591561 genotype when stratified by cognitive diagnosis. sTREM2 measurement in pg/mL.



rs1582763 Minor Allele Interacts with CSF sTREM2 Levels on Select AD Biomarkers of Neuropathology

Table 4.1 compiles interaction results (rs1582763 minor allele presence*CSF sTREM2) from cross-sectional linear regression models across AD biomarkers of interest. The minor allele, rs1582763_A, interacted with sTREM2 levels on select biomarkers of AD neuropathology. As hypothesized, rs1582763_A modified the association between sTREM2 levels and shorter A β species in CSF. Specifically, the presence of rs1582763 minor allele attenuated the positive association between increases in sTREM2 and increases in A β_{x-42} as well as A β_{x-40} in CSF (**Figure 4.3**; $\beta=-0.093$, $p=0.006$ and $\beta=-0.439$, $p=0.017$, respectively). In contrast, we observe insignificant results with A β_{1-42} (**Table 4.1**; $\beta=-0.051$, $p=0.101$) in keeping with a lack of main effect of CSF sTREM2 levels on this particular outcome in VMAP. Interestingly, the positive association between CSF levels of sTREM2 and a marker of increased BBB permeability, CSF/plasma albumin ratio, was driven by rs1582763_A carriers and absent in non-carriers (**Table 4.1** and **Figure 4.3**; $\beta=0.0007$, $p=0.009$). Finally, interaction results revealed that rs1582763_A does not significantly modify the positive association between sTREM2 levels and biomarkers of tau pathology in CSF (**Table 4.1**; t-tau, $\beta=-0.036$, $p=0.108$; tau_{181P}, $\beta=-0.004$, $p=0.114$).

Sensitivity analysis employing models built with an additive (non-carrier=0; heterozygote=1; homozygote=2) as opposed to binary (presence=1; absence=0) interaction term encoding MS4A SNP minor allele genotype yielded similar results.

Table 4.1. sTREM2 * Presence of rs1582763 Minor Allele (A<G) Interaction on CSF AD biomarkers

VMAP Outcome	β	P
$A\beta_{x-42}$	-0.093	0.006*
CSF/plasma Albumin ratio	0.0007	0.009*
$A\beta_{x-40}$	-0.439	0.017*
t-Tau	-0.036	0.108
$A\beta_{1-42}$	-0.051	0.101
Tau_{181P}	-0.004	0.114

Bold represents statistical significance set to a *priori* threshold $P.fdr < 0.05$

* Signifies significance after multiple corrections using the Benjamini & Hochberg (1995) false discovery rate based on number of tests completed

Figure 4.3. rs1582763 X sTREM2 interactions on A β peptides. Genetic regulation of MS4A (presence of rs1582763_A) attenuates the associations between increased sTREM2 and increased shorter A β peptide in CSF including **(A)** A β_{x-42} (pg/mL) and **(B)** A β_{x-40} (pg/mL).

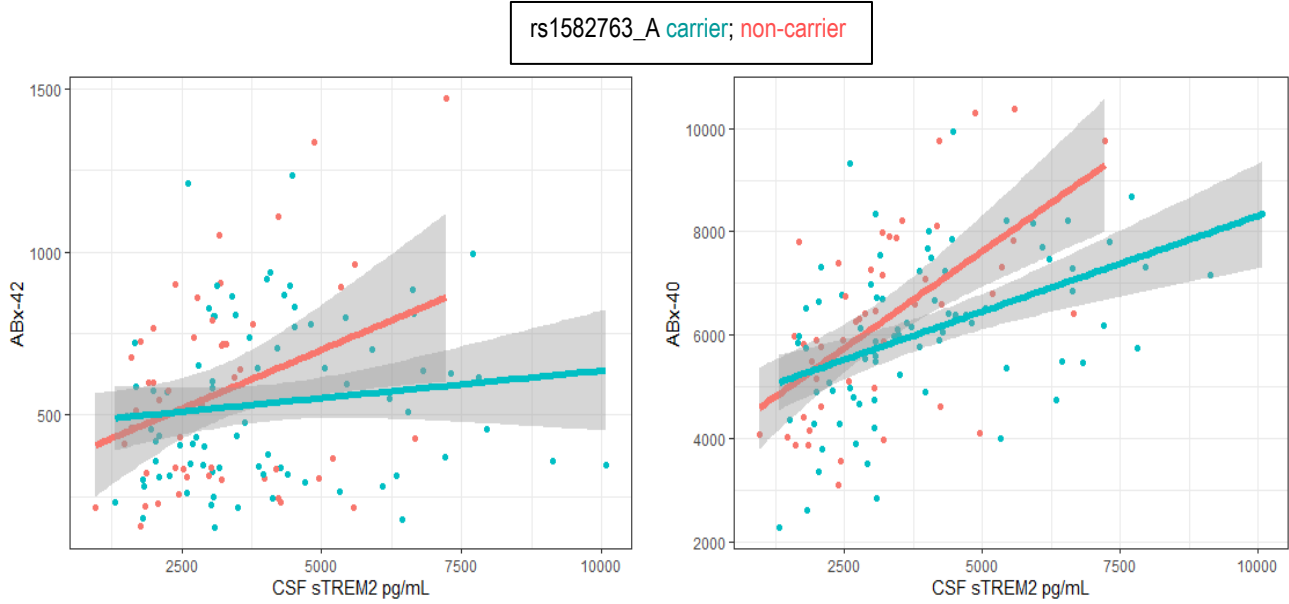
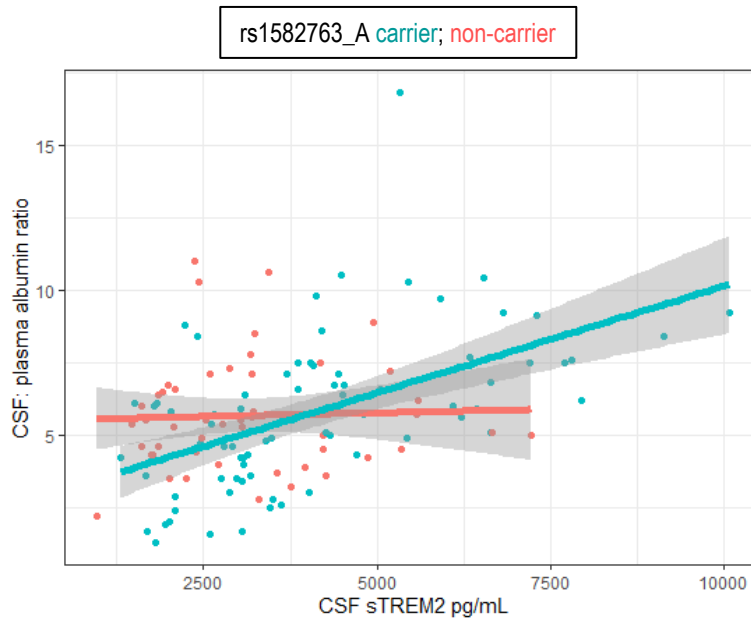


Figure 4.4. rs1582763 X sTREM2 interaction on CSF/plasma albumin. Genetic regulation of MS4A (presence of rs1582763_A) drives the association between increased CSF sTREM2 and increased CSF/plasma Albumin ratio (pg/mL).



rs6591561 Minor Allele Does Not Interact with CSF sTREM2 Levels on AD Biomarkers of Neuropathology

In addition to a lack of association with CSF sTREM2 expression levels in VMAP, the presence of rs6591561 minor allele did not interact with sTREM2 expression on any biomarker of neuropathology. **Table 4.2** summarizes these results including a lack of effect on N-truncated $A\beta_{x-42}$ as well as $A\beta_{x-40}$ (**Figure 4.5**; $\beta=-0.008$, $p=0.757$ and $\beta=0.112$, $p=0.445$, respectively). Similarly, interaction results for CSF/plasma albumin ratio were insignificant (**Table 4.2**; $\beta=-2.190e^{-4}$, $p=0.303$). Positive association between sTREM2 levels and this BBB integrity marker holds amongst both carriers and non-carriers of rs6591561 minor allele, rs6591561_G (**Figure 4.6**).

Sensitivity analysis employing models built with an additive interaction term were also insignificant.

Table 4.2. sTREM2 * Presence of rs6591561 Minor Allele (G<A) Interaction on CSF AD biomarkers

VMAP Outcome	β	P
$A\beta_{x-42}$	-0.008	0.757
CSF/plasma Albumin ratio	-2.190e ⁻⁴	0.303
$A\beta_{x-40}$	0.112	0.445
t-Tau	0.011	0.545
$A\beta_{1-42}$	-0.020	0.411
Tau _{181P}	0.001	0.552

Statistical significance set to a *priori* threshold $P.fdr < 0.05$

Figure 4.5. rs6591561X sTREM2 interactions on A β peptides. There is no significant effect of genetic regulation of MS4A (presence of rs6591561_G) on the associations between increased sTREM2 and increased shorter A β peptide in CSF including **(A)** A β_{x-42} (pg/mL) and **(B)** A β_{x-40} (pg/mL).

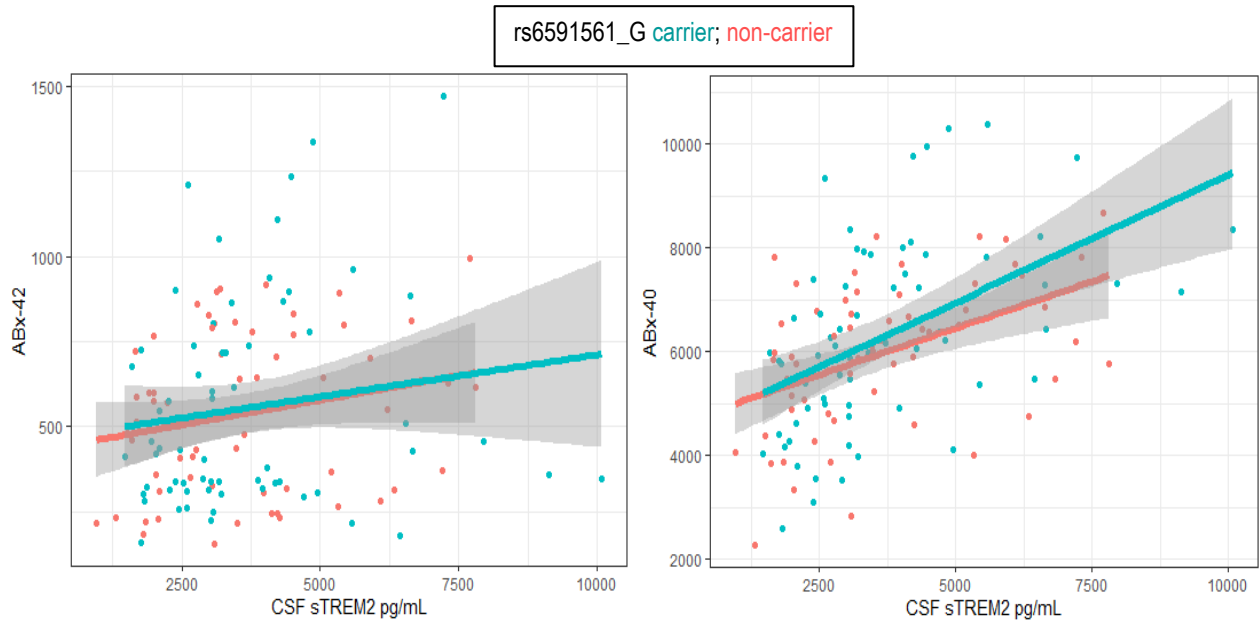
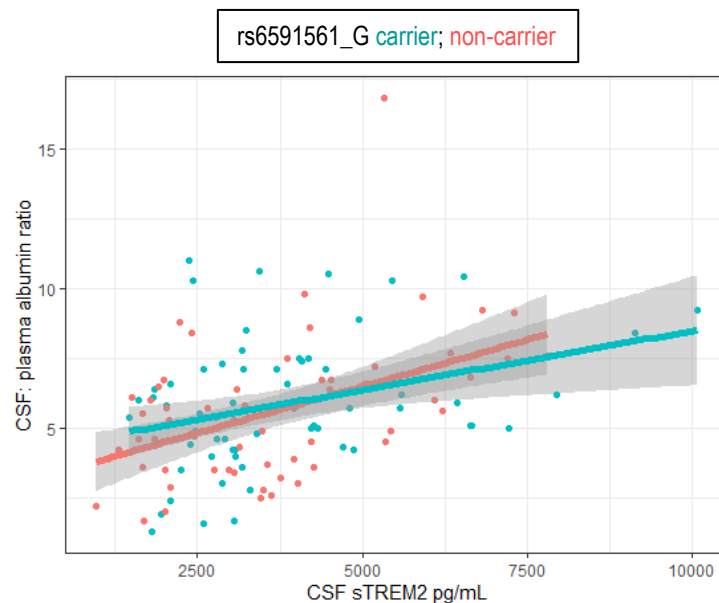


Figure 4.6. rs6591561 X sTREM2 interaction on CSF/plasma albumin. There is no significant effect of genetic regulation of MS4A (presence of rs6591561_G) on the association between increased CSF sTREM2 and increased CSF/plasma Albumin ratio (pg/mL).



ADNI Replication Results

Next, we sought to replicate these novel biomarker interactions in an independent cohort. ADNI participants with available genotype, CSF sTREM2, and A β peptide tandem UPLC mass spectrometry measurements were leveraged yielding a replication cohort of N=440. Demographic characteristics of this cohort are described in **Table 4.3**.

Table 4.3. ADNI Cohort Demographics

Characteristic	Clinical Diagnosis			Total (N=440)
	Normal Cognition (N=138)	Mild Cognitive Impairment (N=270)	Alzheimer's Disease (N=32)	
Male, no. (%)	72 (52)	153 (57)	20 (63)	245 (56)
Age (baseline)	74 \pm 6.03	71 \pm 7.38	76 \pm 10.26	73 \pm 7.39
Education	17 \pm 2.60	16 \pm 2.67	16 \pm 2.64	16 \pm 2.66
sTREM2 CSF pg/mL	4108 \pm 2034.21	3933 \pm 1968.17	4900 \pm 2619.85	4058 \pm 2052.24
<i>APOE</i> - ϵ 4 carriers, no. (%)	35 (25)	125 (46)	22 (69)	182 (41)

Values are presented as mean \pm standard deviation, unless otherwise indicated.

The minor allele of AD protective SNP, rs1582763, interacted with sTREM2 levels on peptide measurements of A β ₁₋₄₀ (**Table 4.4** and **Fig. 4.7A**; β =-0.269, p =0.017), whereby the positive association between sTREM2 and A β ₁₋₄₀ expression was attenuated among carriers of rs1582763_A. Similarly, minor allele carriers had an

attenuated association between sTREM2 and A β ₁₋₃₈ expression, albeit this interaction did not reach statistical significance (**Table 4.4** and **Fig. 4.7B**; β =-0.045, p =0.094). In accordance with initial results using VMAP data, the presence of rs1582763_A did not interact with sTREM2 levels on full-length A β ₁₋₄₂.

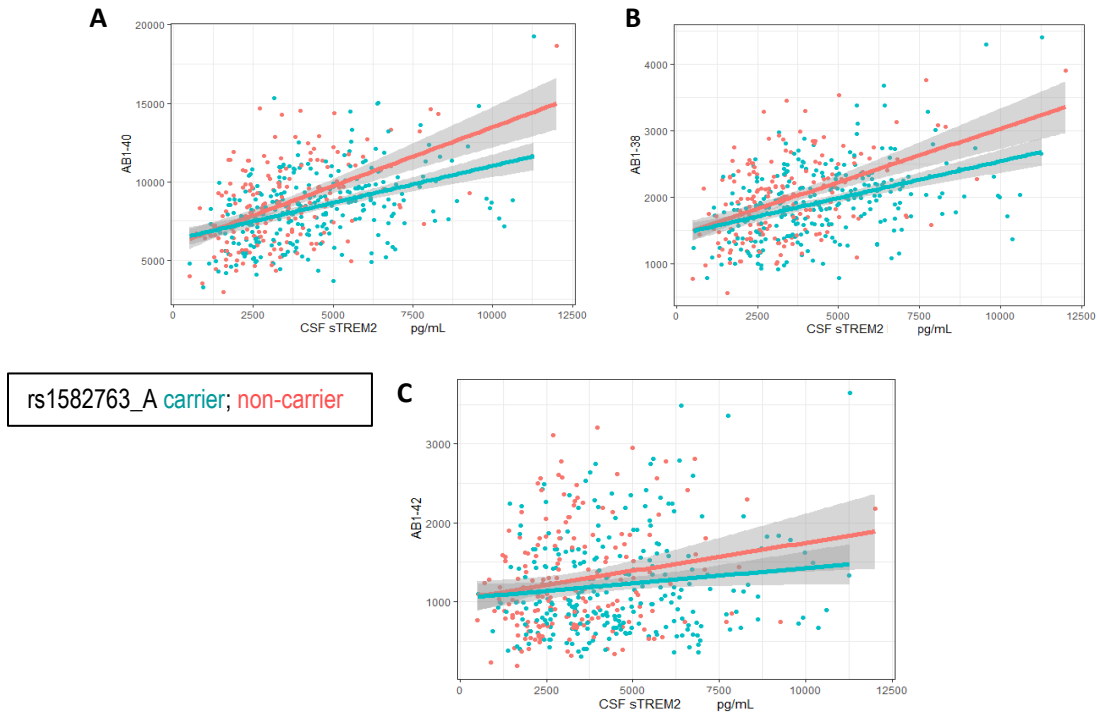
Table 4.4. sTREM2 * Presence of rs1582763 Minor Allele (A<G) Interaction on CSF AD biomarkers in ADNI

ADNI Outcome	β	P
A β ₁₋₄₀	-0.269	0.017*
A β ₁₋₃₈	-0.045	0.094
A β ₁₋₄₂	-0.027	0.396

Bold represents statistical significance set to a *priori* threshold $P.fdr < 0.05$

* Signifies significance after multiple corrections using the Benjamini & Hochberg (1995) false discovery rate based on number of tests completed

Figure 4.7. rs1582763 X sTREM2 interaction on A β peptides ADNI replication. The minor allele of rs1582763 significantly attenuates the positive association between sTREM2 and A β ₁₋₄₀ peptide levels in CSF in ADNI (A). This attenuation is trending but non-significant for both (B) A β ₁₋₃₈ and (C) A β ₁₋₄₂.



In contrast to insignificant results using VMAP data for AD risk SNP rs6591561, in ADNI, the minor allele (G) interacted with CSF sTREM2 levels on A β ₁₋₄₀ expression whereby non-carriers of rs6591561_G had an attenuated association between sTREM2 and A β ₁₋₄₀ levels (**Table 4.5** and **Fig. 4.8A**; $\beta=0.223$, $p=0.028$). Excitingly, the direction of this effect opposes those of rs1582763_A on shorter A β species suggesting results may reflect MS4A biology as opposed to being spurious. However, without significant independent replication between the datasets in our analyses, this novel association remains largely uninterpretable. In keeping with trends across A β peptide outcome measures, A β ₁₋₃₈ and A β ₁₋₄₂ exhibited similar results in terms of direction and magnitude with our discovery cohort (**Table 4.5** and **Fig. 4.8B-C**; $\beta=0.046$, $p=0.054$ and $\beta=0.022$, $p=0.454$, respectively).

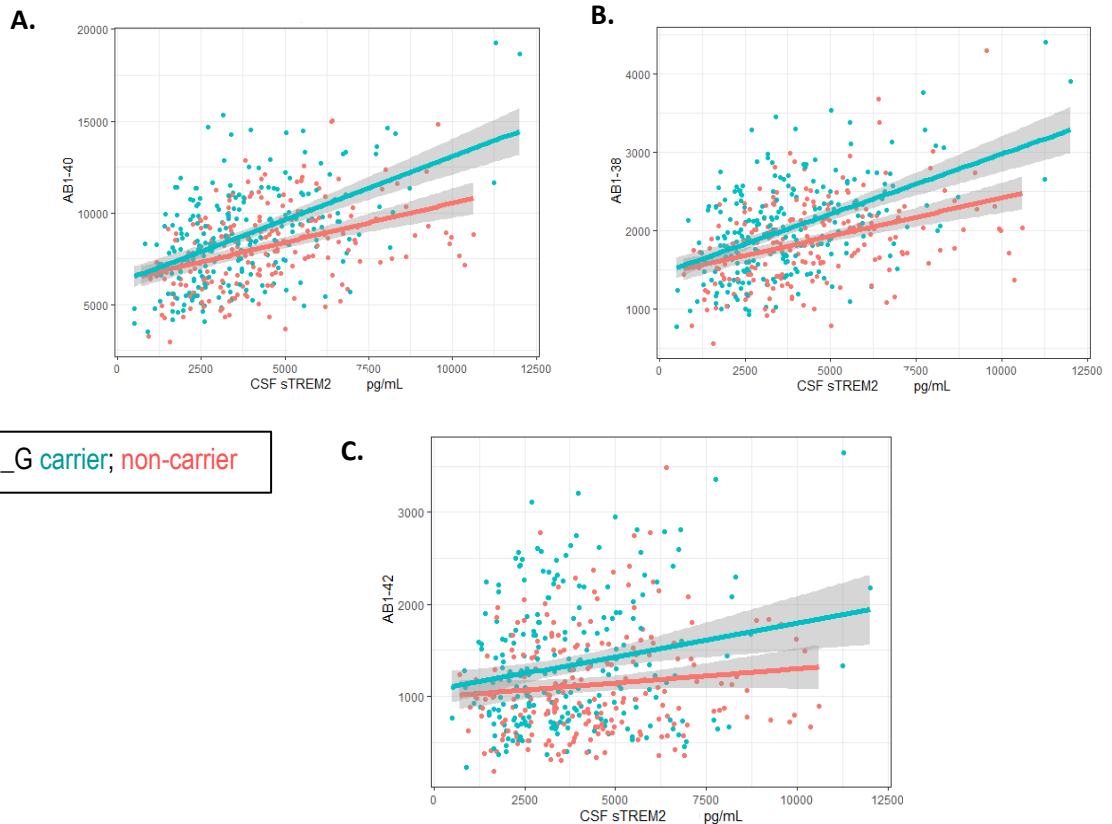
Table 4.5. sTREM2 * Presence of rs6591561 Minor Allele (G<A) Interaction on CSF AD biomarkers in ADNI

ADNI Outcome	β	P
$A\beta_{1-40}$	0.223	0.028*
$A\beta_{1-38}$	0.046	0.054
$A\beta_{1-42}$	0.022	0.454

Bold represents statistical significance set to a *priori* threshold $P.fdr < 0.05$

* Signifies significance after multiple corrections using the Benjamini & Hochberg (1995) false discovery rate based on number of tests completed

Figure 4.8. rs6591561 X sTREM2 interactions on $A\beta$ peptides in ADNI. The minor allele (G) of rs6591561 is associated with a more positive association between sTREM2 and $A\beta_{1-40}$ peptide levels in CSF in ADNI (A). This effect is trending but non-significant for both (B) $A\beta_{1-38}$ and (C) $A\beta_{1-42}$.



rs6591561_G carrier; non-carrier

MS4A SNP Interactions with *TREM2* Transcript Expression on A β Levels at Autopsy

Next, we asked whether MS4A SNP interactions were coupled to *TREM2* transcript abundance. The main effect of *TREM2* mRNA expression on A β neuropathological measurements in ROS/MAP are provided in **Table 4.6**. Using bulk RNA sequencing data and multiple neuropathological measurements of A β species from ROS/MAP we uncover a novel interaction of rs6591561 minor allele with *TREM2* mRNA abundance in the dIPFC on A β_{1-38} measured by mass spectrometry from dIPFC tissue (**Table 4.7** and **Figure 4.9B**; $\beta=0.158$, $p=0.003$).

Secondary analysis, utilizing SRM-quantified AT8 tau peptide as an outcome measure in ROS/MAP yielded insignificant main effect and SNP interaction results. The presence of rs6591561 minor allele predicted lower levels of *TREM2* mRNA ($\beta=-0.122$, $se=0.054$, $p=0.024$) while the minor allele of rs1582763 was not associated with *TREM2* mRNA levels ($\beta=0.055$, $se=0.070$, $p=0.430$).

Table 4.6. Main Effects of *TREM2* mRNA on A β Neuropathology

Neuropathology Outcome Measure	Estimate	P Value
A β_{1-38} (SRM)	0.0974	0.020*
A β (total) (SRM)	0.496	7.43e-04*
A β_{1-42} (IHC)	0.182	5.25e-05*
Silver Stained Neuritic plaque	0.088	3.77e-05*

Bold represents statistical significance set to a *priori* threshold $P.fdr < 0.05$

* Signifies significance after multiple corrections using the Benjamini & Hochberg (1995) false discovery rate based on number of tests completed

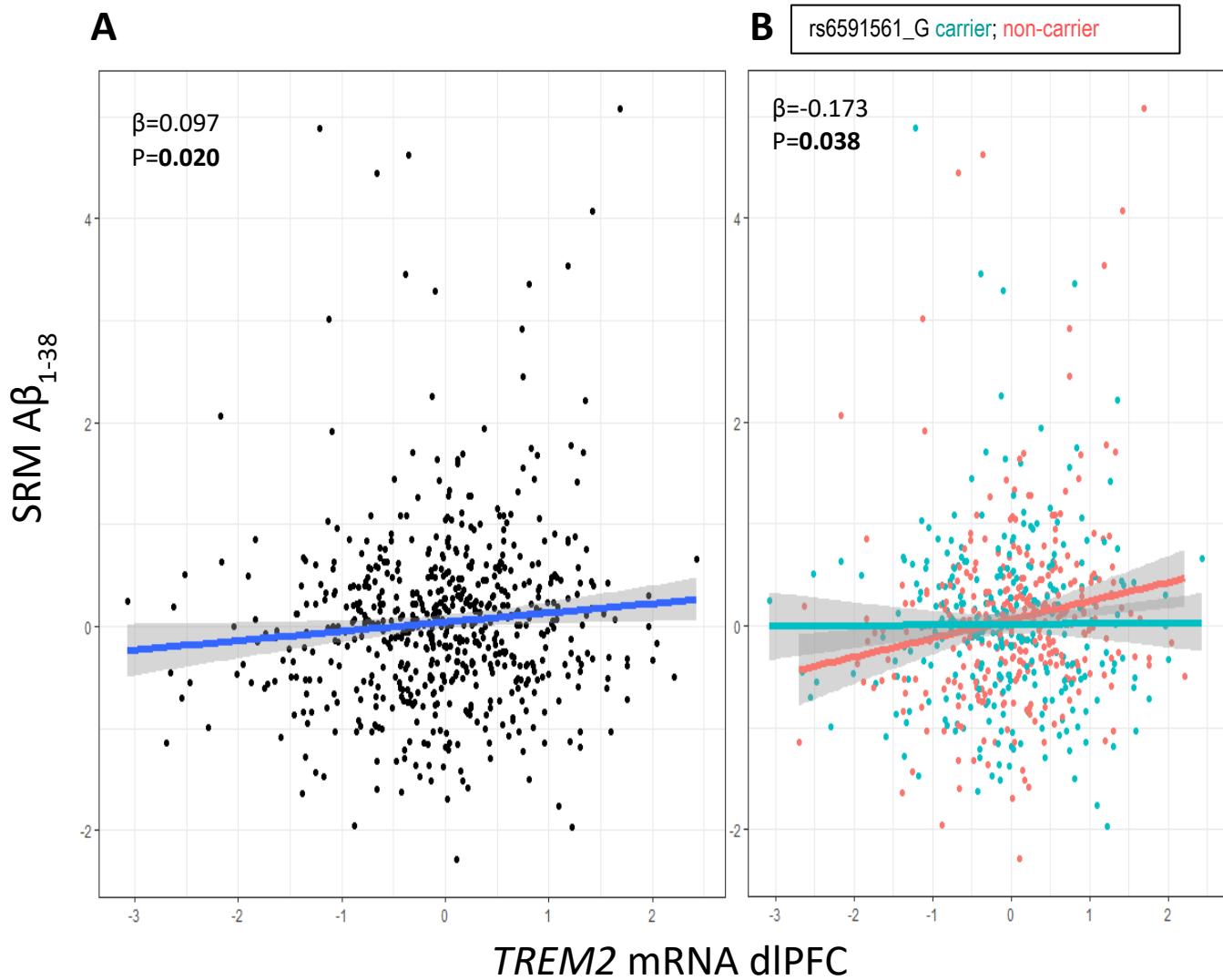
Table 4.7. MS4A SNP * *TREM2* mRNA Interaction on A β Neuropathology

Neuropathology Outcome Measure	<i>rs1582763</i>		<i>rs6591561</i>	
	Estimate	P.int.Value	Estimate	P.int.Value
A β ₁₋₃₈ (SRM)	0.108	0.200	-0.173	0.038*
A β (total) (SRM)	-0.143	0.629	0.043	0.883
A β ₁₋₄₂ (IHC)	-0.058	0.610	0.097	0.384
Silver Stained Neuritic plaque	-0.031	0.546	0.036	0.473

Bold represents statistical significance set to a *priori* threshold P.fdr < 0.05

* Signifies significance after multiple corrections using the Benjamini & Hochberg (1995) false discovery rate based on number of tests completed

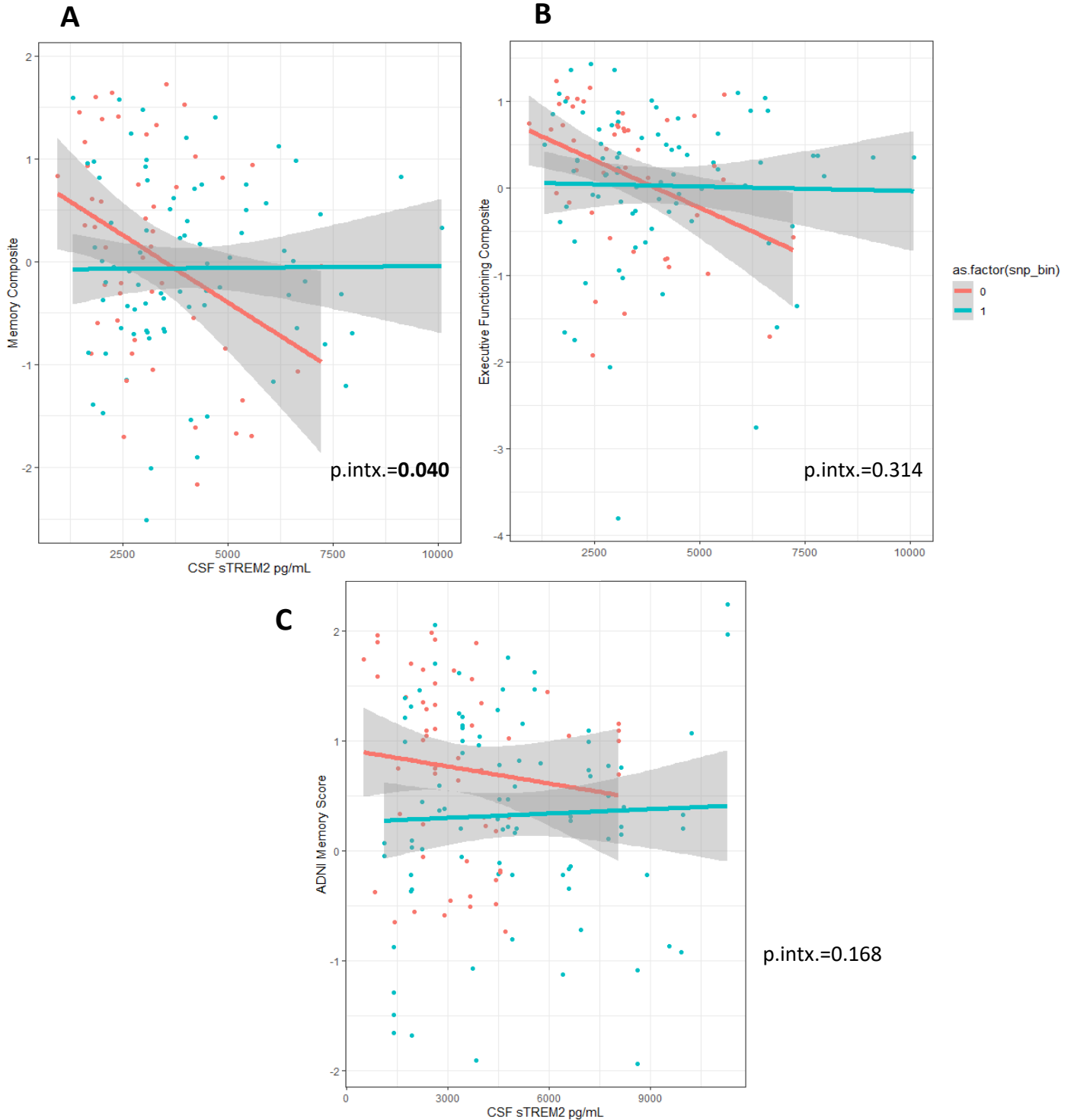
Figure 4.9. *TREM2* X rs6591561 interaction on A β ₁₋₃₈ in ROS/ MAP. (A) *TREM2* mRNA expression is positively associated with A β ₁₋₃₈. (B) *TREM2* mRNA expression association with A β ₁₋₃₈ is driven by non-carriers of rs6591561_G minor allele.



MS4A SNP Interactions with sTREM2 Protein Expression on Cognition

Lastly it was assessed whether MS4A-AD associated SNPs interacted with CSF sTREM2 levels on composite measures of cognition in VMAP. These interaction models were insignificant for the minor allele of rs6591561, whereby rs6591561_G did not interact with sTREM2 expression on either memory or executive functioning composites. By contrast, there was a weak interaction of sTREM2 and the presence of rs1582763_A on the memory composite (**Figure 4.10A**; $\beta=2.35e-4$, $se=1.14e-4$, $p=0.042$), while the interaction of this SNP and sTREM2 on the executive functioning composite is in the same direction (**Figure 4.10B**; $\beta=1.32e-4$, $se=1.05e-4$, $p=0.209$). Replication of this interaction of rs1582763_A on memory scores trended but did not reach statistical significance using ADNI data (**Figure 4.10C**; $p=0.168$).

Figure 4.10. rs1582763 X sTREM2 interactions on cognition. (A) sTREM2 protein significantly interacts with the presence of rs1582763_A on memory but not **(B)** executive functioning, although trending in the same direction. **(C)** In ADNI, this interaction between sTREM2 and rs1582763_A did not replicate, albeit in A-C higher sTREM2 concentration is associated with worse cognitive performance in non-carriers of rs1582763_A.



Discussion

The present analyses assessed whether MS4A AD-associated SNPs modify previously established associations (see Chapter 3) between CSF sTREM2 levels and AD biomarkers of diverse pathology. In summary, we find that genetic regulation at the MS4A locus selectively modifies sTREM2 associations with markers of A β species and BBB integrity but not tau. Moreover, in the brain, MS4A genetic variant rs6591561_G modifies *TREM2* transcript associations with A β ₁₋₃₈ species. Together these results highlight several biological pathways through which these variants (rs1582763_A and rs6591561_G) may regulate AD protection and risk. Results bolster support for the current theory that the TREM2 pathway plays a causal role in AD pathogenesis via inflammatory regulation of neuropathology. Importantly, a novel relationship between sTREM2 levels in CSF and BBB integrity in carriers which is absent in non-carriers of rs1582763_A may suggest that MS4A and TREM2 proteins regulate peripheral-central inflammatory communication.

The association previously described in the literature between MS4A AD-associated rs1582763_A and CSF sTREM2 levels was recapitulated in the VMAP discovery cohort while the rs6591561_G association did not replicate (**Figure 4.2**). Previously described decreases in sTREM2 associated with rs6591561_G were not observed in VMAP, we suspect, due to a much smaller sample size. As expected, protective SNP rs1582763_A was associated with elevated levels of sTREM2 in both VMAP and ADNI whereas rs6591561_G was associated with decreased sTREM2 only in ADNI. This increases confidence that sTREM2 production is genetically regulated by the MS4A locus. The relationship between genotype and sTREM2 protein abundance in

CSF was true across cognitive diagnosis indicating genetic regulation by the MS4A region of sTREM2 production is likely a constitutive as opposed to a disease-specific process.

The main interaction findings from the VMAP discovery cohort demonstrate the presence of rs1582763 minor allele modified previously established amyloid associations including the top association signal, $A\beta_{x-40}$, as well as the relationship between CSF sTREM2 and a fluid biomarker of BBB integrity (**Table 4.1**). Results show that genetic regulation by MS4A rs1582763_A attenuates the positive association between sTREM2 and $A\beta_{x-40}$ abundance in CSF, while also enhancing the positive association between sTREM2 and the CSF/plasma albumin ratio (**Figures 4.3-4.4**). Replication of the sTREM2*rs1582763_A interaction effect using mass spectrometry measurement of $A\beta_{1-40}$ peptide in ADNI yielded significant results (**Table 4.4**). Non-carriers of this allele exhibited decreased memory performance with higher CSF sTREM2 concentration while in minor allele carriers, cognition did not correspond to sTREM2 concentration (**Figure 4.10A**).

It may be the case that given directional associations with cognition and AD protection rs1582763_A decouples sTREM2 from an otherwise pathological process involving soluble $A\beta$ abundance. For example, soluble, low-molecular weight $A\beta$ oligomers may contribute to synapse loss preceding neuronal death¹⁹⁶. $A\beta$ peptides are composed of 36-43 amino acids and are the various cleavage products of their transmembrane parent amyloid precursor protein (APP). While full-length $A\beta_{1-42}$ displays rapid oligomerization and toxicity through the formation of insoluble fibrils¹⁹⁷, there are a number of studies showing neurotoxic effects of shorter $A\beta$ peptide

sequences (i.e., 1-38, 1-40, N-truncated) impacting synapse function and cognition in mice¹⁹⁸⁻²⁰⁰. And notably, A β ₁₋₃₈ truncated at its C-terminal moiety, was identified as the second most abundant form after A β ₁₋₄₀¹⁹⁸ which makes up about 60% of A β species present in CSF²⁰¹. These shorter and truncated forms of A β are understudied and their roles in AD are likely dynamic. In fact, some argue beneficial roles for A β ₁₋₄₀, also A β ₁₋₃₈, in slowing the aggregation of A β ₁₋₄₂²⁰². Therefore, genetic regulation of the MS4A locus modulates the relationship between sTREM2 levels and the most abundant A β species in CSF whereas in rs6591561_G carriers, sTREM2 levels are tightly coupled to soluble A β while in rs1582763_A carriers, sTREM2 levels decouple from soluble A β which may reflect a protective neuroinflammatory response to pathology.

We could expand on this hypothesis by adding that the positive relationship between sTREM2 and increased BBB permeability in carriers, but not non-carriers of AD-protective rs1582763_A may be important for a neuroinflammatory response to early changes in A β dysregulation which involves peripheral-central communication. The lack of sTREM2 coupling to the CSF/plasma albumin ratio in non-carriers may therefore reflect a failure to mount a proper neuroinflammatory response to early changes in the neuropathological landscape. This is supported by evidence showing CSF sTREM2 levels are normalized during neuroinflammation by natalizumab treatment which targets and reduces leukocyte trafficking across the BBB in patients with multiple sclerosis¹⁹². However, in AD, early neuroinflammation (and microglial response) may be beneficial to resolving neuropathology. Therefore, it is possible that in early stages of A β development that peripheral immune involvement may help augment sTREM2 levels in brain or vice versa. sTREM2 has been thought to diffuse to some extent through blood

vessels reaching the brain parenchyma²⁰³. However, peripheral immune cells also express TREM2 and may contribute to the CSF reservoir of sTREM2 concentration. For example, infiltrating T cells also express TREM2 receptor which is attuned to their activation and helps modulate their inflammatory signaling but may also undergo proteolytic cleavage in the brain²⁰⁴.

Alternatively, the coupling of increased CSF sTREM2 and CSF/plasma albumin ratio may be indicative of increased permeability of the choroid plexus (blood-CSF barrier) to solutes which is known to occur in AD²⁰⁵, and subsequently, the increased accumulation of sTREM2 in CSF which had originated in plasma having been cleaved in peripheral tissues. Regardless of the origin of increases in CSF sTREM2, this positive association between CSF sTREM2 and the CSF/plasma albumin ratio occurs selectively in rs1582763_A carriers begging the question and extent of MS4A protein involvement in the BBB and or blood-CSF barrier regulation. The lack of CSF/plasma albumin measurement in ADNI precluded independent replication of this interaction result. Nonetheless, this intersection between barrier integrity, MS4A, and TREM2 proteins remains an uncharted topic which may shed light on early pathophysiological changes in AD and give rise to novel microglial/immunomodulatory therapeutic targets.

However, there was no evidence of rs1582763 genotype significantly interacting with sTREM2 levels on biomarkers of tau pathology. This observation suggests that genetic increases in sTREM2 levels through rs1582763 near MS4A4A likely involves amyloid and BBB regulation but leaves out the very robust and consistent associations we see of CSF sTREM2 and t-tau and p-tau. This is interesting considering increases in CSF sTREM2 have historically been thought to represent microglial response to

neurodegeneration and yet genetic regulation by MS4A-AD associated SNPs did not modify this relationship in our analyses underscoring the importance of trait and environmental factors in the context of innate immunity.

In keeping with the established role of rs1582763_A, and rs6591561_G in AD protection and risk, respectively, it was investigated whether or not these SNP modified the positive relationship between CSF sTREM2 levels and memory in VMAP. This has also been recapitulated in the literature previously¹⁷⁰ as increases in baseline sTREM2 levels are generally thought to improve clinical outcomes in AD as well as cognitive outcomes in AD mouse models. The presence of rs1582763_A interacted with CSF sTREM2 levels on memory composite scores in VMAP (**Figure 4.10A**; $\beta=2.35e-4$, $se=1.14e-4$, $p=0.042$) whereby in non-carriers of this allele, higher sTREM2 concentration was associated with poorer memory performance. This result provides further evidence that this AD protective SNP may decouple sTREM2 expression from an otherwise pathological process important for clinical trajectory, implicating a novel association between this MS4A SNP and an early-affected cognitive outcome measure in preclinical AD progression. Although, it should be noted that this interaction trended but did not significantly replicate in the larger ADNI cohort (**Figure 4.10C**) or extend to a composite measure of executive functioning in VMAP (**Figure 4.10B**), therefore this result should be interpreted cautiously.

Interestingly, rs6591561_G interacted with *TREM2* transcript on A β ₁₋₃₈ peptide levels measured using mass spectrometry and ROS/MAP dIPFC autopsy data (**Table 4.7** and **Figure 4.9**). Furthermore, there is also a lack of interaction with tau peptide here that parallels the findings above from biomarker analyses. This particular finding

highlights a more generalized relationship between MS4A and the TREM2 pathway beyond its known regulation of sTREM2 levels in CSF. Specifically, rs6591561 minor allele related to lower levels of *TREM2* mRNA at autopsy and the relationship between increases in *TREM2* mRNA and increases in A β ₁₋₃₈ peptide were driven by non-carriers, suggesting this AD risk SNP may impair a potential *TREM2* transcriptional response to A β pathology. However, this finding necessitates replication in an independent cohort with available post-mortem data.

There are several strengths to this chapter, including the utilization of multiple independent cohorts of aging and Alzheimer's disease yielding large sample sizes and utilization of several highly sensitive methods of proteomic analysis. Independent replication of interactions using ADNI data increased confidence in these results. However, each cohort is mostly Non-Hispanic, White, and represents little genetic diversity making it hard to generalize findings to more diverse populations. This is especially pertinent given the recent finding²⁰⁶ that on average African Americans, compared to Non-Hispanic White individuals, have lower levels of CSF sTREM2 which has been attributed to their increased likelihood of carrying *TREM2* coding variants associated with decreased levels of sTREM2 and their lowered likelihood of carrying MS4A AD-associated rs1582763_A which we and others have demonstrated is associated with increased sTREM2.

In summary, using VMAP as a discovery cohort, we find evidence that genetic regulation at the MS4A locus may confer protection against AD at least in part via augmentation of the *TREM2* pathway, possibly increases in sTREM2 CSF reservoir in response to soluble A β pathology, replicating results in an independent dataset (N=440)

in ADNI. We also find evidence that this regulation may confer AD risk via a proposed dampening of *TREM2* transcriptional response to A β using available autopsy data in ROS/MAP.

CHAPTER 5

SUMMARY AND FUTURE DIRECTIONS

Alzheimer's disease (AD) is a devastating neurodegenerative disease and a leading cause of death in the U.S. without an efficacious treatment to slow or stop disease progression, including cognitive decline. Triggering receptor expressed on myeloid cells-2 (TREM2) is modulator of neuroinflammation and a nominated therapeutic target for AD. Expression of TREM2 and its soluble fragment (sTREM2) in AD model mice has shown to protect against cognitive deficit and A β plaque formation. Despite this, the exact roles for TREM2 machinery in the development and progression of AD are unknown. Particularly with respect to the various collection of neuropathology that contribute to cognitive decline beyond parenchymal plaque.

This in-depth characterization of *TREM2* mRNA and sTREM2 protein expression associations with diverse and concomitant neuropathology sought to reveal important and novel relationships of the TREM2 pathway with additional drivers of neuroinflammation including cerebrovascular injury. Additionally, genetic regulation of CSF sTREM2 levels within the MS4A gene locus was examined with respect to plausible interactions between SNPs in this region and sTREM2 concentrations on diverse CSF biomarkers of AD neuropathology including a fluid biomarker of BBB integrity. Similarly, interactions between MS4A SNPs and *TREM2* mRNA levels were assessed with respect to post-mortem measurements of AD neuropathology. These analyses helped to answer questions such as what TREM2 and sTREM2 expression represent in brain and CSF, respectively. Also, they paint a more comprehensive picture as to which biological pathways co-occur with elevations in these proteins in AD

expanding the scope of interest on small vessel disease pathology and cerebrovascular integrity and function. Finally, MS4A SNP interaction analyses shed light onto relevant biological pathways where MS4A and TREM2 proteins may interact to regulate the AD neuropathological landscape and thus modulate pathophysiological progression of the disease.

The autopsy approach portion of this dissertation utilized an unprecedented sample size (N=908) of regional post-mortem *TREM2* bulk transcript expression data from the Religious Orders Study and the Rush Memory and Aging Project (ROS/MAP). To our knowledge, this was the largest and most comprehensive examination of *TREM2* gene expression associations in brain to date. As expected, *TREM2* levels, irrespective of subregion, correlated to the microglial cell-type fraction above other cellular fractions examined. *TREM2* mRNA in the dorsolateral prefrontal cortex (dlPFC) and the posterior cingulate cortex (PCC) was significantly greater in individuals diagnosed with AD compared to controls. Additionally, in these cortical regions, *TREM2* mRNA was robustly related to amyloid and weakly related to tau neuropathology. And these associations with classical AD neuropathology, particularly A β , seemed to drive weak associations of *TREM2* levels and retrospective longitudinal global cognition scores. These initial results suggest that we are picking up on a late-life *TREM2* transcriptional response to the accumulation of A β plaque in brain. Cross-sectional results examining *TREM2* mRNA levels and global cognition scores did not reveal a significant association between *TREM2* and cognition. Perhaps the most intriguing finding in this first analytical chapter outlines potential disparate roles for *TREM2* expression and function in cortical versus caudal brain regions. Results from regression models using *TREM2* mRNA

measured from the head of the caudate nucleus (CN) did not reveal significant associations with AD diagnosis, cognitive functioning, or classical AD neuropathology. Instead, higher CN *TREM2* levels related to increased arteriosclerosis severity in the basal ganglia as well as the proportion of activated microglial density (PAM) in the ventral medial caudate. Notably, cortical *TREM2* levels were not related to microglial density measures cis- or trans-regionally. Despite hypothesizing that *TREM2* levels would reflect increased PAM in cortical regions, this was not the case. And we speculate that this may be due to an un-coupling of *TREM2* mRNA expression levels with functional microglial activation at this later time point.

This work supports the hypothesis that cortical *TREM2* upregulation in late life reflects a compensatory response to amyloid progression. Indeed, *TREM2* mRNA was significantly greater in AD vs. control in the prefrontal cortex, a region with robust connections to early affected posterior structures, including the temporal lobe and limbic regions^{207, 208}. However, results also indicate that this pathway may become overwhelmed and decoupled from its basal homeostatic regulatory functions in microglia, specifically their activation. This is in accordance with the fact increased transcription of *TREM2* mRNA followed disease progression instead of being associated with cognitive or neuropathological protection. Therefore, it is possible that *TREM2* is beneficial early-on to the initial deposition of amyloid but as disease progresses, increases in late-life transcription of *TREM2* reflect a failure of microglia to properly respond to the accumulation of neuropathology in the cortex.

Next, a biomarker approach utilizing our in-house cohort of VMAP participants enabled comparison of CSF s*TREM2* protein expression with cerebrovascular as well

as additional AD biomarkers of neuropathology and inflammation. These analyses allowed for further investigation into elevations of sTREM2, archetypal in early MCI-AD converters.

Surprisingly, one of the main findings from main effects analyses defining the biological correlates of elevated CSF sTREM2 demonstrates that sTREM2 is, indeed, very tightly coupled to A β peptide levels, although not in a manner that was necessarily suspected; while increases in sTREM2 robustly related to increases in other CSF biomarkers neurodegeneration, particularly, p-tau₁₈₁, unexpectedly, the top association signal was that of higher CSF A β _{x-40}. This novel association was replicated in the larger independent ADNI cohort using full-length A β ₁₋₄₀ (N=727). While elevation of sTREM2 in VMAP significantly associated with A β _{x-40}, there was an absence of association with full-length A β ₁₋₄₂, and the A β ₁₋₄₂/ A β ₁₋₄₀ ratio – both indicators of A β plaque abundance in brain. This implies the relationship between high sTREM2 and shorter and N-truncated species (i.e., A β ₁₋₄₀, A β _{x-40}, A β _{x-42}, and A β ₁₋₃₈) likely does not reflect A β burden in brain. Additionally, increases of a fluid biomarker of blood-brain barrier integrity (the CSF/plasma albumin ratio) significantly related to increases in sTREM2 bolstering evidence for a role of the TREM2 pathway in early neuroinflammation and BBB integrity. Together, one sees changes in CSF sTREM2 levels correspond to changes in other CSF biomarkers of neurodegeneration, BBB integrity, and most significantly, shorter A β peptides.

Hierarchical linear regression demonstrated independent contributions to and diverse biological correlates of sTREM2 variance. First, a base model including age, sex, education, and cognitive diagnosis explained 11.8% of variance in sTREM2 protein

measurement in VMAP. In competitive models, p-tau₁₈₁, A β _{x-40}, and the CSF/plasma albumin ratio independently explained 17.7%, 21.2%, and 21.2% of variance in sTREM2 levels, respectively. Jointly, all three biological correlates explained a significant 36% of variance while the inclusion of all three biological correlates and the base model covariates explained nearly half (48%) of variance in sTREM2 expression. Interestingly, post-hoc interaction models revealed these observations were present regardless of tau status.

Linear mixed-effects models investigated sTREM2 associations with future cognitive performance. Increases in baseline sTREM2 significantly predicted a favorable longitudinal memory performance in VMAP, consistent with other reports. However, sTREM2 levels did not significantly predict changes in longitudinal executive functioning, suggesting regional specificity of this biomarker to functional areas affected early-on in the process of AD-related cognitive decline (i.e., hippocampal memory). When accounting for residual variance due to other biological correlates, sTREM2 remained predictive of memory performance with the exception of when the model was adjusted for A β _{x-40} values. Importantly, this suggests that sTREM2 expression which is related to A β species abundance in CSF may be relevant to cognitive trajectory. Therefore, this relationship may have notable clinical relevance in the early stages of cognitive decline. Additionally, we posit that the sTREM2/p-tau ratio may relate to cognitive outcomes due to a decoupling of sTREM2 and tau as AD progresses. In contrast to tau, A β _{x-40} explained a larger percentage of sTREM2 variance, and this association did not differ by cognitive diagnosis. In summary, sTREM2 expression is deconvolved in CSF from a subset of participants in VMAP and a surprisingly large

percentage of variance in sTREM2 levels may be explained by just three biomarkers. While it has been hypothesized sTREM2 production may be a response to the onset of neurodegeneration, functional relationships between TREM2 proteins and NVU components such as the BBB, as well as regulation of soluble A β abundance remain almost completely unexplored. This is despite the fact this present analysis draws connections between these pathways and clinically relevant outcome measures.

To better understand the influence of genetic regulation of sTREM2 levels in CSF, MS4A SNPs were investigated with respect to potential modulation of the above associations between sTREM2 and AD biomarkers in VMAP. As found previously, MS4A SNPs, rs1582763 and rs6591561 are associated (in opposing directions) with AD risk modulation and constitutive levels of CSF sTREM2. In line with this finding, individuals in VMAP carrying the minor allele (A<G) of rs1582763 had higher concentrations of sTREM2 in CSF as compared to non-carriers, and this was dose dependent. However, previously demonstrated decreases in sTREM2 in rs6591561 minor allele (G<A) carriers was not observed in this cohort, most likely due to a significantly smaller sample size and differences in clinical characterization between VMAP and the ADNI subsample used by Deming et. al. The rs6591561 minor allele did not interact with sTREM2 expression on any of the AD biomarker outcomes, in part, we suspect due to the lack of main effect between sTREM2 levels and SNP genotype status. Therefore, we focused the following analyses on rs1582763. The minor allele of rs1582763 did, in fact, interact with sTREM2 on select AD biomarkers of neuropathology including attenuation of the association between sTREM2 with shorter A β peptides including A β _{x-40}. This interaction effect was replicated in the larger ADNI

cohort using mass spectrometry. Additionally, there was a significant interaction between this minor allele and sTREM2 on the CSF/plasma albumin ratio and stratified models revealed that carriers are driving the association whereas it is absent in non-carriers of the rs1582763_A allele. In contrast, rs1582763_A did not interact with sTREM2 on tau outcomes. These findings suggest that genetic regulation by the MS4A locus modifies the relationships between microglial activation, and BBB integrity, as well as levels of soluble A β species. Yet there was a lack of evidence that MS4A and TREM2 pathways interact on tau neuropathology in aging or AD.

Lastly, these two MS4A tool SNPs were investigated with respect to interactions with *TREM2* transcript abundance on A β neuropathology outcome measures including selected reaction monitoring (SRM) tandem mass spectrometry of total A β and A β ₁₋₃₈, as well as immunohistochemistry of A β ₁₋₄₂ and silver-stained neuritic plaques. *TREM2* mRNA expression was positively associated across the board with amyloid outcomes in main effects models. Interestingly, in keeping with the lack of main effects surrounding sTREM2 and correlates of parenchymal plaque, there were no significant interactions of MS4A SNPs on total A β , full-length A β ₁₋₄₂, or silver staining of parenchymal plaque. However, there was a significant interaction between the minor allele of rs6591561 and *TREM2* mRNA abundance on SRM quantification of A β ₁₋₃₈ whereas this association is stronger in non-carriers than carriers of this AD risk allele. This was accompanied by a similar trending interaction between *TREM2* mRNA abundance and rs1582763_A in the opposite direction on A β ₁₋₃₈ levels. These final analyses bolster evidence supporting the hypothesis that MS4A proteins regulate the TREM2 pathway with respect to both *TREM2* transcription and sTREM2 production and that the relationship between MS4A

and TREM2 proteins may have implications on downstream AD neuropathology, including amyloid and BBB alterations.

Results from brain and CSF reveal a somewhat unexpected insight into TREM2's relationship with tau. Whereas using post-mortem quantification of *TREM2* mRNA, there was a lack of robust association with tau neuropathology indicating transcription of *TREM2* is more closely coupled to amyloid processes. Additionally, although CSF sTREM2 associations with tau biomarkers were quite strong, these associations did not drive the relationship between sTREM2 levels and cognition (as did A β _{x-40} species) or contribute to the majority of variance in sTREM2 levels. In fact, sTREM2 levels decoupled from tau biomarkers in CSF as disease progressed using both VMAP and ADNI data. Variant level analyses also stressed a lack of evidence for tau in TREM2-mediated contributions to AD. Specifically, the intersection of MS4A and TREM2 seems to converge, rather, with amyloid and increased blood-brain barrier permeability. This suggests that TREM2 associations with tau may be a consequence rather than cause of AD progression, while underscoring TREM2's relationship to earlier pathological events such as increases in soluble A β species.

In addition to insights into the relationship between TREM2 proteins and tau, analyses bring forth a deeper understanding of how the TREM2 pathway relates to clinical outcome measures in aging and AD. TREM2 isoforms were established as a predictors of cognitive functioning; importantly this connection between TREM2 and sTREM2 upregulation and cognitive outcomes are amyloid-dependent as opposed to tau-dependent suggesting dysregulation microglial TREM2 function in disease occurs primarily due to amyloidosis. Furthermore, a novel relationship discovered between

sTREM2 and soluble A β species highlighted herein reveals an earlier biological relationship between TREM2 and amyloid which may be amenable to therapeutic intervention during the prodromal period of AD.

Additionally, we provide novel evidence that the MS4A locus may modify or respond to levels of these shorter A β isoforms in conjunction with the TREM2 pathway. Additional functional studies, clarifying the mechanism which links MS4A4A and MS4A6A proteins to the regulation of sTREM2 production are needed to provide context to the results herein. Specifically, as to why we see interactions of MS4A variants with both sTREM2 and *TREM2* mRNA abundance. Up to this report, it was largely untested how MS4A SNPs might confer AD protection and risk apart from Deming et al, showing their directional associations with CSF sTREM2 and co-localization with TREM2 protein in macrophage membranes. We add to this, finding that MS4A and TREM2 proteins may interact to regulate early AD neuropathology (soluble A β abundance and BBB integrity) as opposed to later AD neuropathology (neuritic plaque abundance, p-tau, and neurofibrillary tangles) and this relationship may involve complex interplay between central and peripheral immune compartments.

To our knowledge, for the first time, an in-depth look at baseline CSF sTREM2 associations with neuroimaging measures of cerebrovascular structure and function was carried out. This provided a lack of support for sTREM2 involvement in global measures of cerebrovascular injury beyond alterations in BBB integrity as indicated by the robust relationship between sTREM2 and a fluid biomarker of BBB integrity. Despite these negative results, future longitudinal measurement of sTREM2 may provide a clearer picture of NVU dynamics over the course of disease, including those of BBB and

arteriolosclerosis. Furthermore, regional measurements of cerebrovascular neuropathology may help inform future TREM2 studies as microglial activation and pathway associations with select neuropathology as evidence by this report are regionally specific.

We hypothesize that with accompanying glial activation at the onset of neurodegeneration, sTREM2 abundance, together with increases in shorter A β peptides, likely reflects an increase in synaptic activity thus dynamic regulation of free and abundant A β species in ISF/CSF. Despite the lack of nuanced understanding surrounding the heterogeneity of A β pools in brain, synapse dysfunction is now well-characterized as an early event in AD resultant of neuronal hyperactivity, and A β is indeed intricately tight to this by multiple mechanisms^{172-174, 196}. For example, hippocampal hyperactivity as detected by fMRI has been observed during memory tasks in individuals with MCI²⁰⁹⁻²¹¹ as well as presymptomatic individuals carrying the *APOE- ϵ 4* allele²¹²⁻²¹⁴. In fact, oligomeric A β are regarded as the most pathogenic form as opposed to monomers or plaques as they are thought to instigate neuronal damage, fluctuate in accordance with neuronal hyperactivity, and have been shown to precede plaque development³. One theory is that A β plaques create reservoirs of A β oligomers which help to sustain and exacerbate synaptic and neuronal loss²¹⁵. Human A β ₁₋₄₀ monomers and dimers applied to cultured hippocampal neurons and in hippocampal slices induced release of synaptic vesicles and subsequent hyperactivity of excitatory synapses²¹⁶. Along these lines, soluble A β is thought to disturb glutamate/GABA homeostasis by a number of different mechanisms¹⁹⁷. It is possible that during this shift

towards hyperexcitability of neurons, that TREM2 is cleaved and increases in sTREM2 become detectable in CSF.

The selectivity of results throughout analyses for shorter A β peptide species, namely A β_{40} and A β_{1-38} but not full-length A β_{1-42} , suggests we may be picking up on a biological signal that is not specific to A β plaque abundance, but rather soluble more abundant forms in CSF. If CSF sTREM2 were to be found to respond to increases in A β secretion or neuronal hyperactivity, this may help explain the lack of functional connection between sTREM2 and tau proteins in the literature, whereby the relationship of sTREM2 to neurons reflects early-stage synapse loss as opposed to the structural progression of tau and neurofibrillary tangles themselves. Adding to this, sTREM2 tracks closely with biomarkers of neurodegeneration in CSF, however, this relationship decouples with disease progression (see Chapter 3 **Figure 3.4** and **Supplemental Figure 3.6**), further suggesting that sTREM2 may reflect early stages of neuronal degeneration, which include synapse loss, signaling imbalances, increases in local soluble A β peptides, and secreted forms of tau. In contrast we found that the relationship between sTREM2 and A β_{x-40} does not change with disease progression (see Chapter 3 **Figure 3.5**) and is genetically regulated by MS4A AD-associated SNPs suggesting these biological pathways (soluble A β homeostasis and sTREM2-associated microglial activation) intersect to modulate AD risk. It is indeed a fascinating theory that CSF sTREM2 levels respond to levels of soluble A β_{1-40} and its N-truncated forms regardless of cognitive status, particularly given recent findings in ADNI highlight subtle age-independent increases in CSF A β_{1-40} in AD (this was historically contested in earlier studies with smaller sample sizes) while a robust positive correlation between this

peptide and p-tau₁₈₁ was highlighted in AD and was more pronounced in cognitively normal individuals, suggesting A β ₁₋₄₀ may play a role in development of disease²¹⁷.

The overarching hypothesis taken from these analyses is that elevation of CSF sTREM2 marks the intersection between microglial activation and neuroinflammation, the onset of neurodegeneration, and increases in soluble A β species - possibly due to neuronal hyperexcitability. All of these may contribute and or respond in some degree to concomitant BBB permeability. Therefore, future sTREM2 analyses in animal models should prioritize expanding current knowledge of sTREM2 function with respect to alterations of the NVU including glial-neuronal communication. One significant gap in understanding remains the potential contribution of BBB permeability to sTREM2 levels in brain. Future work is needed to determine whether sTREM2 elevations in CSF are in fact dependent to some extent on peripheral-central immune and inflammatory crosstalk. Quantification of early changes in A β kinetics in relationship to microglial activation and sTREM2 cleavage may be another important avenue to elucidating the therapeutic relevance of sTREM2 as a target for AD.

In summary, TREM2 appears to be directly related to A β species abundance, this relationship is relevant to cognition, and is modulated by known AD variants in the MS4A locus. The role of the TREM2 pathway in abundance of soluble A β species may be causally contributing to AD pathogenesis and a fundamental component of the TREM2 relationship to AD. TREM2 additionally showed a strong and understudied association with blood-brain barrier permeability and this association was also modulated by a known protective AD variant in the MS4A locus. Finally, TREM2

associations with tau may be robust in CSF, however, the relationship of the TREM2 pathway with tau may be primarily a consequence of AD progression.

APPENDIX

Supplemental Tables

Supplemental Table 3.1 Commercially Available Assay Information

CSF Analyte	Assay Kit Name	Company	Catalogue Number
A β _{x-40}	MSD® A β Triplex Assay	Meso Scale Discovery, Rockville, MD	K15148
A β _{x-42}	MSD® A β Triplex Assay	Meso Scale Discovery, Rockville, MD	K15148
A β ₁₋₄₂	INNOTEST® β -Amyloid (1-42)	Fujirebio, Ghent, Belgium	81583
p-tau ₁₈₁	INNOTEST® PHOSPHO-Tau (181P)	Fujirebio, Ghent, Belgium	81581
t-tau	INNOTEST® hTau Ag	Fujirebio, Ghent, Belgium	81579
NfL	NF-light™ ELISA RUO	UmanDiagnostics, Umeå, Sweden	10-7002 RUO
albumin†	IMMAGE® Immunochemistry System	Beckman Coulter, Brea, CA	447600

† CSF and plasma albumin measurements were determined from the same kit.

Supplemental Table 3.2 ADNI Cohort Demographics

Characteristic	Clinical Diagnosis			Total (N=727)
	Normal Cognition (N=229)	Mild Cognitive Impairment (N=381)	Alzheimer's Dementia (N=117)	
Male, no. (%)	122 (48)	217(57)	71(61)	400(55)
Age (baseline)	73±6.13	71±7.34	74±8.58	72±7.30
Education(yrs.)	17±2.51	16±2.66	16±2.62	16±2.63
sTREM2 CSF pg/mL	3940±1979.11	3894±2075.57	4039±2145.60	3932±2055.03
<i>APOE</i> -ε4 carriers, no. (%)	64(28)	194(51)	77(66)	335(46)

Values are presented as mean±standard deviation, unless otherwise indicated.
 93% participants are White; less than 1% reported as more than one or unknown racial category

Supplemental Table 3.3 Baseline CSF Biomarker Interactions on sTREM2

CSF Biomarker Interactions on sTREM2									
Biomarker	APOE-ε4 carrier status			Sex			MCI diagnosis		
	β	P	P.fdr	β	P	P.fdr	β	P	P.fdr
Aβ _{x-40}	0.051	0.781	0.781	-0.158	0.329	0.768	-0.140	0.368	0.676
p-tau ₁₈₁	-28.272	0.006	0.021	-20.211	0.045	0.158	-22.242	0.033	0.116
CSF/plasma Albumin ratio	-118.316	0.289	0.506	77.000	0.589	0.981	-55.097	0.627	0.732
t-tau	-3.698	0.002	0.014	-2.852	0.015	0.105	-4.057	0.003	0.021
NfL	-1.006	0.072	0.168	-0.171	0.749	0.981	-0.466	0.386	0.676
Aβ _{x-42}	1.031	0.517	0.693	-0.170	0.981	0.981	0.024	0.998	0.998
Aβ ₁₋₄₂	0.804	0.594	0.693	-0.135	0.917	0.981	0.601	0.611	0.732

Bold represents statistical significance set to a *priori* threshold P/P.fdr < 0.05 (Benjamini & Hochberg 1995).

Supplemental Table 3.4 Sensitivity Analysis: Main Effects of AD Biomarkers on Baseline CSF sTREM2 Measurement Adjusted for CSF Collection Date

Biomarker	Original Results				Sensitivity Results			
	β	SE	DF	P	β	SE	DF	P
A β _{x-40}	0.490	0.076	149	1.532e-09*	0.446	0.074	148	1.331e-8*
P-tau ₁₈₁	30.513	5.126	149	1.818e-08*	28.473	0.005	148	3.948e-8*
CSF/plasma albumin ratio	327.552	59.077	145	1.355e-07*	286.021	0.584	144	2.606e-6*
T-tau	3.146	0.604	149	6.137e-07*	2.919	0.578	148	1.277e-6*
Nfl	0.969	0.263	144	3.185e-04*	0.792	0.257	143	2.503e-3*
A β _{x-42}	1.448	0.536	149	7.728e-03*	1.445	0.507	148	4.953e-3*
A β ₁₋₄₂	0.678	0.599	149	2.599e-01	0.619	0.569	148	2.790e-1

Models included an additional covariate, CSF collection date, to adjust for potential storage/degradation effects (i.e., sTREM2 ~ AD Biomarker + age + sex + education + cognitive diagnosis + CSF collection date). Statistical results from the sensitivity analysis are colored green. Bold represents statistical significance set to a *priori* threshold $P < 0.05$. An asterisk indicates survival for multiple comparisons by FDR correction across each primary model (Benjamini & Hochberg 1995).

**Supplementary Table 3.5 Competitive Hierarchical Linear Regression Results
Adjusted for CSF Collection Date**

Model	Formula	Original Results						Sensitivity Results					
		DF	AIC	BIC	R ²	Adjusted R ²	ΔR ²	DF	AIC	BIC	R ²	Adjusted R ²	ΔR ²
base	CSF sTREM2 ~ age + sex + education + cognitive diagnosis	150	2778	2798	0.118	0.089	N/A	149	2762	2786	0.211	0.180	N/A
1	CSF sTREM2 ~ base covariates + p- tau ₁₈₁	149	2747	2770	0.288	0.259	0.169	148	2733	2759	0.357	0.327	0.146
2	CSF sTREM2 ~ base covariates + p- tau ₁₈₁ + Aβ _{x-40}	148	2738	2765	0.333	0.302	0.046	147	2727	2756	0.390	0.357	0.033
3	CSF sTREM2 ~ base covariates + p- tau ₁₈₁ + Aβ _{x-40} + CSF/plasma Albumin ratio	143	2636	2664	0.481	0.452	0.148	142	2631	2662	0.504	0.473	0.114

Statistical results from the sensitivity analysis are colored green. Sensitivity models included an additional covariate, CSF collection date, to adjust for potential storage/degradation effects. ΔR² = change in R² from previous nested model. Akaike information criterion (AIC) and Bayesian information criterion (BIC) calculations derived as follows: AIC = 2K – 2ln(L); where K = number of model parameters, and ln(L) = model log-likelihood. BIC = (RSS+log(n)df²) / n; where RSS = residual sum of squares, n = total observations, d = number of predictors, and σ² = estimate of variance of the error associated with each response measurement.

Supplemental Table 3.6. Main Effects of Baseline CSF Biomarkers on sTREM2 Measurement with Updated MCI Criteria

Biomarker	Original Results				Sensitivity Results			
	β	SE	DF	P	β	SE	DF	P
A β _{x-40}	0.490	0.076	149	1.532e-09*	0.495	0.078	136	2.917e-09*
p-tau ₁₈₁	30.513	5.126	149	1.818e-08*	30.734	5.450	136	9.306e-08*
CSF/plasma albumin ratio	327.552	59.077	145	1.355e-07*	332.156	60.641	132	2.105e-07*
t-tau	3.146	0.604	149	6.137e-07*	3.278	0.649	136	1.394e-06*
NfL	0.969	0.263	144	3.185e-04*	1.121	0.284	131	1.284e-04*
A β _{x-42}	1.448	0.536	149	7.728e-03*	1.627	0.553	136	3.867e-03*
A β ₁₋₄₂	0.678	0.599	149	2.599e-01	0.870	0.634	136	1.721e-01

To more accurately reflect ADNI MCI criteria, 8 individuals with MCI and a CDR score of 0 were removed. Additionally, 5 individuals with MCI and a Montreal Cognitive Assessment (MoCA) score of 17 or below were removed yielding a sample size for this sensitivity analysis of 142 individuals (originally 155). Statistical results from the sensitivity analysis are colored green. Bold represents statistical significance set to a *priori* threshold $P < 0.05$. An asterisk indicates survival for multiple comparisons by FDR correction across each primary model (Benjamini & Hochberg 1995). Significance value (P), degrees of freedom (DF), standard error (SE) and estimate of coefficient (β) represented for each model.

Supplemental Table 3.7 Baseline CSF Biomarker Interactions on sTREM2 with Updated MCI Criteria

CSF Biomarker Interactions on sTREM2						
Biomarker	APOE-ε4 carrier status					
	Original Results			Sensitivity Results		
	β	P	P.fdr	β	P	P.fdr
Aβ _{x-40}	0.051	0.781	0.781	0.038	0.835	0.835
p-tau ₁₈₁	-28.272	0.006	0.021	-30.121	0.005	0.018
CSF/plasma Albumin ratio	-118.316	0.289	0.506	-117.334	0.313	0.548
t-tau	-3.698	0.002	0.014	-4.398	0.0004	0.003
NfL	-1.006	0.072	0.168	-0.798	0.308	0.548
Aβ _{x-42}	1.031	0.517	0.693	0.983	0.545	0.760
Aβ ₁₋₄₂	0.804	0.594	0.693	0.701	0.652	0.760
Biomarker	Sex					
Aβ _{x-40}	-0.158	0.329	0.768	-0.141	0.401	0.865
p-tau ₁₈₁	-20.211	0.045	0.158	-18.569	0.086	0.302
CSF/plasma Albumin ratio	77.000	0.589	0.981	72.855	0.618	0.865
t-tau	-2.852	0.015	0.105	-2.527	0.047	0.302
NfL	-0.171	0.749	0.981	-0.368	0.513	0.865
Aβ _{x-42}	-0.170	0.981	0.981	-0.081	0.950	0.969
Aβ ₁₋₄₂	-0.135	0.917	0.981	-0.053	0.969	0.969
Biomarker	MCI diagnosis					
Aβ _{x-40}	-0.140	0.368	0.676	-0.146	0.370	0.717
p-tau ₁₈₁	-22.242	0.033	0.116	-23.629	0.031	0.108
CSF/plasma Albumin ratio	-55.097	0.627	0.732	-59.303	0.615	0.717
t-tau	-4.057	0.003	0.021	-4.186	0.002	0.011
NfL	-0.466	0.386	0.676	-0.332	0.555	0.717
Aβ _{x-42}	0.024	0.998	0.998	0.330	0.764	0.764
Aβ ₁₋₄₂	0.601	0.611	0.732	0.100	0.424	0.717

Statistical results from the sensitivity analysis are colored green. To more accurately reflect ADNI MCI criteria, 8 individuals with MCI and a CDR score of 0 were removed. Additionally, 5 individuals with MCI and a Montreal Cognitive Assessment (MoCA) score of 17 or below were removed yielding a sample size for this sensitivity analysis of 142 individuals (originally 155). Bold represents statistical significance set to a *priori* threshold P/P.fdr < 0.05 (Benjamini & Hochberg 1995).

Supplemental Table 3.8 Main Effects of Baseline CSF Biomarkers on sTREM2 Measurement After Outlier Removal

Biomarker	Original Results				Sensitivity Results			
	β	SE	DF	P	β	SE	DF	P
p-tau ₁₈₁	30.513	5.126	149	1.818e-08*	33.652	5.356	148	3.511e-09*
CSF/plasma albumin ratio	327.552	59.077	145	1.355e-07*	350.849	64.043	144	1.865e-07*
t-tau	3.146	0.604	149	6.137e-07*	3.767	0.654	148	4.762e-08*
NfL	0.969	0.263	144	3.185e-04*	1.360	0.349	141	1.514e-04*

Statistical results from the sensitivity analysis removing statistical and visual outliers (N=6 total; 1 t-tau, 1 CSF/plasma albumin, 3 NfL, and one visual p-tau₁₈₁ outliers) are colored green. Bold represents statistical significance set to a *priori* threshold P<0.05. An asterisk indicates survival for multiple comparisons by FDR correction across each primary model (Benjamini & Hochberg 1995). Significance value (P), degrees of freedom (DF), standard error (SE) and estimate of coefficient (β) represented for

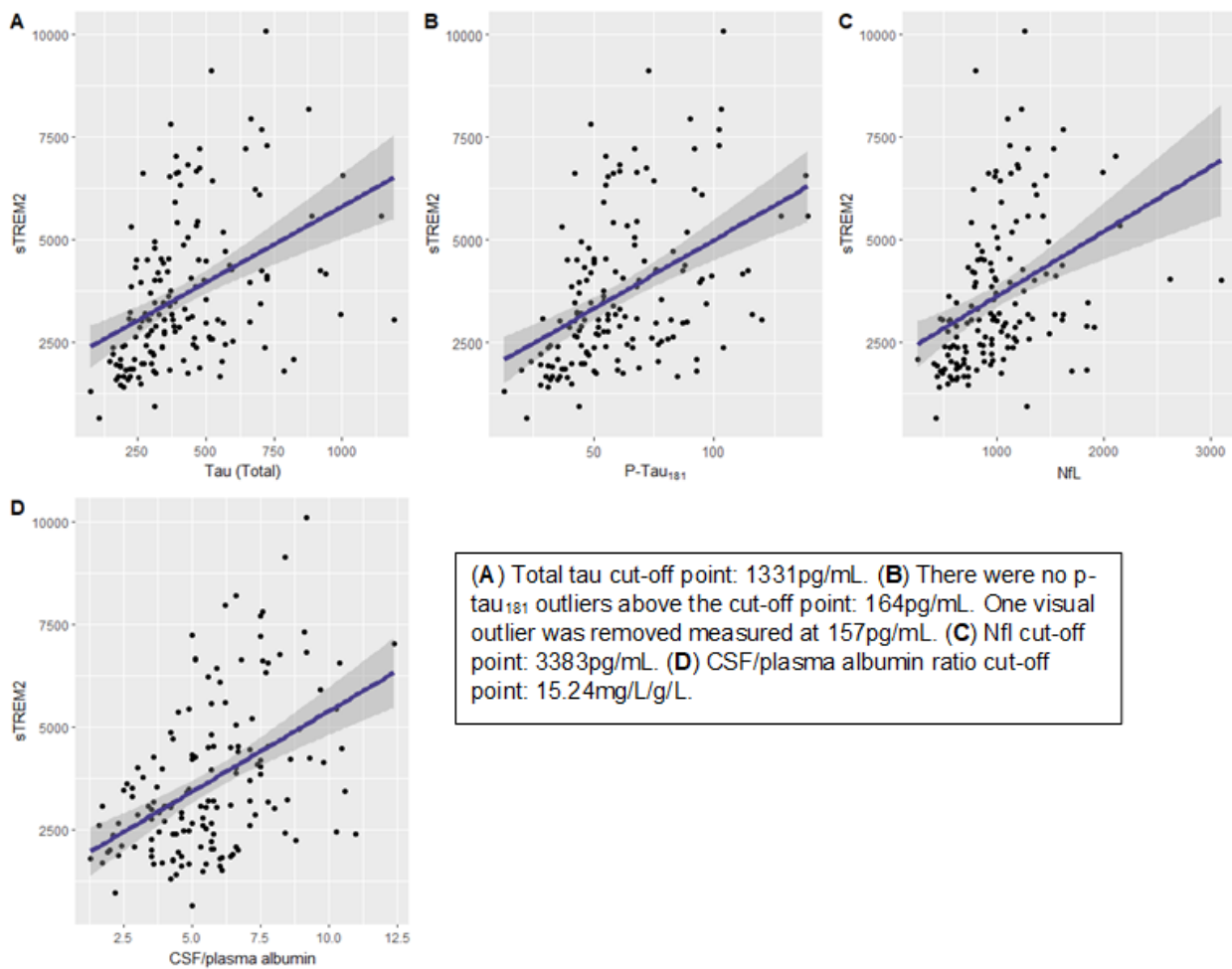
Supplemental Table 3.9 Baseline CSF Biomarker Interactions on sTREM2 After Outlier Removal

CSF Biomarker Interactions on sTREM2						
Biomarker	APOE-ε4 carrier status					
	Original Results			Sensitivity Results		
	β	P	P.fdr	β	P	P.fdr
p-tau ₁₈₁	-28.272	0.006	0.021	-24.828	0.009	0.036
CSF/plasma Albumin ratio	-118.316	0.289	0.506	-94.695	0.441	0.693
t-tau	-3.698	0.002	0.014	-3.152	0.010	0.036
NfL	-1.006	0.072	0.168	-1.150	0.151	0.693
Biomarker	Sex					
p-tau ₁₈₁	-20.211	0.045	0.158	-15.856	0.134	0.312
CSF/plasma Albumin ratio	77.000	0.589	0.981	50.600	0.729	0.917
t-tau	-2.852	0.015	0.105	-2.153	0.086	0.312
NfL	-0.171	0.749	0.981	-1.013	0.116	0.312
Biomarker	MCI diagnosis					
p-tau ₁₈₁	-22.242	0.033	0.116	-18.481	0.085	0.198
CSF/plasma Albumin ratio	-55.097	0.627	0.732	-11.357	0.928	0.998
t-tau	-4.057	0.003	0.021	-3.507	0.008	0.035
NfL	-0.466	0.386	0.676	-1.465	0.044	0.156

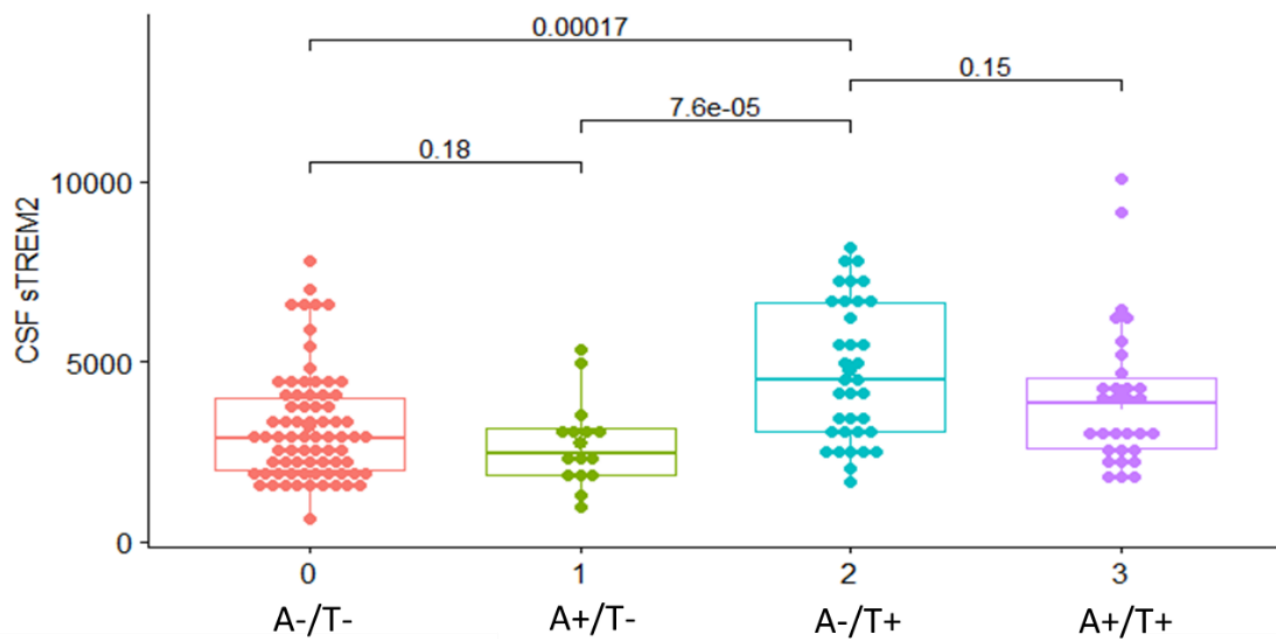
Statistical results from the sensitivity analysis after removal of statistical and visual outliers (N=6 total; 1 t-tau, 1 CSF/plasma albumin, 3 NfL, and one visual p-tau₁₈₁ outliers) are colored green. Bold represents statistical significance set to a *priori* threshold P/P.fdr < 0.05 (Benjamini & Hochberg

Supplemental Figures

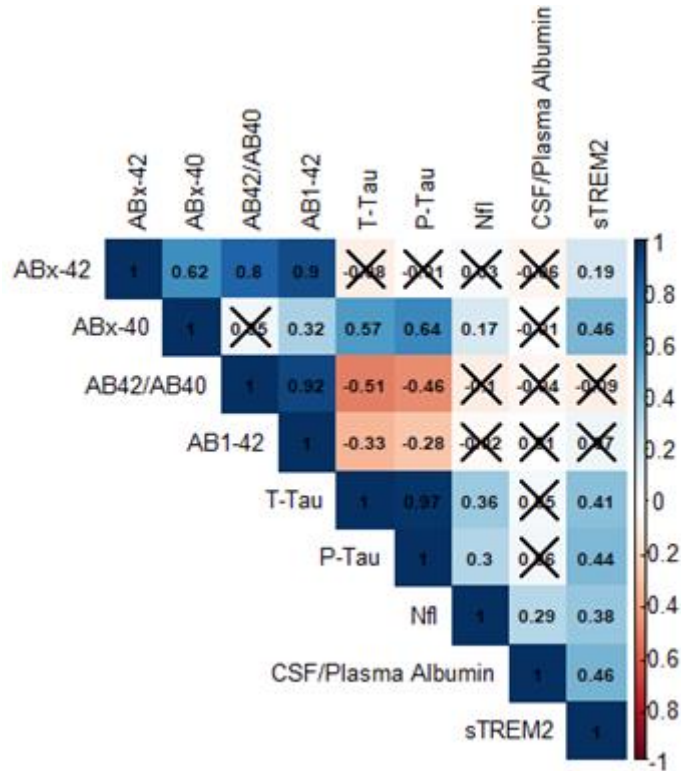
Supplemental Figure 3.1. Unadjusted scatter plots showing CSF AD biomarkers (x axis) by CSF sTREM2 (y axis) after visual and statistical outlier removal. Statistical outliers were determined by values 4 standard deviations outside of the mean measurement.



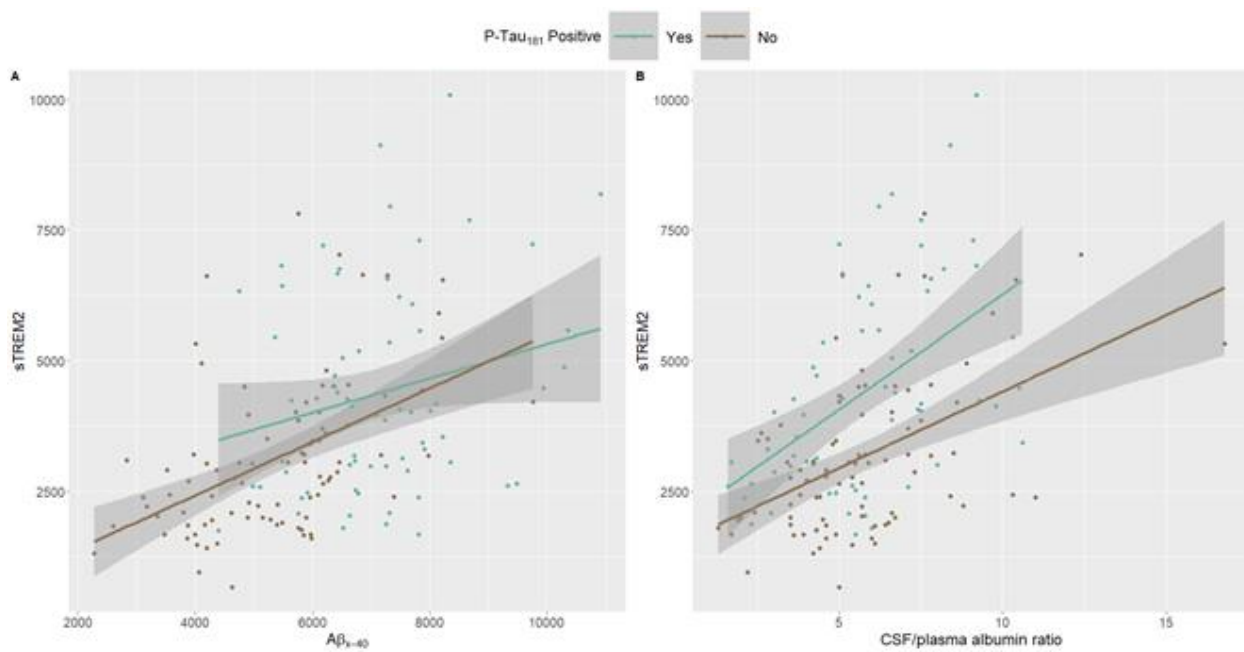
Supplemental Figure 3.2. CSF sTREM2 levels across amyloid and tau classification. AT=0 (Amyloid and Tau Negative); AT=1 (Amyloid Positive/Tau Negative); AT=2 (Amyloid Negative/Tau Positive); AT=3 (Amyloid and Tau Positive). sTREM2 measured in pg/mL.



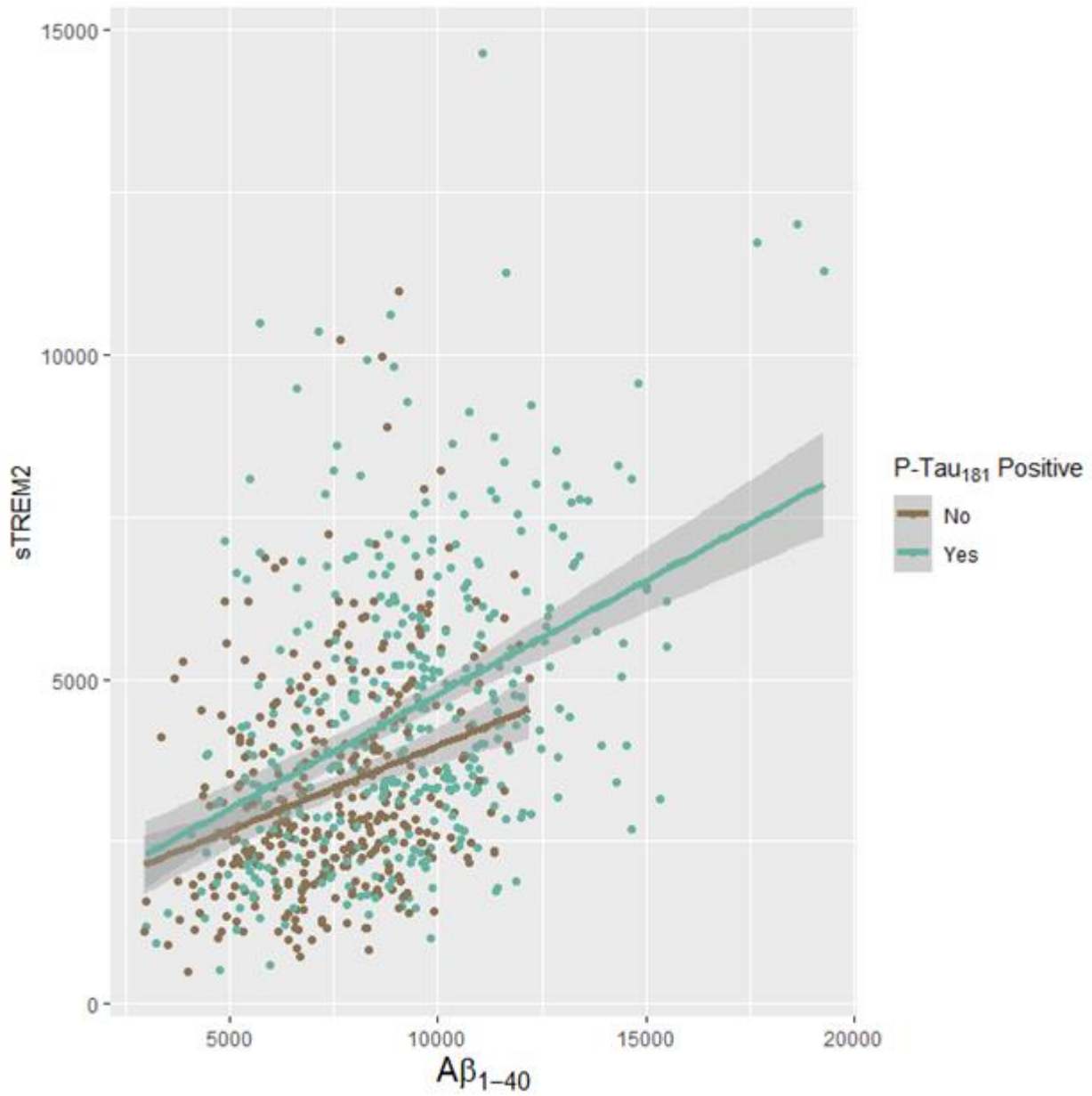
Supplemental Figure 3.3. Correlation matrix between sTREM2 and additional CSF biomarker measurements in VMAP. Non-significant Pearson's correlation coefficients are denoted by an "X".



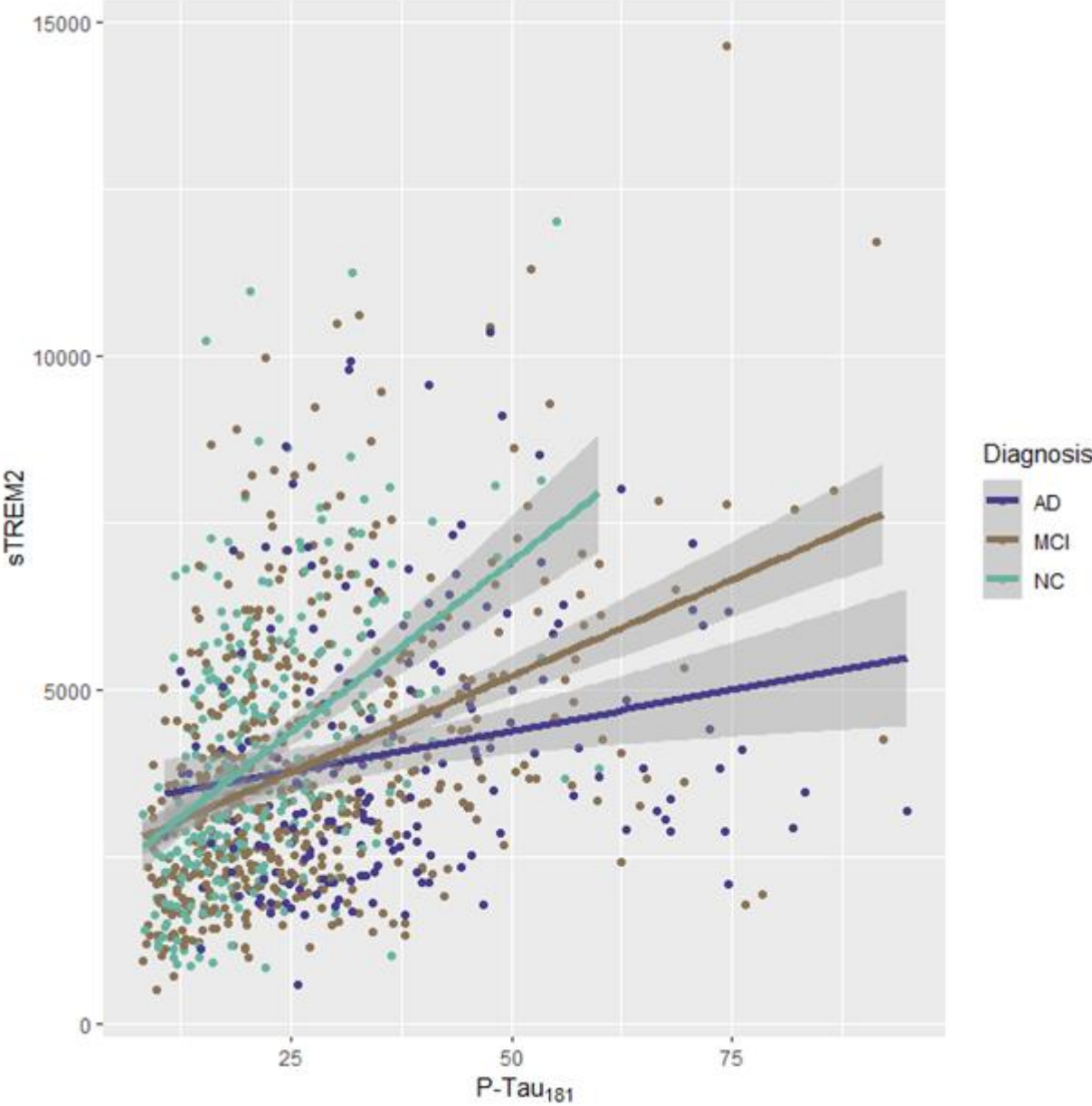
Supplemental Figure 3.4. A β and BBB biomarkers do not significantly interact with tau status on sTREM2 levels in CSF: **(A)** A β_{x-40} * tau status, p.int.=0.64, and **(B)** CSF/plasma albumin ratio * tau status, p.int.=0.25. Protein measurements given in pg/mL.



Supplemental Figure 3.5. Replication of $A\beta_{40}$ * tau status interaction on sTREM2. $A\beta_{1-40}$ does not significantly interact with tau status on sTREM2 levels in CSF using ADNI data: $A\beta_{1-40}$ * tau status, $p.int. = 0.22$. Protein measurements given in pg/mL.



Supplemental Figure 3.6. Using ADNI data, sTREM2 decouples from tau as disease progresses. Protein measurements given in pg/mL.



References

1. 2021 Alzheimer's disease facts and figures. *Alzheimers Dement.* 2021;17:327-406.
2. Wisniewski T and Drummond E. APOE-amyloid interaction: Therapeutic targets. *Neurobiol Dis.* 2020;138:104784.
3. Cline EN, Bicca MA, Viola KL and Klein WL. The Amyloid-beta Oligomer Hypothesis: Beginning of the Third Decade. *J Alzheimers Dis.* 2018;64:S567-S610.
4. Alzheimer's disease facts and figures. *Alzheimers Dement.* 2022;18:700-789.
5. Kirmess KM, Meyer MR, Holubasch MS, Knapik SS, Hu Y, Jackson EN, Harpstrite SE, Verghese PB, West T, Fogelman I, Braunstein JB, Yarasheski KE and Contois JH. The PrecivityAD test: Accurate and reliable LC-MS/MS assays for quantifying plasma amyloid beta 40 and 42 and apolipoprotein E proteotype for the assessment of brain amyloidosis. *Clin Chim Acta.* 2021;519:267-275.
6. West T, Kirmess KM, Meyer MR, Holubasch MS, Knapik SS, Hu Y, Contois JH, Jackson EN, Harpstrite SE, Bateman RJ, Holtzman DM, Verghese PB, Fogelman I, Braunstein JB and Yarasheski KE. A blood-based diagnostic test incorporating plasma A β 42/40 ratio, ApoE proteotype, and age accurately identifies brain amyloid status: findings from a multi cohort validity analysis. *Mol Neurodegener.* 2021;16:30.
7. Gale SA, Acar D and Daffner KR. Dementia. *Am J Med.* 2018;131:1161-1169.
8. Albert MS, DeKosky ST, Dickson D, Dubois B, Feldman HH, Fox NC, Gamst A, Holtzman DM, Jagust WJ, Petersen RC, Snyder PJ, Carrillo MC, Thies B and Phelps CH. The diagnosis of mild cognitive impairment due to Alzheimer's disease: recommendations from the National Institute on Aging-Alzheimer's Association workgroups on diagnostic guidelines for Alzheimer's disease. *Alzheimers Dement.* 2011;7:270-9.
9. Ward A, Tardiff S, Dye C and Arrighi HM. Rate of conversion from prodromal Alzheimer's disease to Alzheimer's dementia: a systematic review of the literature. *Dement Geriatr Cogn Dis Extra.* 2013;3:320-32.
10. Kapasi A, DeCarli C and Schneider JA. Impact of multiple pathologies on the threshold for clinically overt dementia. *Acta Neuropathol.* 2017;134:171-186.
11. Attems J and Jellinger KA. The overlap between vascular disease and Alzheimer's disease--lessons from pathology. *BMC Med.* 2014;12:206.
12. Toledo JB, Arnold SE, Raible K, Brettschneider J, Xie SX, Grossman M, Monsell SE, Kukull WA and Trojanowski JQ. Contribution of cerebrovascular disease in autopsy confirmed neurodegenerative disease cases in the National Alzheimer's Coordinating Centre. *Brain.* 2013;136:2697-706.
13. Custodio N, Montesinos R, Lira D, Herrera-Perez E, Bardales Y and Valeriano-Lorenzo L. Mixed dementia: A review of the evidence. *Dement Neuropsychol.* 2017;11:364-370.
14. Azarpazhooh MR, Avan A, Cipriano LE, Munoz DG, Sposato LA and Hachinski V. Concomitant vascular and neurodegenerative pathologies double the risk of dementia. *Alzheimers Dement.* 2018;14:148-156.
15. Gorelick PB, Scuteri A, Black SE, Decarli C, Greenberg SM, Iadecola C, Launer LJ, Laurent S, Lopez OL, Nyenhuis D, Petersen RC, Schneider JA, Tzourio C, Arnett DK, Bennett DA, Chui HC, Higashida RT, Lindquist R, Nilsson PM, Roman GC, Sellke FW, Seshadri S, American Heart Association Stroke Council CoE, Prevention CoNCOCR, Intervention, Council on Cardiovascular S and Anesthesia. Vascular contributions to cognitive impairment and dementia: a statement for healthcare professionals from the american heart association/american stroke association. *Stroke.* 2011;42:2672-713.

16. Stephan BC, Matthews FE, Ma B, Muniz G, Hunter S, Davis D, McKeith IG, Foster G, Ince PG and Brayne C. Alzheimer and vascular neuropathological changes associated with different cognitive States in a non-demented sample. *J Alzheimers Dis.* 2012;29:309-18.
17. Snowdon DA, Greiner LH, Mortimer JA, Riley KP, Greiner PA and Markesbery WR. Brain infarction and the clinical expression of Alzheimer disease. The Nun Study. *JAMA.* 1997;277:813-7.
18. Esiri MM, Nagy Z, Smith MZ, Barnetson L and Smith AD. Cerebrovascular disease and threshold for dementia in the early stages of Alzheimer's disease. *Lancet.* 1999;354:919-20.
19. Jellinger KA. Alzheimer disease and cerebrovascular pathology: an update. *J Neural Transm (Vienna).* 2002;109:813-36.
20. Kalaria RN. The role of cerebral ischemia in Alzheimer's disease. *Neurobiol Aging.* 2000;21:321-30.
21. Zekry D, Duyckaerts C, Moulia R, Belmin J, Geoffre C, Herrmann F and Hauw JJ. Degenerative and vascular lesions of the brain have synergistic effects in dementia of the elderly. *Acta Neuropathol.* 2002;103:481-7.
22. Heyman A, Fillenbaum GG, Welsh-Bohmer KA, Gearing M, Mirra SS, Mohs RC, Peterson BL and Pieper CF. Cerebral infarcts in patients with autopsy-proven Alzheimer's disease: CERAD, part XVIII. Consortium to Establish a Registry for Alzheimer's Disease. *Neurology.* 1998;51:159-62.
23. Esiri MM, Wilcock GK and Morris JH. Neuropathological assessment of the lesions of significance in vascular dementia. *J Neurol Neurosurg Psychiatry.* 1997;63:749-53.
24. Lee JH, Olichney JM, Hansen LA, Hofstetter CR and Thal LJ. Small concomitant vascular lesions do not influence rates of cognitive decline in patients with Alzheimer disease. *Arch Neurol.* 2000;57:1474-9.
25. Smallwood A, Oulhaj A, Joachim C, Christie S, Sloan C, Smith AD and Esiri M. Cerebral subcortical small vessel disease and its relation to cognition in elderly subjects: a pathological study in the Oxford Project to Investigate Memory and Ageing (OPTIMA) cohort. *Neuropathol Appl Neurobiol.* 2012;38:337-43.
26. Mehlig K, Skoog I, Waern M, Miao Jonasson J, Lapidus L, Bjorkelund C, Ostling S and Lissner L. Physical activity, weight status, diabetes and dementia: a 34-year follow-up of the population study of women in Gothenburg. *Neuroepidemiology.* 2014;42:252-9.
27. Sweeney MD, Sagare AP and Zlokovic BV. Blood-brain barrier breakdown in Alzheimer disease and other neurodegenerative disorders. *Nat Rev Neurol.* 2018;14:133-150.
28. Golde TE. Alzheimer's disease - the journey of a healthy brain into organ failure. *Mol Neurodegener.* 2022;17:18.
29. Iadecola C and Gottesman RF. Cerebrovascular Alterations in Alzheimer Disease. *Circ Res.* 2018;123:406-408.
30. Canepa E and Fossati S. Impact of Tau on Neurovascular Pathology in Alzheimer's Disease. *Front Neurol.* 2020;11:573324.
31. Kling MA, Trojanowski JQ, Wolk DA, Lee VM and Arnold SE. Vascular disease and dementias: paradigm shifts to drive research in new directions. *Alzheimers Dement.* 2013;9:76-92.
32. Ninomiya T, Ohara T, Hiraoka Y, Yoshida D, Doi Y, Hata J, Kanba S, Iwaki T and Kiyohara Y. Midlife and late-life blood pressure and dementia in Japanese elderly: the Hisayama study. *Hypertension.* 2011;58:22-8.
33. Dickstein DL, Walsh J, Brautigam H, Stockton SD, Jr., Gandy S and Hof PR. Role of vascular risk factors and vascular dysfunction in Alzheimer's disease. *Mt Sinai J Med.* 2010;77:82-102.
34. Laing KK, Simoes S, Baena-Caldas GP, Lao PJ, Kothiyi M, Igwe KC, Chesebro AG, Houck AL, Pedraza L, Hernandez AI, Li J, Zimmerman ME, Luchsinger JA, Barone FC, Moreno H, Brickman AM and Alzheimer's Disease Neuroimaging I. Cerebrovascular disease promotes tau pathology in Alzheimer's disease. *Brain Commun.* 2020;2:fcaa132.

35. Kalaria RN, Akinyemi R and Ihara M. Does vascular pathology contribute to Alzheimer changes? *J Neurol Sci.* 2012;322:141-7.
36. Zlokovic BV. Neurovascular pathways to neurodegeneration in Alzheimer's disease and other disorders. *Nat Rev Neurosci.* 2011;12:723-38.
37. Toledo JB, Toledo E, Weiner MW, Jack CR, Jr., Jagust W, Lee VM, Shaw LM, Trojanowski JQ and Alzheimer's Disease Neuroimaging I. Cardiovascular risk factors, cortisol, and amyloid-beta deposition in Alzheimer's Disease Neuroimaging Initiative. *Alzheimers Dement.* 2012;8:483-9.
38. Weller RO, Subash M, Preston SD, Mazanti I and Carare RO. Perivascular drainage of amyloid-beta peptides from the brain and its failure in cerebral amyloid angiopathy and Alzheimer's disease. *Brain Pathol.* 2008;18:253-66.
39. Raz L, Bhaskar K, Weaver J, Marini S, Zhang Q, Thompson JF, Espinoza C, Iqbal S, Maphis NM, Weston L, Sillerud LO, Caprihan A, Pesko JC, Erhardt EB and Rosenberg GA. Hypoxia promotes tau hyperphosphorylation with associated neuropathology in vascular dysfunction. *Neurobiol Dis.* 2019;126:124-136.
40. Iadecola C. The Neurovascular Unit Coming of Age: A Journey through Neurovascular Coupling in Health and Disease. *Neuron.* 2017;96:17-42.
41. Iturria-Medina Y, Sotero RC, Toussaint PJ, Mateos-Perez JM, Evans AC and Alzheimer's Disease Neuroimaging I. Early role of vascular dysregulation on late-onset Alzheimer's disease based on multifactorial data-driven analysis. *Nat Commun.* 2016;7:11934.
42. Shen Z, Bao X and Wang R. Clinical PET Imaging of Microglial Activation: Implications for Microglial Therapeutics in Alzheimer's Disease. *Front Aging Neurosci.* 2018;10:314.
43. Bettcher BM, Tansey MG, Dorothee G and Heneka MT. Peripheral and central immune system crosstalk in Alzheimer disease - a research prospectus. *Nat Rev Neurol.* 2021;17:689-701.
44. Moore Z, Taylor JM and Crack PJ. The involvement of microglia in Alzheimer's disease: a new dog in the fight. *Br J Pharmacol.* 2019;176:3533-3543.
45. Knopman DS, Jones DT and Greicius MD. Failure to demonstrate efficacy of aducanumab: An analysis of the EMERGE and ENGAGE trials as reported by Biogen, December 2019. *Alzheimers Dement.* 2021;17:696-701.
46. Mullard A. Landmark Alzheimer's drug approval confounds research community. *Nature.* 2021;594:309-310.
47. Bateman RJ, Benzinger TL, Berry S, Clifford DB, Duggan C, Fagan AM, Fanning K, Farlow MR, Hassenstab J, McDade EM, Mills S, Paumier K, Quintana M, Salloway SP, Santacruz A, Schneider LS, Wang G, Xiong C and Network D-TPCftDIA. The DIAN-TU Next Generation Alzheimer's prevention trial: Adaptive design and disease progression model. *Alzheimers Dement.* 2017;13:8-19.
48. Mintun MA, Lo AC, Duggan Evans C, Wessels AM, Ardayfio PA, Andersen SW, Shcherbinin S, Sparks J, Sims JR, Brys M, Apostolova LG, Salloway SP and Skovronsky DM. Donanemab in Early Alzheimer's Disease. *N Engl J Med.* 2021;384:1691-1704.
49. Demattos RB, Lu J, Tang Y, Racke MM, Delong CA, Tzaferis JA, Hole JT, Forster BM, McDonnell PC, Liu F, Kinley RD, Jordan WH and Hutton ML. A plaque-specific antibody clears existing beta-amyloid plaques in Alzheimer's disease mice. *Neuron.* 2012;76:908-20.
50. Cummings J, Lee G, Zhong K, Fonseca J and Taghva K. Alzheimer's disease drug development pipeline: 2021. *Alzheimers Dement (N Y).* 2021;7:e12179.
51. Wang S, Mustafa M, Yuede CM, Salazar SV, Kong P, Long H, Ward M, Siddiqui O, Paul R, Gilfillan S, Ibrahim A, Rhinn H, Tassi I, Rosenthal A, Schwabe T and Colonna M. Anti-human TREM2 induces microglia proliferation and reduces pathology in an Alzheimer's disease model. *J Exp Med.* 2020;217.
52. Bennett T, Bray D and Neville MW. Suvorexant, a dual orexin receptor antagonist for the management of insomnia. *P T.* 2014;39:264-6.

53. Ma L, Allen M, Sakae N, Ertekin-Taner N, Graff-Radford NR, Dickson DW, Younkin SG and Sevlever D. Expression and processing analyses of wild type and p.R47H TREM2 variant in Alzheimer's disease brains. *Mol Neurodegener.* 2016;11:72.
54. Angiulli F, Conti E, Zoia CP, Da Re F, Appollonio I, Ferrarese C and Tremolizzo L. Blood-Based Biomarkers of Neuroinflammation in Alzheimer's Disease: A Central Role for Periphery? *Diagnostics (Basel).* 2021;11.
55. Jay TR, Hirsch AM, Broihier ML, Miller CM, Neilson LE, Ransohoff RM, Lamb BT and Landreth GE. Disease Progression-Dependent Effects of TREM2 Deficiency in a Mouse Model of Alzheimer's Disease. *J Neurosci.* 2017;37:637-647.
56. Hu N, Tan MS, Yu JT, Sun L, Tan L, Wang YL, Jiang T and Tan L. Increased expression of TREM2 in peripheral blood of Alzheimer's disease patients. *J Alzheimers Dis.* 2014;38:497-501.
57. Casati M, Ferri E, Gussago C, Mazzola P, Abbate C, Bellelli G, Mari D, Cesari M and Arosio B. Increased expression of TREM2 in peripheral cells from mild cognitive impairment patients who progress into Alzheimer's disease. *Eur J Neurol.* 2018;25:805-810.
58. Daws MR, Sullam PM, Niemi EC, Chen TT, Tchao NK and Seaman WE. Pattern recognition by TREM-2: binding of anionic ligands. *J Immunol.* 2003;171:594-9.
59. Kober DL and Brett TJ. TREM2-Ligand Interactions in Health and Disease. *J Mol Biol.* 2017;429:1607-1629.
60. Zheng H, Jia L, Liu CC, Rong Z, Zhong L, Yang L, Chen XF, Fryer JD, Wang X, Zhang YW, Xu H and Bu G. TREM2 Promotes Microglial Survival by Activating Wnt/beta-Catenin Pathway. *J Neurosci.* 2017;37:1772-1784.
61. Kleinberger G, Yamanishi Y, Suarez-Calvet M, Czirr E, Lohmann E, Cuyvers E, Struyfs H, Pettkus N, Wenninger-Weinzierl A, Mazaheri F, Tahirovic S, Lleo A, Alcolea D, Fortea J, Willem M, Lammich S, Molinuevo JL, Sanchez-Valle R, Antonell A, Ramirez A, Heneka MT, Slegers K, van der Zee J, Martin JJ, Engelborghs S, Demirtas-Tatlidede A, Zetterberg H, Van Broeckhoven C, Gurvit H, Wyss-Coray T, Hardy J, Colonna M and Haass C. TREM2 mutations implicated in neurodegeneration impair cell surface transport and phagocytosis. *Sci Transl Med.* 2014;6:243ra86.
62. Linnartz-Gerlach B, Bodea LG, Klaus C, Ginolhac A, Halder R, Sinkkonen L, Walter J, Colonna M and Neumann H. TREM2 triggers microglial density and age-related neuronal loss. *Glia.* 2019;67:539-550.
63. Wu R, Li X, Xu P, Huang L, Cheng J, Huang X, Jiang J, Wu LJ and Tang Y. TREM2 protects against cerebral ischemia/reperfusion injury. *Mol Brain.* 2017;10:20.
64. Ulland TK, Song WM, Huang SC, Ulrich JD, Sergushichev A, Beatty WL, Loboda AA, Zhou Y, Cairns NJ, Kambal A, Loginicheva E, Gilfillan S, Cella M, Virgin HW, Unanue ER, Wang Y, Artyomov MN, Holtzman DM and Colonna M. TREM2 Maintains Microglial Metabolic Fitness in Alzheimer's Disease. *Cell.* 2017;170:649-663 e13.
65. Poliani PL, Wang Y, Fontana E, Robinette ML, Yamanishi Y, Gilfillan S and Colonna M. TREM2 sustains microglial expansion during aging and response to demyelination. *J Clin Invest.* 2015;125:2161-70.
66. Piccio L, Buonsanti C, Cella M, Tassi I, Schmidt RE, Fenoglio C, Rinker J, 2nd, Naismith RT, Panina-Bordignon P, Passini N, Galimberti D, Scarpini E, Colonna M and Cross AH. Identification of soluble TREM-2 in the cerebrospinal fluid and its association with multiple sclerosis and CNS inflammation. *Brain.* 2008;131:3081-91.
67. Del-Aguila JL, Benitez BA, Li Z, Dube U, Mihindikulasuriya KA, Budde JP, Farias FHG, Fernandez MV, Ibanez L, Jiang S, Perrin RJ, Cairns NJ, Morris JC, Harari O and Cruchaga C. TREM2 brain transcript-specific studies in AD and TREM2 mutation carriers. *Mol Neurodegener.* 2019;14:18.
68. Thornton P, Sevalle J, Deery MJ, Fraser G, Zhou Y, Stahl S, Franssen EH, Dodd RB, Qamar S, Gomez Perez-Nievas B, Nicol LS, Eketjall S, Revell J, Jones C, Billinton A, St George-Hyslop PH, Chessell I and

- Crowther DC. TREM2 shedding by cleavage at the H157-S158 bond is accelerated for the Alzheimer's disease-associated H157Y variant. *EMBO Mol Med.* 2017;9:1366-1378.
69. Feuerbach D, Schindler P, Barske C, Joller S, Beng-Louka E, Worringer KA, Kommineni S, Kaykas A, Ho DJ, Ye C, Welzenbach K, Elain G, Klein L, Brzak I, Mir AK, Farady CJ, Aichholz R, Popp S, George N and Neumann U. ADAM17 is the main sheddase for the generation of human triggering receptor expressed in myeloid cells (hTREM2) ectodomain and cleaves TREM2 after Histidine 157. *Neurosci Lett.* 2017;660:109-114.
70. Wunderlich P, Glebov K, Kemmerling N, Tien NT, Neumann H and Walter J. Sequential proteolytic processing of the triggering receptor expressed on myeloid cells-2 (TREM2) protein by ectodomain shedding and gamma-secretase-dependent intramembranous cleavage. *J Biol Chem.* 2013;288:33027-36.
71. Wu K, Byers DE, Jin X, Agapov E, Alexander-Brett J, Patel AC, Cella M, Gilfilan S, Colonna M, Kober DL, Brett TJ and Holtzman MJ. TREM-2 promotes macrophage survival and lung disease after respiratory viral infection. *J Exp Med.* 2015;212:681-97.
72. Szykowska A, Chen Y, Smith TB, Preger C, Yang J, Qian D, Mukhopadhyay SM, Wigren E, Neame SJ, Graslund S, Persson H, Atkinson PJ, Di Daniel E, Mead E, Wang J, Davis JB, Burgess-Brown NA and Bullock AN. Selection and structural characterization of anti-TREM2 scFvs that reduce levels of shed ectodomain. *Structure.* 2021;29:1241-1252 e5.
73. Schlepckow K, Monroe KM, Kleinberger G, Cantuti-Castelvetri L, Parhizkar S, Xia D, Willem M, Werner G, Pettkus N, Brunner B, Sulzen A, Nuscher B, Hampel H, Xiang X, Feederle R, Tahirovic S, Park JJ, Prorok R, Mahon C, Liang CC, Shi J, Kim DJ, Sabelstrom H, Huang F, Di Paolo G, Simons M, Lewcock JW and Haass C. Enhancing protective microglial activities with a dual function TREM2 antibody to the stalk region. *EMBO Mol Med.* 2020;12:e11227.
74. Zhong L, Chen XF, Wang T, Wang Z, Liao C, Wang Z, Huang R, Wang D, Li X, Wu L, Jia L, Zheng H, Painter M, Atagi Y, Liu CC, Zhang YW, Fryer JD, Xu H and Bu G. Soluble TREM2 induces inflammatory responses and enhances microglial survival. *J Exp Med.* 2017;214:597-607.
75. Michaelson DM. APOE epsilon4: the most prevalent yet understudied risk factor for Alzheimer's disease. *Alzheimers Dement.* 2014;10:861-8.
76. Guerreiro R, Wojtas A, Bras J, Carrasquillo M, Rogaeva E, Majounie E, Cruchaga C, Sassi C, Kauwe JS, Younkin S, Hazrati L, Collinge J, Pocock J, Lashley T, Williams J, Lambert JC, Amouyel P, Goate A, Rademakers R, Morgan K, Powell J, St George-Hyslop P, Singleton A, Hardy J and Alzheimer Genetic Analysis G. TREM2 variants in Alzheimer's disease. *N Engl J Med.* 2013;368:117-27.
77. Jonsson T, Stefansson H, Steinberg S, Jonsdottir I, Jonsson PV, Snaedal J, Bjornsson S, Huttenlocher J, Levey AI, Lah JJ, Rujescu D, Hampel H, Giegling I, Andreassen OA, Engedal K, Ulstein I, Djurovic S, Ibrahim-Verbaas C, Hofman A, Ikram MA, van Duijn CM, Thorsteinsdottir U, Kong A and Stefansson K. Variant of TREM2 associated with the risk of Alzheimer's disease. *N Engl J Med.* 2013;368:107-16.
78. Paloneva J, Kestila M, Wu J, Salminen A, Bohling T, Ruotsalainen V, Hakola P, Bakker AB, Phillips JH, Pekkarinen P, Lanier LL, Timonen T and Peltonen L. Loss-of-function mutations in TYROBP (DAP12) result in a presenile dementia with bone cysts. *Nat Genet.* 2000;25:357-61.
79. Paloneva J, Manninen T, Christman G, Hovanes K, Mandelin J, Adolfsson R, Bianchin M, Bird T, Miranda R, Salmaggi A, Tranebjaerg L, Konttinen Y and Peltonen L. Mutations in two genes encoding different subunits of a receptor signaling complex result in an identical disease phenotype. *Am J Hum Genet.* 2002;71:656-62.
80. Soragna D, Papi L, Ratti MT, Sestini R, Tupler R and Montalbetti L. An Italian family affected by Nasu-Hakola disease with a novel genetic mutation in the TREM2 gene. *J Neurol Neurosurg Psychiatry.* 2003;74:825-6.
81. Borroni B, Ferrari F, Galimberti D, Nacmias B, Barone C, Bagnoli S, Fenoglio C, Piaceri I, Archetti S, Bonvicini C, Gennarelli M, Turla M, Scarpini E, Sorbi S and Padovani A. Heterozygous TREM2 mutations in frontotemporal dementia. *Neurobiol Aging.* 2014;35:934 e7-10.

82. Rayaprolu S, Mullen B, Baker M, Lynch T, Finger E, Seeley WW, Hatanpaa KJ, Lomen-Hoerth C, Kertesz A, Bigio EH, Lippa C, Josephs KA, Knopman DS, White CL, 3rd, Caselli R, Mackenzie IR, Miller BL, Boczarska-Jedynak M, Opala G, Krygowska-Wajs A, Barcikowska M, Younkin SG, Petersen RC, Ertekin-Taner N, Uitti RJ, Meschia JF, Boylan KB, Boeve BF, Graff-Radford NR, Wszolek ZK, Dickson DW, Rademakers R and Ross OA. TREM2 in neurodegeneration: evidence for association of the p.R47H variant with frontotemporal dementia and Parkinson's disease. *Mol Neurodegener.* 2013;8:19.
83. Sasaki A, Kakita A, Yoshida K, Konno T, Ikeuchi T, Hayashi S, Matsuo H and Shioda K. Variable expression of microglial DAP12 and TREM2 genes in Nasu-Hakola disease. *Neurogenetics.* 2015;16:265-76.
84. Zhong L, Xu Y, Zhuo R, Wang T, Wang K, Huang R, Wang D, Gao Y, Zhu Y, Sheng X, Chen K, Wang N, Zhu L, Can D, Marten Y, Shinohara M, Liu CC, Du D, Sun H, Wen L, Xu H, Bu G and Chen XF. Soluble TREM2 ameliorates pathological phenotypes by modulating microglial functions in an Alzheimer's disease model. *Nat Commun.* 2019;10:1365.
85. Leyns CEG, Gratuze M, Narasimhan S, Jain N, Koscal LJ, Jiang H, Manis M, Colonna M, Lee VMY, Ulrich JD and Holtzman DM. TREM2 function impedes tau seeding in neuritic plaques. *Nat Neurosci.* 2019;22:1217-1222.
86. Bemiller SM, McCray TJ, Allan K, Formica SV, Xu G, Wilson G, Kokiko-Cochran ON, Crish SD, Lasagna-Reeves CA, Ransohoff RM, Landreth GE and Lamb BT. TREM2 deficiency exacerbates tau pathology through dysregulated kinase signaling in a mouse model of tauopathy. *Mol Neurodegener.* 2017;12:74.
87. Wang Y, Ulland TK, Ulrich JD, Song W, Tzaferis JA, Hole JT, Yuan P, Mahan TE, Shi Y, Gilfillan S, Cella M, Grutzendler J, DeMattos RB, Cirrito JR, Holtzman DM and Colonna M. TREM2-mediated early microglial response limits diffusion and toxicity of amyloid plaques. *J Exp Med.* 2016;213:667-75.
88. Jay TR, Miller CM, Cheng PJ, Graham LC, Bemiller S, Broihier ML, Xu G, Margevicius D, Karlo JC, Sousa GL, Cotleur AC, Butovsky O, Bekris L, Staugaitis SM, Leverenz JB, Pimplikar SW, Landreth GE, Howell GR, Ransohoff RM and Lamb BT. TREM2 deficiency eliminates TREM2+ inflammatory macrophages and ameliorates pathology in Alzheimer's disease mouse models. *J Exp Med.* 2015;212:287-95.
89. Edison P and Brooks DJ. Role of Neuroinflammation in the Trajectory of Alzheimer's Disease and in vivo Quantification Using PET. *J Alzheimers Dis.* 2018;64:S339-S351.
90. Lue LF, Schmitz CT, Serrano G, Sue LI, Beach TG and Walker DG. TREM2 Protein Expression Changes Correlate with Alzheimer's Disease Neurodegenerative Pathologies in Post-Mortem Temporal Cortices. *Brain Pathol.* 2015;25:469-80.
91. Toomey CE, Heywood W, Benson BC, Packham G, Mills K and Lashley T. Investigation of pathology, expression and proteomic profiles in human TREM2 variant postmortem brains with and without Alzheimer's disease. *Brain Pathol.* 2020;30:794-810.
92. Deming Y, Filipello F, Cignarella F, Cantoni C, Hsu S, Mikesell R, Li Z, Del-Aguila JL, Dube U, Farias FG, Bradley J, Budde J, Ibanez L, Fernandez MV, Blennow K, Zetterberg H, Heslegrave A, Johansson PM, Svensson J, Nellgard B, Lleo A, Alcolea D, Clarimon J, Rami L, Molinuevo JL, Suarez-Calvet M, Morenas-Rodriguez E, Kleinberger G, Ewers M, Harari O, Haass C, Brett TJ, Benitez BA, Karch CM, Piccio L and Cruchaga C. The MS4A gene cluster is a key modulator of soluble TREM2 and Alzheimer's disease risk. *Sci Transl Med.* 2019;11.
93. Hollingworth P, Harold D, Sims R, Gerrish A, Lambert JC, Carrasquillo MM, Abraham R, Hamshere ML, Pahwa JS, Moskvina V, Dowzell K, Jones N, Stretton A, Thomas C, Richards A, Ivanov D, Widdowson C, Chapman J, Lovestone S, Powell J, Proitsi P, Lupton MK, Brayne C, Rubinsztein DC, Gill M, Lawlor B, Lynch A, Brown KS, Passmore PA, Craig D, McGuinness B, Todd S, Holmes C, Mann D, Smith AD, Beaumont H, Warden D, Wilcock G, Love S, Kehoe PG, Hooper NM, Vardy ER, Hardy J, Mead S, Fox NC, Rossor M, Collinge J, Maier W, Jessen F, Ruther E, Schurmann B, Heun R, Kolsch H, van den Bussche H, Heuser I, Kornhuber J, Wiltfang J, Dichgans M, Frolich L, Hampel H, Gallacher J, Hull M, Rujescu D, Giegling I, Goate

AM, Kauwe JS, Cruchaga C, Nowotny P, Morris JC, Mayo K, Slegers K, Bettens K, Engelborghs S, De Deyn PP, Van Broeckhoven C, Livingston G, Bass NJ, Gurling H, McQuillin A, Gwilliam R, Deloukas P, Al-Chalabi A, Shaw CE, Tsolaki M, Singleton AB, Guerreiro R, Muhleisen TW, Nothen MM, Moebus S, Jockel KH, Klopp N, Wichmann HE, Pankratz VS, Sando SB, Aasly JO, Barcikowska M, Wszolek ZK, Dickson DW, Graff-Radford NR, Petersen RC, Alzheimer's Disease Neuroimaging I, van Duijn CM, Breteler MM, Ikram MA, DeStefano AL, Fitzpatrick AL, Lopez O, Launer LJ, Seshadri S, consortium C, Berr C, Champion D, Epelbaum J, Dartigues JF, Tzourio C, Alperovitch A, Lathrop M, consortium E, Feulner TM, Friedrich P, Riehle C, Krawczak M, Schreiber S, Mayhaus M, Nicolhaus S, Wagenpfeil S, Steinberg S, Stefansson H, Stefansson K, Snaedal J, Bjornsson S, Jonsson PV, Chouraki V, Genier-Boley B, Hiltunen M, Soininen H, Combarros O, Zelenika D, Delepine M, Bullido MJ, Pasquier F, Mateo I, Frank-Garcia A, Porcellini E, Hanon O, Coto E, Alvarez V, Bosco P, Siciliano G, Mancuso M, Panza F, Solfrizzi V, Nacmias B, Sorbi S, Bossu P, Piccardi P, Arosio B, Annoni G, Seripa D, Pilotto A, Scarpini E, Galimberti D, Brice A, Hannequin D, Licastrò F, Jones L, Holmans PA, Jonsson T, Riemenschneider M, Morgan K, Younkin SG, Owen MJ, O'Donovan M, Amouyel P and Williams J. Common variants at ABCA7, MS4A6A/MS4A4E, EPHA1, CD33 and CD2AP are associated with Alzheimer's disease. *Nat Genet.* 2011;43:429-35.

94. Naj AC, Jun G, Beecham GW, Wang LS, Vardarajan BN, Buross J, Gallins PJ, Buxbaum JD, Jarvik GP, Crane PK, Larson EB, Bird TD, Boeve BF, Graff-Radford NR, De Jager PL, Evans D, Schneider JA, Carrasquillo MM, Ertekin-Taner N, Younkin SG, Cruchaga C, Kauwe JS, Nowotny P, Kramer P, Hardy J, Huentelman MJ, Myers AJ, Barmada MM, Demirci FY, Baldwin CT, Green RC, Rogava E, St George-Hyslop P, Arnold SE, Barber R, Beach T, Bigio EH, Bowen JD, Boxer A, Burke JR, Cairns NJ, Carlson CS, Carney RM, Carroll SL, Chui HC, Clark DG, Corneveaux J, Cotman CW, Cummings JL, DeCarli C, DeKosky ST, Diaz-Arrastia R, Dick M, Dickson DW, Ellis WG, Faber KM, Fallon KB, Farlow MR, Ferris S, Frosch MP, Galasko DR, Ganguli M, Gearing M, Geschwind DH, Ghetti B, Gilbert JR, Gilman S, Giordani B, Glass JD, Growdon JH, Hamilton RL, Harrell LE, Head E, Honig LS, Hulette CM, Hyman BT, Jicha GA, Jin LW, Johnson N, Karlawish J, Karydas A, Kaye JA, Kim R, Koo EH, Kowall NW, Lah JJ, Levey AI, Lieberman AP, Lopez OL, Mack WJ, Marson DC, Martiniuk F, Mash DC, Masliah E, McCormick WC, McCurry SM, McDavid AN, McKee AC, Mesulam M, Miller BL, Miller CA, Miller JW, Parisi JE, Perl DP, Peskind E, Petersen RC, Poon WW, Quinn JF, Rajbhandary RA, Raskind M, Reisberg B, Ringman JM, Roberson ED, Rosenberg RN, Sano M, Schneider LS, Seeley W, Shelanski ML, Slifer MA, Smith CD, Sonnen JA, Spina S, Stern RA, Tanzi RE, Trojanowski JQ, Troncoso JC, Van Deerlin VM, Vinters HV, Vonsattel JP, Weintraub S, Welsh-Bohmer KA, Williamson J, Woltjer RL, Cantwell LB, Dombroski BA, Beekly D, Lunetta KL, Martin ER, Kamboh MI, Saykin AJ, Reiman EM, Bennett DA, Morris JC, Montine TJ, Goate AM, Blacker D, Tsuang DW, Hakonarson H, Kukull WA, Foroud TM, Haines JL, Mayeux R, Pericak-Vance MA, Farrer LA and Schellenberg GD. Common variants at MS4A4/MS4A6E, CD2AP, CD33 and EPHA1 are associated with late-onset Alzheimer's disease. *Nat Genet.* 2011;43:436-41.

95. Yuetiva Deming FF, Francesca Cignarella, Marc Suárez-Calvet, Estrella Morenas-Rodríguez, Carol A. Van Hulle, Erin M. Jonaitis, Kaj Blennow, Henrik Zetterberg, Sanjay Asthana, Sterling C. Johnson, Cynthia M. Carlsson, Barbara B. Bendlin, Corinne D. Engelman, Michael Ewers, Christian Haass, Bruno Benitez, Celeste M. Karch, Laura Piccio, Carlos Cruchaga Protective genetic variants in the MS4A gene cluster modulate microglial activity. *Alzheimer's & Dementia.* 2020;16.

96. Wang Y, Cella M, Mallinson K, Ulrich JD, Young KL, Robinette ML, Gilfillan S, Krishnan GM, Sudhakar S, Zinselmeyer BH, Holtzman DM, Cirrito JR and Colonna M. TREM2 lipid sensing sustains the microglial response in an Alzheimer's disease model. *Cell.* 2015;160:1061-71.

97. Jiang T, Tan L, Zhu XC, Zhou JS, Cao L, Tan MS, Wang HF, Chen Q, Zhang YD and Yu JT. Silencing of TREM2 exacerbates tau pathology, neurodegenerative changes, and spatial learning deficits in P301S tau transgenic mice. *Neurobiol Aging.* 2015;36:3176-3186.

98. Jiang T, Zhang YD, Chen Q, Gao Q, Zhu XC, Zhou JS, Shi JQ, Lu H, Tan L and Yu JT. TREM2 modifies microglial phenotype and provides neuroprotection in P301S tau transgenic mice. *Neuropharmacology.* 2016;105:196-206.

99. Hakola HP. Neuropsychiatric and genetic aspects of a new hereditary disease characterized by progressive dementia and lipomembranous polycystic osteodysplasia. *Acta Psychiatr Scand Suppl.* 1972;232:1-173.
100. Cady J, Koval ED, Benitez BA, Zaidman C, Jockel-Balsarotti J, Allred P, Baloh RH, Ravits J, Simpson E, Appel SH, Pestronk A, Goate AM, Miller TM, Cruchaga C and Harms MB. TREM2 variant p.R47H as a risk factor for sporadic amyotrophic lateral sclerosis. *JAMA Neurol.* 2014;71:449-53.
101. Jay TR, von Saucken VE and Landreth GE. TREM2 in Neurodegenerative Diseases. *Mol Neurodegener.* 2017;12:56.
102. Parhizkar S, Arzberger T, Brendel M, Kleinberger G, Deussing M, Focke C, Nuscher B, Xiong M, Ghasemigharagoz A, Katzmarski N, Krasemann S, Lichtenthaler SF, Muller SA, Colombo A, Monasor LS, Tahirovic S, Herms J, Willem M, Pettkus N, Butovsky O, Bartenstein P, Edbauer D, Rominger A, Erturk A, Grathwohl SA, Neher JJ, Holtzman DM, Meyer-Luehmann M and Haass C. Loss of TREM2 function increases amyloid seeding but reduces plaque-associated ApoE. *Nat Neurosci.* 2019;22:191-204.
103. Yuan P, Condello C, Keene CD, Wang Y, Bird TD, Paul SM, Luo W, Colonna M, Baddeley D and Grutzendler J. TREM2 Haplodeficiency in Mice and Humans Impairs the Microglia Barrier Function Leading to Decreased Amyloid Compaction and Severe Axonal Dystrophy. *Neuron.* 2016;90:724-39.
104. Yeh FL, Wang Y, Tom I, Gonzalez LC and Sheng M. TREM2 Binds to Apolipoproteins, Including APOE and CLU/APOJ, and Thereby Facilitates Uptake of Amyloid-Beta by Microglia. *Neuron.* 2016;91:328-40.
105. Zhao Y, Wu X, Li X, Jiang LL, Gui X, Liu Y, Sun Y, Zhu B, Pina-Crespo JC, Zhang M, Zhang N, Chen X, Bu G, An Z, Huang TY and Xu H. TREM2 Is a Receptor for beta-Amyloid that Mediates Microglial Function. *Neuron.* 2018;97:1023-1031 e7.
106. Wolfe CM, Fitz NF, Nam KN, Lefterov I and Koldamova R. The Role of APOE and TREM2 in Alzheimer's Disease-Current Understanding and Perspectives. *Int J Mol Sci.* 2018;20.
107. Ulrich JD, Ulland TK, Colonna M and Holtzman DM. Elucidating the Role of TREM2 in Alzheimer's Disease. *Neuron.* 2017;94:237-248.
108. Raha-Chowdhury R, Henderson JW, Raha AA, Stott SRW, Vuono R, Foscarin S, Wilson L, Annus T, Fincham R, Allinson K, Devalia V, Friedland RP, Holland A and Zaman SH. Erythromyeloid-Derived TREM2: A Major Determinant of Alzheimer's Disease Pathology in Down Syndrome. *J Alzheimers Dis.* 2018;61:1143-1162.
109. Carbajosa G, Malki K, Lawless N, Wang H, Ryder JW, Wozniak E, Wood K, Mein CA, Dobson RJB, Collier DA, O'Neill MJ, Hodges AK and Newhouse SJ. Loss of Trem2 in microglia leads to widespread disruption of cell coexpression networks in mouse brain. *Neurobiol Aging.* 2018;69:151-166.
110. Bekris LM, Khrestian M, Dyne E, Shao Y, Pillai JA, Rao SM, Bemiller SM, Lamb B, Fernandez HH and Leverenz JB. Soluble TREM2 and biomarkers of central and peripheral inflammation in neurodegenerative disease. *J Neuroimmunol.* 2018;319:19-27.
111. Jaitin DA, Adlung L, Thaiss CA, Weiner A, Li B, Descamps H, Lundgren P, Blieriot C, Liu Z, Deczkowska A, Keren-Shaul H, David E, Zmora N, Eldar SM, Lubezky N, Shibolet O, Hill DA, Lazar MA, Colonna M, Ginhoux F, Shapiro H, Elinav E and Amit I. Lipid-Associated Macrophages Control Metabolic Homeostasis in a Trem2-Dependent Manner. *Cell.* 2019;178:686-698 e14.
112. Perez SE, Nadeem M, He B, Miguel JC, Malek-Ahmadi MH, Chen K and Mufson EJ. Neocortical and hippocampal TREM2 protein levels during the progression of Alzheimer's disease. *Neurobiol Aging.* 2017;54:133-143.
113. Zhao Y, Bhattacharjee S, Jones BM, Dua P, Alexandrov PN, Hill JM and Lukiw WJ. Regulation of TREM2 expression by an NF-small ka, CyrillicB-sensitive miRNA-34a. *Neuroreport.* 2013;24:318-23.
114. Celarain N, Sanchez-Ruiz de Gordo J, Zelaya MV, Roldan M, Larumbe R, Pulido L, Echavarri C and Mendioroz M. TREM2 upregulation correlates with 5-hydroxymethylcytosine enrichment in Alzheimer's disease hippocampus. *Clin Epigenetics.* 2016;8:37.

115. Frank S, Burbach GJ, Bonin M, Walter M, Streit W, Bechmann I and Deller T. TREM2 is upregulated in amyloid plaque-associated microglia in aged APP23 transgenic mice. *Glia*. 2008;56:1438-47.
116. Felsky D, Roostaei T, Nho K, Risacher SL, Bradshaw EM, Petyuk V, Schneider JA, Saykin A, Bennett DA and De Jager PL. Neuropathological correlates and genetic architecture of microglial activation in elderly human brain. *Nat Commun*. 2019;10:409.
117. Davies DS, Ma J, Jegathees T and Goldsbury C. Microglia show altered morphology and reduced arborization in human brain during aging and Alzheimer's disease. *Brain Pathol*. 2017;27:795-808.
118. Serrano-Pozo A, Gomez-Isla T, Growdon JH, Frosch MP and Hyman BT. A phenotypic change but not proliferation underlies glial responses in Alzheimer disease. *Am J Pathol*. 2013;182:2332-44.
119. Rosenberg GA, Wallin A, Wardlaw JM, Markus HS, Montaner J, Wolfson L, Iadecola C, Zlokovic BV, Joutel A, Dichgans M, Duering M, Schmidt R, Korczyn AD, Grinberg LT, Chui HC and Hachinski V. Consensus statement for diagnosis of subcortical small vessel disease. *J Cereb Blood Flow Metab*. 2016;36:6-25.
120. Poggesi A, Pasi M, Pescini F, Pantoni L and Inzitari D. Circulating biologic markers of endothelial dysfunction in cerebral small vessel disease: A review. *J Cereb Blood Flow Metab*. 2016;36:72-94.
121. Gorenjak V, Aldasoro Arguinano AA, Dade S, Stathopoulou MG, Vance DR, Masson C and Visvikis-Siest S. The polymorphism rs6918289 located in the downstream region of the TREM2 gene is associated with TNF-alpha levels and IMT-F. *Sci Rep*. 2018;8:7160.
122. Stanimirovic DB and Friedman A. Pathophysiology of the neurovascular unit: disease cause or consequence? *J Cereb Blood Flow Metab*. 2012;32:1207-21.
123. Oveisgharan S, Buchman AS, Yu L, Farfel J, Hachinski V, Gaiteri C, De Jager PL, Schneider JA and Bennett DA. APOE epsilon2epsilon4 genotype, incident AD and MCI, cognitive decline, and AD pathology in older adults. *Neurology*. 2018;90:e2127-e2134.
124. Bennett DA, Schneider JA, Buchman AS, Barnes LL, Boyle PA and Wilson RS. Overview and findings from the rush Memory and Aging Project. *Curr Alzheimer Res*. 2012;9:646-63.
125. Bennett DA, Wilson RS, Arvanitakis Z, Boyle PA, de Toledo-Morrell L and Schneider JA. Selected findings from the Religious Orders Study and Rush Memory and Aging Project. *J Alzheimers Dis*. 2013;33 Suppl 1:S397-403.
126. Bennett DA, Buchman AS, Boyle PA, Barnes LL, Wilson RS and Schneider JA. Religious Orders Study and Rush Memory and Aging Project. *J Alzheimers Dis*. 2018;64:S161-S189.
127. Mathys H, Davila-Velderrain J, Peng Z, Gao F, Mohammadi S, Young JZ, Menon M, He L, Abdurrob F, Jiang X, Martorell AJ, Ransohoff RM, Hafler BP, Bennett DA, Kellis M and Tsai LH. Single-cell transcriptomic analysis of Alzheimer's disease. *Nature*. 2019;570:332-337.
128. Habib N, Avraham-Davidi I, Basu A, Burks T, Shekhar K, Hofree M, Choudhury SR, Aguet F, Gelfand E, Ardlie K, Weitz DA, Rozenblatt-Rosen O, Zhang F and Regev A. Massively parallel single-nucleus RNA-seq with DroNc-seq. *Nat Methods*. 2017;14:955-+.
129. Grothe MJ, Barthel H, Sepulcre J, Dyrba M, Sabri O, Teipel SJ and Alzheimer's Disease Neuroimaging I. In vivo staging of regional amyloid deposition. *Neurology*. 2017;89:2031-2038.
130. Leyns CEG, Ulrich JD, Finn MB, Stewart FR, Koscal LJ, Remolina Serrano J, Robinson GO, Anderson E, Colonna M and Holtzman DM. TREM2 deficiency attenuates neuroinflammation and protects against neurodegeneration in a mouse model of tauopathy. *Proc Natl Acad Sci U S A*. 2017;114:11524-11529.
131. Pascoal TA, Benedet AL, Ashton NJ, Kang MS, Therriault J, Chamoun M, Savard M, Lussier FZ, Tissot C, Karikari TK, Ottoy J, Mathotaarachchi S, Stevenson J, Massarweh G, Scholl M, de Leon MJ, Soucy JP, Edison P, Blennow K, Zetterberg H, Gauthier S and Rosa-Neto P. Microglial activation and tau propagate jointly across Braak stages. *Nat Med*. 2021;27:1592-1599.
132. Tan YL, Yuan Y and Tian L. Microglial regional heterogeneity and its role in the brain. *Mol Psychiatry*. 2020;25:351-367.

133. Keren-Shaul H, Spinrad A, Weiner A, Matcovitch-Natan O, Dvir-Szternfeld R, Ulland TK, David E, Baruch K, Lara-Astaiso D, Toth B, Itzkovitz S, Colonna M, Schwartz M and Amit I. A Unique Microglia Type Associated with Restricting Development of Alzheimer's Disease. *Cell*. 2017;169:1276-1290 e17.
134. Masuda T, Sankowski R, Staszewski O, Bottcher C, Amann L, Sagar, Scheiwe C, Nessler S, Kunz P, van Loo G, Coenen VA, Reinacher PC, Michel A, Sure U, Gold R, Grun D, Priller J, Stadelmann C and Prinz M. Spatial and temporal heterogeneity of mouse and human microglia at single-cell resolution. *Nature*. 2019;566:388-392.
135. Porsch F, KMG, Goederle L., Hendriks T., Hladik A., Knapp S., et al. Haematopoietic TREM2 Deficiency Modulates Atherosclerosis and Lipid Metabolism. *Atherosclerosis*. 2020;315:e58–e59.
136. Kawabori M, Kacimi R, Kauppinen T, Calosing C, Kim JY, Hsieh CL, Nakamura MC and Yenari MA. Triggering receptor expressed on myeloid cells 2 (TREM2) deficiency attenuates phagocytic activities of microglia and exacerbates ischemic damage in experimental stroke. *J Neurosci*. 2015;35:3384-96.
137. Yang AC, Vest RT, Kern F, Lee DP, Agam M, Maat CA, Losada PM, Chen MB, Schaum N, Houry N, Toland A, Calcuttawala K, Shin H, Palovics R, Shin A, Wang EY, Luo J, Gate D, Schulz-Schaeffer WJ, Chu P, Siegenthaler JA, McNerney MW, Keller A and Wyss-Coray T. A human brain vascular atlas reveals diverse mediators of Alzheimer's risk. *Nature*. 2022;603:885-892.
138. Fahrenhold M, Rakic S, Classey J, Brayne C, Ince PG, Nicoll JAR, Boche D and Mrc C. TREM2 expression in the human brain: a marker of monocyte recruitment? *Brain Pathol*. 2018;28:595-602.
139. Serrano-Pozo A, Frosch MP, Masliah E and Hyman BT. Neuropathological alterations in Alzheimer disease. *Cold Spring Harb Perspect Med*. 2011;1:a006189.
140. Baik SH, Kang S, Lee W, Choi H, Chung S, Kim JI and Mook-Jung I. A Breakdown in Metabolic Reprogramming Causes Microglia Dysfunction in Alzheimer's Disease. *Cell Metab*. 2019;30:493-507 e6.
141. Kleinberger G, Brendel M, Mracsko E, Wefers B, Groeneweg L, Xiang X, Focke C, Deussing M, Suarez-Calvet M, Mazaheri F, Parhizkar S, Pettkus N, Wurst W, Feederle R, Bartenstein P, Mueggler T, Arzberger T, Knuesel I, Rominger A and Haass C. The FTD-like syndrome causing TREM2 T66M mutation impairs microglia function, brain perfusion, and glucose metabolism. *EMBO J*. 2017;36:1837-1853.
142. Jack CR, Jr. and Holtzman DM. Biomarker modeling of Alzheimer's disease. *Neuron*. 2013;80:1347-58.
143. Jack CR, Jr., Bennett DA, Blennow K, Carrillo MC, Feldman HH, Frisoni GB, Hampel H, Jagust WJ, Johnson KA, Knopman DS, Petersen RC, Scheltens P, Sperling RA and Dubois B. A/T/N: An unbiased descriptive classification scheme for Alzheimer disease biomarkers. *Neurology*. 2016;87:539-47.
144. Heslegrave A, Heywood W, Paterson R, Magdalinou N, Svensson J, Johansson P, Ohrfelt A, Blennow K, Hardy J, Schott J, Mills K and Zetterberg H. Increased cerebrospinal fluid soluble TREM2 concentration in Alzheimer's disease. *Mol Neurodegener*. 2016;11:3.
145. Hao J, Qiao Y, Li T, Yang J, Song Y, Jia L and Jia J. Investigating Changes in the Serum Inflammatory Factors in Alzheimer's Disease and Their Correlation with Cognitive Function. *J Alzheimers Dis*. 2021;84:835-842.
146. Bostrom G, Freyhult E, Virhammar J, Alcolea D, Tumani H, Otto M, Brundin RM, Kilander L, Lowenmark M, Giedraitis V, Lleo A, von Arnim CAF, Kultima K and Ingelsson M. Different Inflammatory Signatures in Alzheimer's Disease and Frontotemporal Dementia Cerebrospinal Fluid. *J Alzheimers Dis*. 2021;81:629-640.
147. Kober DL, Stuchell-Brereton MD, Kluender CE, Dean HB, Strickland MR, Steinberg DF, Nelson SS, Baban B, Holtzman DM, Frieden C, Alexander-Brett J, Roberson ED, Song Y and Brett TJ. Functional insights from biophysical study of TREM2 interactions with apoE and Abeta1-42. *Alzheimers Dement*. 2020.
148. Song WM, Joshita S, Zhou Y, Ulland TK, Gilfillan S and Colonna M. Humanized TREM2 mice reveal microglia-intrinsic and -extrinsic effects of R47H polymorphism. *J Exp Med*. 2018;215:745-760.

149. Gratuze M, Leyns CE, Sauerbeck AD, St-Pierre MK, Xiong M, Kim N, Serrano JR, Tremblay ME, Kummer TT, Colonna M, Ulrich JD and Holtzman DM. Impact of TREM2R47H variant on tau pathology-induced gliosis and neurodegeneration. *J Clin Invest*. 2020;130:4954-4968.
150. Jiang T, Zhang YD, Gao Q, Ou Z, Gong PY, Shi JQ, Wu L and Zhou JS. TREM2 Ameliorates Neuronal Tau Pathology Through Suppression of Microglial Inflammatory Response. *Inflammation*. 2018;41:811-823.
151. Lee SH, Meilandt WJ, Xie L, Gandham VD, Ngu H, Barck KH, Rezzonico MG, Imperio J, Lalehzadeh G, Huntley MA, Stark KL, Foreman O, Carano RAD, Friedman BA, Sheng M, Easton A, Bohlen CJ and Hansen DV. Trem2 restrains the enhancement of tau accumulation and neurodegeneration by beta-amyloid pathology. *Neuron*. 2021;109:1283-1301 e6.
152. Wang Q, Yang W, Zhang J, Zhao Y and Xu Y. TREM2 Overexpression Attenuates Cognitive Deficits in Experimental Models of Vascular Dementia. *Neural Plast*. 2020;2020:8834275.
153. Taylor X, Cisternas P, You Y, You Y, Xiang S, Marambio Y, Zhang J, Vidal R and Lasagna-Reeves CA. A1 reactive astrocytes and a loss of TREM2 are associated with an early stage of pathology in a mouse model of cerebral amyloid angiopathy. *J Neuroinflammation*. 2020;17:223.
154. Hamerman JA, Jarjoura JR, Humphrey MB, Nakamura MC, Seaman WE and Lanier LL. Cutting edge: inhibition of TLR and FcR responses in macrophages by triggering receptor expressed on myeloid cells (TREM)-2 and DAP12. *J Immunol*. 2006;177:2051-5.
155. Turnbull IR, Gilfillan S, Cella M, Aoshi T, Miller M, Piccio L, Hernandez M and Colonna M. Cutting edge: TREM-2 attenuates macrophage activation. *J Immunol*. 2006;177:3520-4.
156. Liu AH, Chu M and Wang YP. Up-Regulation of Trem2 Inhibits Hippocampal Neuronal Apoptosis and Alleviates Oxidative Stress in Epilepsy via the PI3K/Akt Pathway in Mice. *Neurosci Bull*. 2019;35:471-485.
157. Liu D, Cao B, Zhao Y, Huang H, McIntyre RS, Rosenblat JD and Zhou H. Soluble TREM2 changes during the clinical course of Alzheimer's disease: A meta-analysis. *Neurosci Lett*. 2018;686:10-16.
158. Suarez-Calvet M, Kleinberger G, Araque Caballero MA, Brendel M, Rominger A, Alcolea D, Fortea J, Lleó A, Blesa R, Gispert JD, Sanchez-Valle R, Antonell A, Rami L, Molinuevo JL, Brosseron F, Trasciatti A, Heneka MT, Struyfs H, Engelborghs S, Sleegers K, Van Broeckhoven C, Zetterberg H, Nellgard B, Blennow K, Crispin A, Ewers M and Haass C. sTREM2 cerebrospinal fluid levels are a potential biomarker for microglia activity in early-stage Alzheimer's disease and associate with neuronal injury markers. *EMBO Mol Med*. 2016;8:466-76.
159. Henjum K, Almdahl IS, Arskog V, Minthon L, Hansson O, Fladby T and Nilsson LN. Cerebrospinal fluid soluble TREM2 in aging and Alzheimer's disease. *Alzheimers Res Ther*. 2016;8:17.
160. Suarez-Calvet M, Morenas-Rodriguez E, Kleinberger G, Schlepckow K, Araque Caballero MA, Franzmeier N, Capell A, Fellerer K, Nuscher B, Eren E, Levin J, Deming Y, Piccio L, Karch CM, Cruchaga C, Shaw LM, Trojanowski JQ, Weiner M, Ewers M, Haass C and Alzheimer's Disease Neuroimaging I. Early increase of CSF sTREM2 in Alzheimer's disease is associated with tau related-neurodegeneration but not with amyloid-beta pathology. *Mol Neurodegener*. 2019;14:1.
161. Jefferson AL, Gifford KA, Acosta LM, Bell SP, Donahue MJ, Davis LT, Gottlieb J, Gupta DK, Hohman TJ, Lane EM, Libon DJ, Mendes LA, Niswender K, Pechman KR, Rane S, Ruberg FL, Su YR, Zetterberg H and Liu D. The Vanderbilt Memory & Aging Project: Study Design and Baseline Cohort Overview. *J Alzheimers Dis*. 2016;52:539-59.
162. Kresge HA, Khan OA, Wagener MA, Liu D, Terry JG, Nair S, Cambronero FE, Gifford KA, Osborn KE, Hohman TJ, Pechman KR, Bell SP, Wang TJ, Carr JJ and Jefferson AL. Subclinical Compromise in Cardiac Strain Relates to Lower Cognitive Performances in Older Adults. *J Am Heart Assoc*. 2018;7.
163. Jensen CS, Bahl JM, Ostergaard LB, Høgh P, Wermuth L, Heslegrave A, Zetterberg H, Heegaard NHH, Hasselbalch SG and Simonsen AH. Exercise as a potential modulator of inflammation in patients with Alzheimer's disease measured in cerebrospinal fluid and plasma. *Exp Gerontol*. 2019;121:91-98.

164. Korecka M, Waligorska T, Figurski M, Toledo JB, Arnold SE, Grossman M, Trojanowski JQ and Shaw LM. Qualification of a surrogate matrix-based absolute quantification method for amyloid-beta(4)(2) in human cerebrospinal fluid using 2D UPLC-tandem mass spectrometry. *J Alzheimers Dis*. 2014;41:441-51.
165. Korecka M, Figurski MJ, Landau SM, Brylska M, Alexander J, Blennow K, Zetterberg H, Jagust WJ, Trojanowski JQ, Shaw LM and Alzheimer's Disease Neuroimaging I. Analytical and Clinical Performance of Amyloid-Beta Peptides Measurements in CSF of ADNIGO/2 Participants by an LC-MS/MS Reference Method. *Clin Chem*. 2020;66:587-597.
166. Shaw LM, Vanderstichele H, Knapik-Czajka M, Clark CM, Aisen PS, Petersen RC, Blennow K, Soares H, Simon A, Lewczuk P, Dean R, Siemers E, Potter W, Lee VM, Trojanowski JQ and Alzheimer's Disease Neuroimaging I. Cerebrospinal fluid biomarker signature in Alzheimer's disease neuroimaging initiative subjects. *Ann Neurol*. 2009;65:403-13.
167. Suarez-Calvet M, Araque Caballero MA, Kleinberger G, Bateman RJ, Fagan AM, Morris JC, Levin J, Danek A, Ewers M, Haass C and Dominantly Inherited Alzheimer N. Early changes in CSF sTREM2 in dominantly inherited Alzheimer's disease occur after amyloid deposition and neuronal injury. *Sci Transl Med*. 2016;8:369ra178.
168. Wardlaw JM, Smith EE, Biessels GJ, Cordonnier C, Fazekas F, Frayne R, Lindley RI, O'Brien JT, Barkhof F, Benavente OR, Black SE, Brayne C, Breteler M, Chabriat H, Decarli C, de Leeuw FE, Doubal F, Duering M, Fox NC, Greenberg S, Hachinski V, Kilimann I, Mok V, Oostenbrugge R, Pantoni L, Speck O, Stephan BC, Teipel S, Viswanathan A, Werring D, Chen C, Smith C, van Buchem M, Norrving B, Gorelick PB, Dichgans M and nEuroimaging STfRVco. Neuroimaging standards for research into small vessel disease and its contribution to ageing and neurodegeneration. *Lancet Neurol*. 2013;12:822-38.
169. Trzepacz PT, Hochstetler H, Wang S, Walker B, Saykin AJ and Alzheimer's Disease Neuroimaging I. Relationship between the Montreal Cognitive Assessment and Mini-mental State Examination for assessment of mild cognitive impairment in older adults. *BMC Geriatr*. 2015;15:107.
170. Ewers M, Franzmeier N, Suarez-Calvet M, Morenas-Rodriguez E, Caballero MAA, Kleinberger G, Piccio L, Cruchaga C, Deming Y, Dichgans M, Trojanowski JQ, Shaw LM, Weiner MW, Haass C and Alzheimer's Disease Neuroimaging I. Increased soluble TREM2 in cerebrospinal fluid is associated with reduced cognitive and clinical decline in Alzheimer's disease. *Sci Transl Med*. 2019;11.
171. Edwin TH, Henjum K, Nilsson LNG, Watne LO, Persson K, Eldholm RS, Saltvedt I, Halaas NB, Selbaek G, Engedal K, Strand BH and Knapskog AB. A high cerebrospinal fluid soluble TREM2 level is associated with slow clinical progression of Alzheimer's disease. *Alzheimers Dement (Amst)*. 2020;12:e12128.
172. Bero AW, Yan P, Roh JH, Cirrito JR, Stewart FR, Raichle ME, Lee JM and Holtzman DM. Neuronal activity regulates the regional vulnerability to amyloid-beta deposition. *Nat Neurosci*. 2011;14:750-6.
173. Cirrito JR, Yamada KA, Finn MB, Sloviter RS, Bales KR, May PC, Schoepp DD, Paul SM, Mennerick S and Holtzman DM. Synaptic activity regulates interstitial fluid amyloid-beta levels in vivo. *Neuron*. 2005;48:913-22.
174. Kamenetz F, Tomita T, Hsieh H, Seabrook G, Borchelt D, Iwatsubo T, Sisodia S and Malinow R. APP processing and synaptic function. *Neuron*. 2003;37:925-37.
175. Wei W, Nguyen LN, Kessels HW, Hagiwara H, Sisodia S and Malinow R. Amyloid beta from axons and dendrites reduces local spine number and plasticity. *Nat Neurosci*. 2010;13:190-6.
176. da Fonseca AC, Matias D, Garcia C, Amaral R, Geraldo LH, Freitas C and Lima FR. The impact of microglial activation on blood-brain barrier in brain diseases. *Front Cell Neurosci*. 2014;8:362.
177. Harold D, Abraham R, Hollingworth P, Sims R, Gerrish A, Hamshere ML, Pahwa JS, Moskvina V, Dowzell K, Williams A, Jones N, Thomas C, Stretton A, Morgan AR, Lovestone S, Powell J, Proitsi P, Lupton MK, Brayne C, Rubinsztein DC, Gill M, Lawlor B, Lynch A, Morgan K, Brown KS, Passmore PA, Craig D, McGuinness B, Todd S, Holmes C, Mann D, Smith AD, Love S, Kehoe PG, Hardy J, Mead S, Fox N, Rossor M, Collinge J, Maier W, Jessen F, Schurmann B, Heun R, van den Bussche H, Heuser I, Kornhuber J, Wiltfang J, Dichgans M, Frolich L, Hampel H, Hull M, Rujescu D, Goate AM, Kauwe JS, Cruchaga C, Nowotny P, Morris

- JC, Mayo K, Sleegers K, Bettens K, Engelborghs S, De Deyn PP, Van Broeckhoven C, Livingston G, Bass NJ, Gurling H, McQuillin A, Gwilliam R, Deloukas P, Al-Chalabi A, Shaw CE, Tsolaki M, Singleton AB, Guerreiro R, Muhleisen TW, Nothen MM, Moebus S, Jockel KH, Klopp N, Wichmann HE, Carrasquillo MM, Pankratz VS, Younkin SG, Holmans PA, O'Donovan M, Owen MJ and Williams J. Genome-wide association study identifies variants at CLU and PICALM associated with Alzheimer's disease. *Nat Genet.* 2009;41:1088-93.
178. Antunez C, Boada M, Gonzalez-Perez A, Gayan J, Ramirez-Lorca R, Marin J, Hernandez I, Moreno-Rey C, Moron FJ, Lopez-Arrieta J, Mauleon A, Rosende-Roca M, Noguera-Perea F, Legaz-Garcia A, Vivancos-Moreau L, Velasco J, Carrasco JM, Alegret M, Antequera-Torres M, Manzanares S, Romo A, Blanca I, Ruiz S, Espinosa A, Castano S, Garcia B, Martinez-Herrada B, Vinyes G, Lafuente A, Becker JT, Galan JJ, Serrano-Rios M, Alzheimer's Disease Neuroimaging I, Vazquez E, Tarraga L, Saez ME, Lopez OL, Real LM and Ruiz A. The membrane-spanning 4-domains, subfamily A (MS4A) gene cluster contains a common variant associated with Alzheimer's disease. *Genome Med.* 2011;3:33.
179. Deng YL, Liu LH, Wang Y, Tang HD, Ren RJ, Xu W, Ma JF, Wang LL, Zhuang JP, Wang G and Chen SD. The prevalence of CD33 and MS4A6A variant in Chinese Han population with Alzheimer's disease. *Hum Genet.* 2012;131:1245-9.
180. Tan L, Yu JT, Zhang W, Wu ZC, Zhang Q, Liu QY, Wang W, Wang HF, Ma XY and Cui WZ. Association of GWAS-linked loci with late-onset Alzheimer's disease in a northern Han Chinese population. *Alzheimers Dement.* 2013;9:546-53.
181. Efthymiou AG and Goate AM. Late onset Alzheimer's disease genetics implicates microglial pathways in disease risk. *Mol Neurodegener.* 2017;12:43.
182. Silva-Gomes R, Mapelli SN, Boutet MA, Mattioli I, Sironi M, Grizzi F, Colombo F, Supino D, Carnevale S, Pasqualini F, Stravalaci M, Porte R, Gianatti A, Pitzalis C, Locati M, Oliveira MJ, Bottazzi B and Mantovani A. Differential expression and regulation of MS4A family members in myeloid cells in physiological and pathological conditions. *J Leukoc Biol.* 2022;111:817-836.
183. Roach CA and Cross AH. Anti-CD20 B Cell Treatment for Relapsing Multiple Sclerosis. *Front Neurol.* 2020;11:595547.
184. Pavlasova G and Mraz M. The regulation and function of CD20: an "enigma" of B-cell biology and targeted therapy. *Haematologica.* 2020;105:1494-1506.
185. Yan Y, Li Z, Zhang GX, Williams MS, Carey GB, Zhang J, Rostami A and Xu H. Anti-MS4a4B treatment abrogates MS4a4B-mediated protection in T cells and ameliorates experimental autoimmune encephalomyelitis. *Apoptosis.* 2013;18:1106-19.
186. Ma J, Yu JT and Tan L. MS4A Cluster in Alzheimer's Disease. *Mol Neurobiol.* 2015;51:1240-8.
187. Dong H, Zhang X and Qian Y. Mast cells and neuroinflammation. *Med Sci Monit Basic Res.* 2014;20:200-6.
188. Laurent C, Dorothee G, Hunot S, Martin E, Monnet Y, Duchamp M, Dong Y, Legeron FP, Leboucher A, Burnouf S, Faivre E, Carvalho K, Caillierez R, Zommer N, Demeyer D, Jouy N, Sazdovitch V, Schraen-Maschke S, Delarasse C, Buee L and Blum D. Hippocampal T cell infiltration promotes neuroinflammation and cognitive decline in a mouse model of tauopathy. *Brain.* 2017;140:184-200.
189. Unger MS, Li E, Scharnagl L, Poupardin R, Altendorfer B, Mrowetz H, Hutter-Paier B, Weiger TM, Heneka MT, Attems J and Aigner L. CD8(+) T-cells infiltrate Alzheimer's disease brains and regulate neuronal- and synapse-related gene expression in APP-PS1 transgenic mice. *Brain Behav Immun.* 2020;89:67-86.
190. Franzmeier N, Suarez-Calvet M, Frontzkowski L, Moore A, Hohman TJ, Morenas-Rodriguez E, Nuscher B, Shaw L, Trojanowski JQ, Dichgans M, Kleinberger G, Haass C, Ewers M and Alzheimer's Disease Neuroimaging I. Higher CSF sTREM2 attenuates ApoE4-related risk for cognitive decline and neurodegeneration. *Mol Neurodegener.* 2020;15:57.
191. Ewers M, Biechele G, Suarez-Calvet M, Sacher C, Blume T, Morenas-Rodriguez E, Deming Y, Piccio L, Cruchaga C, Kleinberger G, Shaw L, Trojanowski JQ, Herms J, Dichgans M, Alzheimer's Disease

- Neuroimaging I, Brendel M, Haass C and Franzmeier N. Higher CSF sTREM2 and microglia activation are associated with slower rates of beta-amyloid accumulation. *EMBO Mol Med*. 2020;12:e12308.
192. Ohrfelt A, Axelsson M, Malmstrom C, Novakova L, Heslegrave A, Blennow K, Lycke J and Zetterberg H. Soluble TREM-2 in cerebrospinal fluid from patients with multiple sclerosis treated with natalizumab or mitoxantrone. *Mult Scler*. 2016;22:1587-1595.
193. Petyuk VA, Qian WJ, Smith RD and Smith DJ. Mapping protein abundance patterns in the brain using voxelation combined with liquid chromatography and mass spectrometry. *Methods*. 2010;50:77-84.
194. Andreev VP, Petyuk VA, Brewer HM, Karpievitch YV, Xie F, Clarke J, Camp D, Smith RD, Lieberman AP, Albin RL, Nawaz Z, El Hokayem J and Myers AJ. Label-free quantitative LC-MS proteomics of Alzheimer's disease and normally aged human brains. *J Proteome Res*. 2012;11:3053-67.
195. MacLean B, Tomazela DM, Shulman N, Chambers M, Finney GL, Frewen B, Kern R, Tabb DL, Liebler DC and MacCoss MJ. Skyline: an open source document editor for creating and analyzing targeted proteomics experiments. *Bioinformatics*. 2010;26:966-8.
196. Brouillette J. The effects of soluble Abeta oligomers on neurodegeneration in Alzheimer's disease. *Curr Pharm Des*. 2014;20:2506-19.
197. Hector A and Brouillette J. Hyperactivity Induced by Soluble Amyloid-beta Oligomers in the Early Stages of Alzheimer's Disease. *Front Mol Neurosci*. 2020;13:600084.
198. Dunys J, Valverde A and Checler F. Are N- and C-terminally truncated Abeta species key pathological triggers in Alzheimer's disease? *J Biol Chem*. 2018;293:15419-15428.
199. Ghasemi-Tarie R, Kiasalari Z, Fakour M, Khorasani M, Keshtkar S, Baluchnejadmojarad T and Roghani M. Nobiletin prevents amyloid beta1-40-induced cognitive impairment via inhibition of neuroinflammation and oxidative/nitrosative stress. *Metab Brain Dis*. 2022;37:1337-1349.
200. Park J, Lee SY, Shon J, Kim K, Lee HJ, Kim KA, Lee BY, Oh SH, Kim NK and Kim OJ. Adalimumab improves cognitive impairment, exerts neuroprotective effects and attenuates neuroinflammation in an Abeta1-40-injected mouse model of Alzheimer's disease. *Cytotherapy*. 2019;21:671-682.
201. Wiltfang J, Esselmann H, Bibl M, Smirnov A, Otto M, Paul S, Schmidt B, Klafki HW, Maler M, Dyrks T, Bienert M, Beyermann M, Ruther E and Kornhuber J. Highly conserved and disease-specific patterns of carboxyterminally truncated Abeta peptides 1-37/38/39 in addition to 1-40/42 in Alzheimer's disease and in patients with chronic neuroinflammation. *J Neurochem*. 2002;81:481-96.
202. Quartey MO, Nyarko JNK, Maley JM, Barnes JR, Bolanos MAC, Heistad RM, Knudsen KJ, Pennington PR, Buttigieg J, De Carvalho CE, Leary SC, Parsons MP and Mousseau DD. The Abeta(1-38) peptide is a negative regulator of the Abeta(1-42) peptide implicated in Alzheimer disease progression. *Sci Rep*. 2021;11:431.
203. Pugazhenti S, Qin L and Reddy PH. Common neurodegenerative pathways in obesity, diabetes, and Alzheimer's disease. *Biochim Biophys Acta Mol Basis Dis*. 2017;1863:1037-1045.
204. Yang J, Fu Z, Zhang X, Xiong M, Meng L and Zhang Z. TREM2 ectodomain and its soluble form in Alzheimer's disease. *J Neuroinflammation*. 2020;17:204.
205. Raha-Chowdhury R, Henderson JW, Raha AA, Vuono R, Bickerton A, Jones E, Fincham R, Allinson K, Holland A and Zaman SH. Choroid Plexus Acts as Gatekeeper for TREM2, Abnormal Accumulation of ApoE, and Fibrillary Tau in Alzheimer's Disease and in Down Syndrome Dementia. *J Alzheimers Dis*. 2019;69:91-109.
206. Schindler SE, Cruchaga C, Joseph A, McCue L, Farias FHG, Wilkins CH, Deming Y, Henson RL, Mikesell RJ, Piccio L, Llibre-Guerra JJ, Moulder KL, Fagan AM, Ances BM, Benzinger TLS, Xiong C, Holtzman DM and Morris JC. African Americans Have Differences in CSF Soluble TREM2 and Associated Genetic Variants. *Neurol Genet*. 2021;7:e571.
207. Salat DH, Kaye JA and Janowsky JS. Selective preservation and degeneration within the prefrontal cortex in aging and Alzheimer disease. *Arch Neurol*. 2001;58:1403-8.

208. Giannakopoulos P, Hof PR, Michel JP, Guimon J and Bouras C. Cerebral cortex pathology in aging and Alzheimer's disease: a quantitative survey of large hospital-based geriatric and psychiatric cohorts. *Brain Res Brain Res Rev.* 1997;25:217-45.
209. Dickerson BC, Salat DH, Greve DN, Chua EF, Rand-Giovannetti E, Rentz DM, Bertram L, Mullin K, Tanzi RE, Blacker D, Albert MS and Sperling RA. Increased hippocampal activation in mild cognitive impairment compared to normal aging and AD. *Neurology.* 2005;65:404-11.
210. Celone KA, Calhoun VD, Dickerson BC, Atri A, Chua EF, Miller SL, DePeau K, Rentz DM, Selkoe DJ, Blacker D, Albert MS and Sperling RA. Alterations in memory networks in mild cognitive impairment and Alzheimer's disease: an independent component analysis. *J Neurosci.* 2006;26:10222-31.
211. Bakker A, Krauss GL, Albert MS, Speck CL, Jones LR, Stark CE, Yassa MA, Bassett SS, Shelton AL and Gallagher M. Reduction of hippocampal hyperactivity improves cognition in amnesic mild cognitive impairment. *Neuron.* 2012;74:467-74.
212. Bookheimer SY, Strojwas MH, Cohen MS, Saunders AM, Pericak-Vance MA, Mazziotta JC and Small GW. Patterns of brain activation in people at risk for Alzheimer's disease. *N Engl J Med.* 2000;343:450-6.
213. Trivedi MA, Schmitz TW, Ries ML, Hess TM, Fitzgerald ME, Atwood CS, Rowley HA, Asthana S, Sager MA and Johnson SC. fMRI activation during episodic encoding and metacognitive appraisal across the lifespan: risk factors for Alzheimer's disease. *Neuropsychologia.* 2008;46:1667-78.
214. Filippini N, MacIntosh BJ, Hough MG, Goodwin GM, Frisoni GB, Smith SM, Matthews PM, Beckmann CF and Mackay CE. Distinct patterns of brain activity in young carriers of the APOE-epsilon4 allele. *Proc Natl Acad Sci U S A.* 2009;106:7209-14.
215. Hefendehl JK, LeDue J, Ko RW, Mahler J, Murphy TH and MacVicar BA. Mapping synaptic glutamate transporter dysfunction in vivo to regions surrounding Abeta plaques by iGluSnFR two-photon imaging. *Nat Commun.* 2016;7:13441.
216. Fogel H, Frere S, Segev O, Bharill S, Shapira I, Gazit N, O'Malley T, Slomowitz E, Berdichevsky Y, Walsh DM, Isacoff EY, Hirsch JA and Slutsky I. APP homodimers transduce an amyloid-beta-mediated increase in release probability at excitatory synapses. *Cell Rep.* 2014;7:1560-1576.
217. Lehmann S, Dumurgier J, Aygnac X, Marelli C, Alcolea D, Ormaechea JF, Thouvenot E, Delaby C, Hirtz C, Vialaret J, Ginestet N, Bouaziz-Amar E, Laplanche JL, Labauge P, Paquet C, Lleo A, Gabelle A and Alzheimer's Disease Neuroimaging I. Cerebrospinal fluid A beta 1-40 peptides increase in Alzheimer's disease and are highly correlated with phospho-tau in control individuals. *Alzheimers Res Ther.* 2020;12:123.